

# From Molecules to Cells- Towards whole cell simulations

**Dr. Jeffrey Skolnick**

**Director**

**Center for the Study of Systems Biology  
Georgia Institute of Technology**

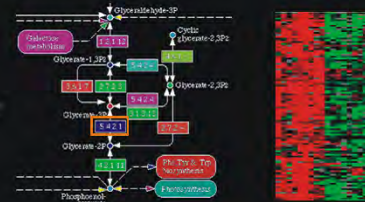
# Overview of General Approach

# Sequence to Function

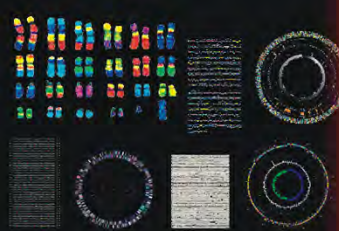
EFICAZ<sup>2</sup>

AG_VVICDT	EC 4.2.1.1	TLAEPNG.A
GGIV.ICES	YWRP.MGHL	WKIDQGG.G
A.TI.ICES	YURR.IGRL	TIAD.NAYG
A.SVVLCD	TUKYHMAN.	SLAE.QAYG
G.TLIICET	FWRKRLGR.	SLAE.NAFA
EC 1.2.1.3	YWKRMGH.	EC 5.4.1.1

Enzyme Function Inference



# Sequence to Structure



PROSPECTOR\_3.5



TASSER

FINDSITE<sup>LHM</sup>

FINDSITE

Binding Site Prediction

multi-FINDSITE

Prediction of Protein-Protein Interactions

m-TASSER

# Structure to Function

Computational Metabolomics



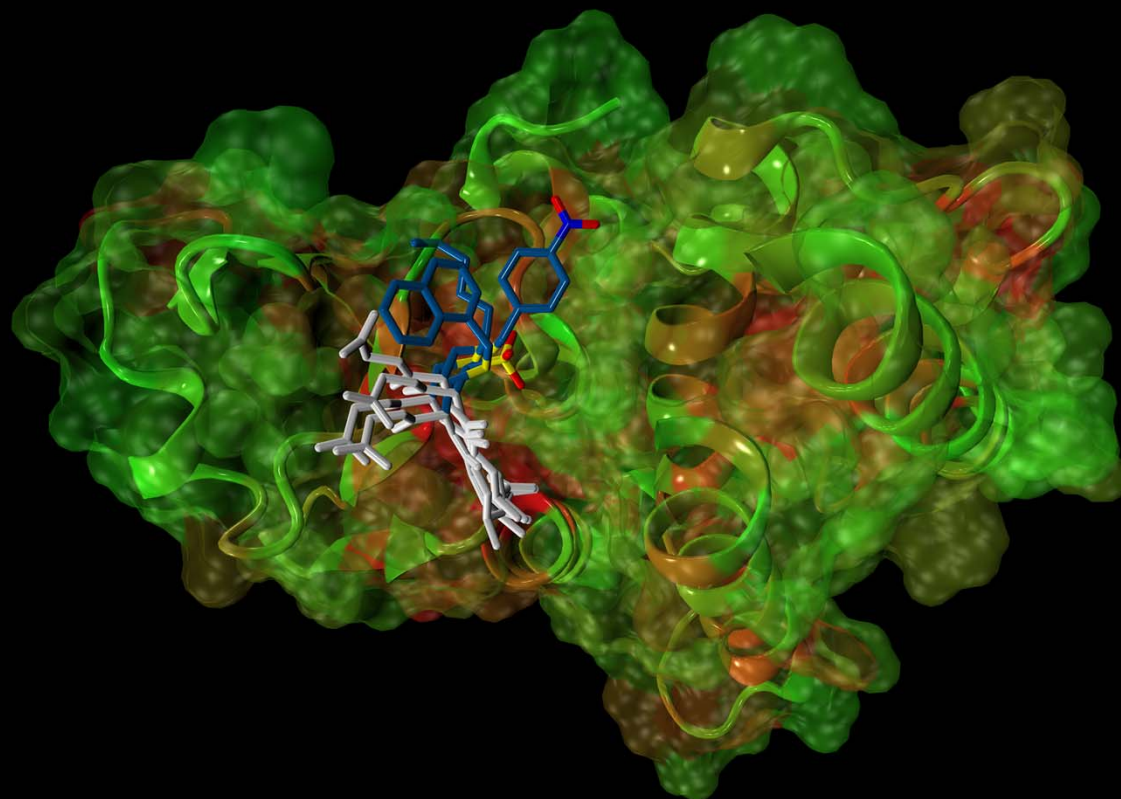
Cancer Biology



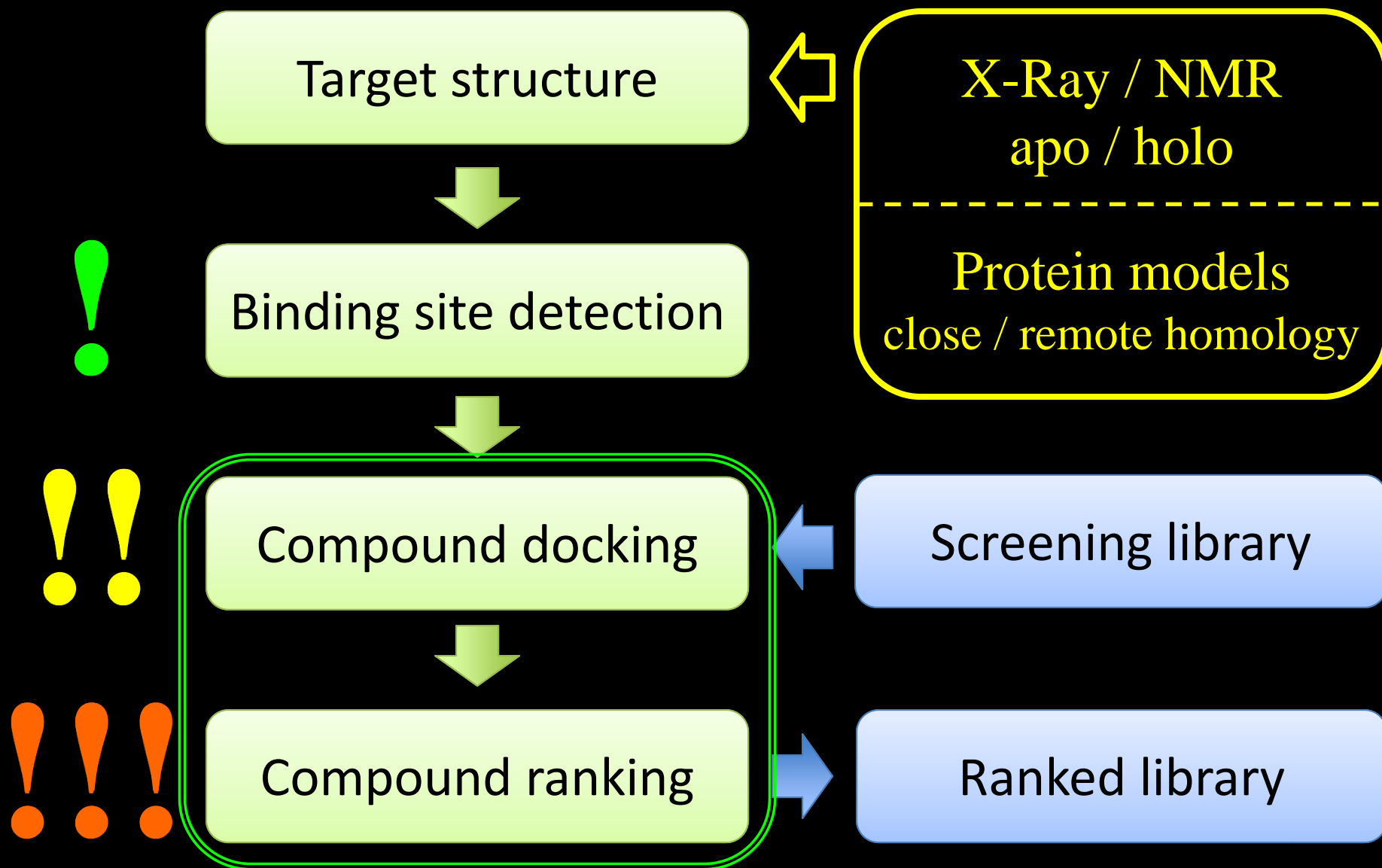
Druggable Target Prediction



LIGAND HOMOMOLOGY MODELING AS A  
NEW COMPUTATIONAL PLATFORM TO  
SUPPORT MODERN DRUG DEVELOPMENT



# Structure-based virtual screening in drug discovery



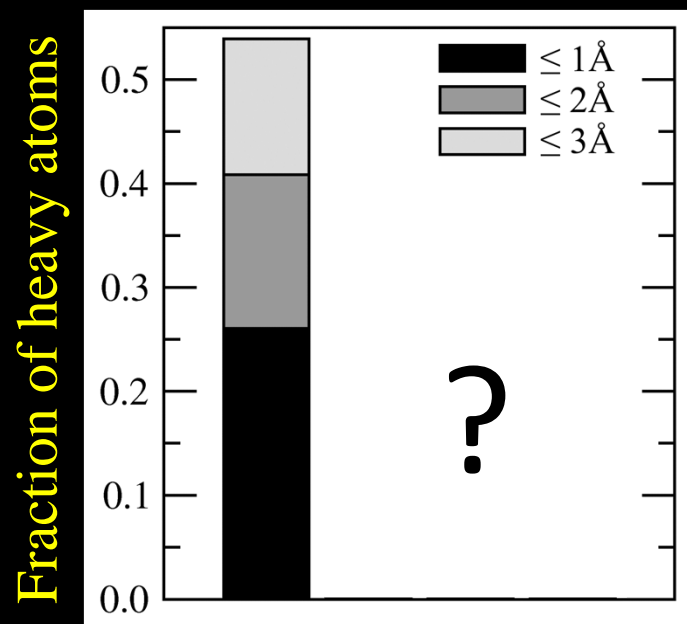
### Requirements for ligand docking/scoring approaches:

- ① Accurate ligand binding pose prediction
- ② Reliable compound ranking in virtual screening

# LIGAND HOMOLOGY MODELING: CHALLENGES

Most ligand docking algorithms are inapplicable to protein models

*AUTODOCK3*



Crystal structures

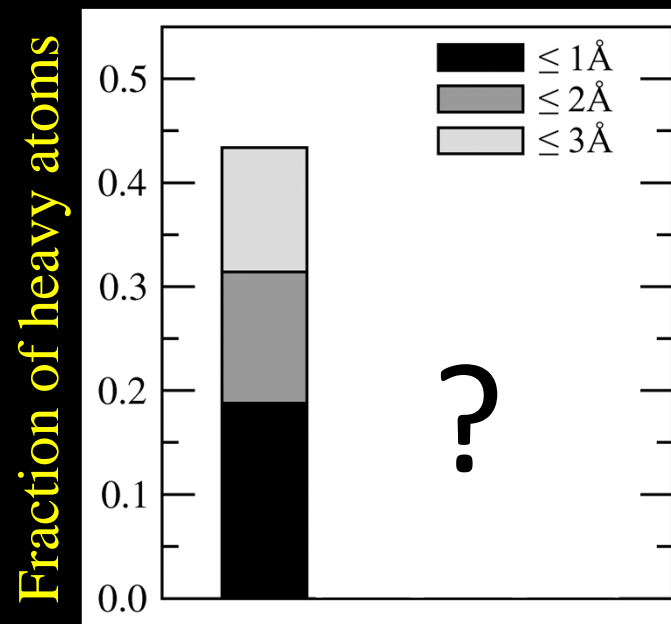
3.8Å

5.7Å

7.3Å

(C $\alpha$ -RMSD)

*LIGIN*



Crystal structures

3.8Å

5.7Å

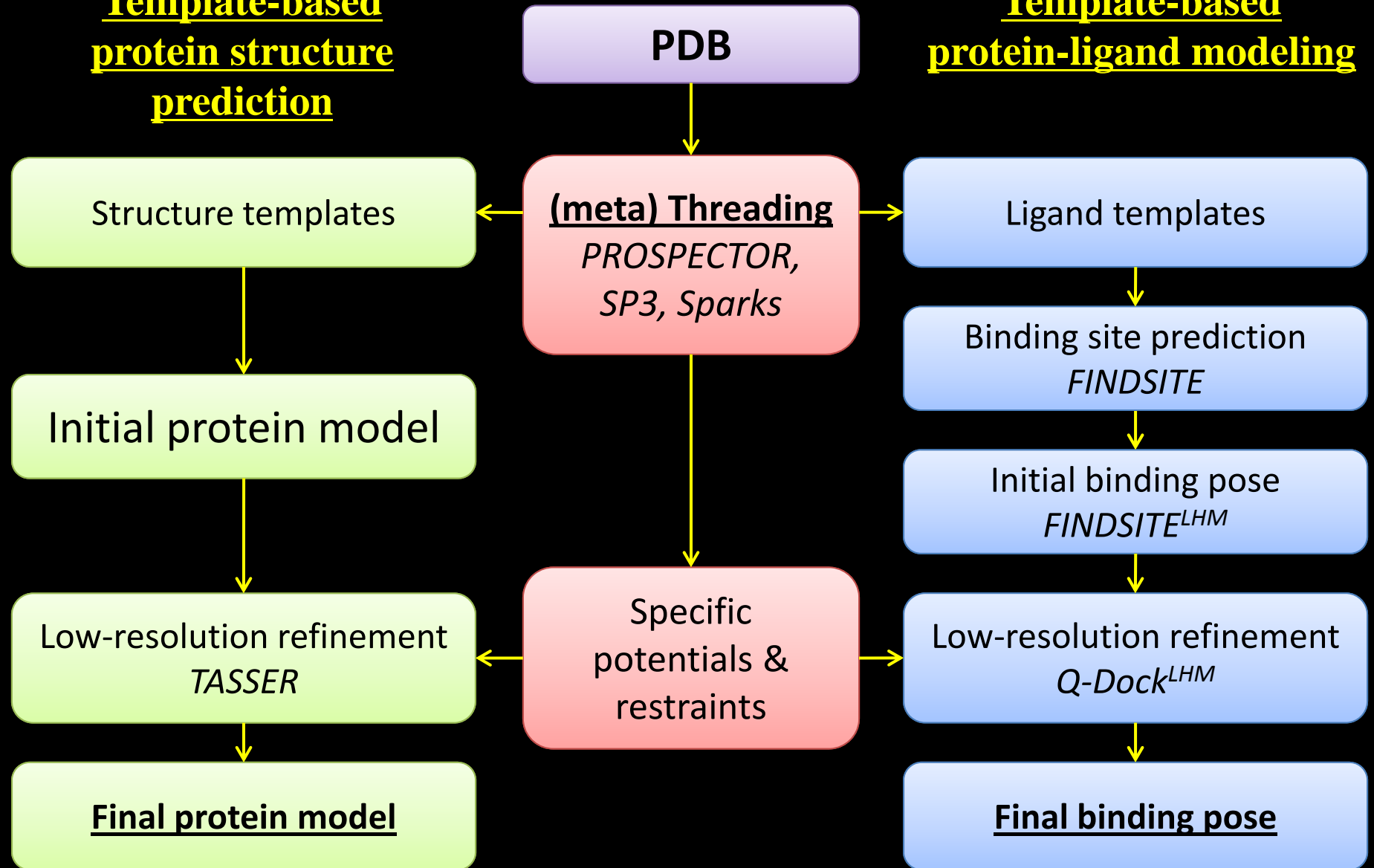
7.3Å

(C $\alpha$ -RMSD)

# LIGAND HOMOMOLOGY MODELING: OVERVIEW

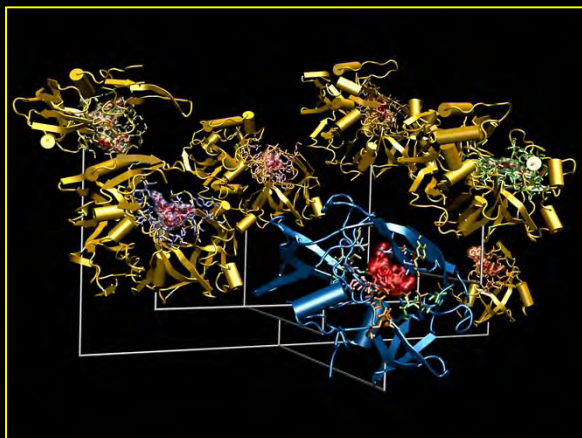
## Template-based protein structure prediction

## Template-based protein-ligand modeling



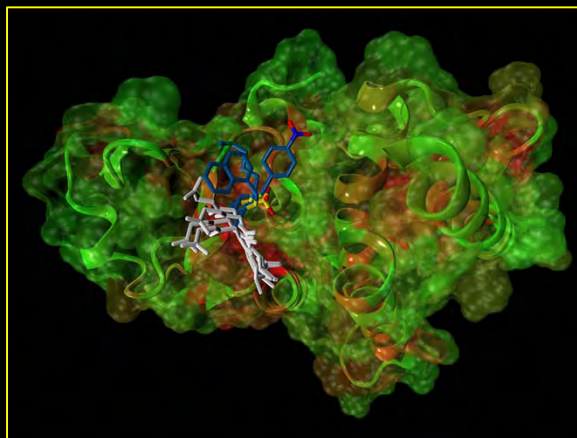
# LIGAND HOMOMOLOGY MODELING: TECHNOLOGY & APPLICATION

## FINDSITE



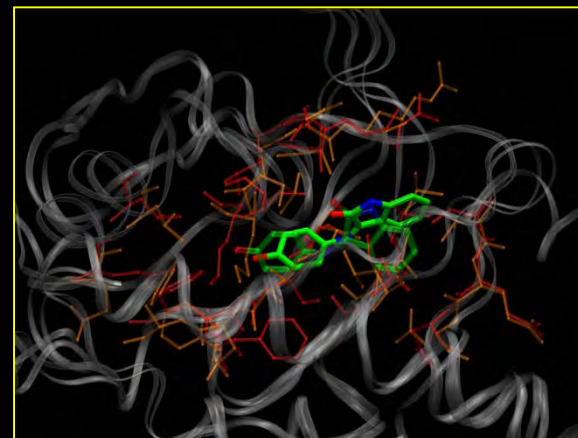
Ligand binding site  
prediction

## FINDSITE<sup>LHM</sup>

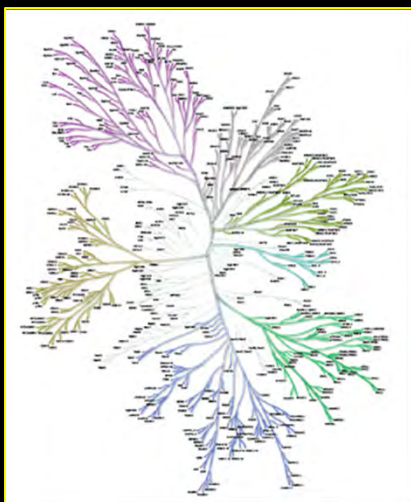


Similarity-based  
ligand docking

## Q-Dock<sup>LHM</sup>



Low-resolution ligand  
docking/refinement

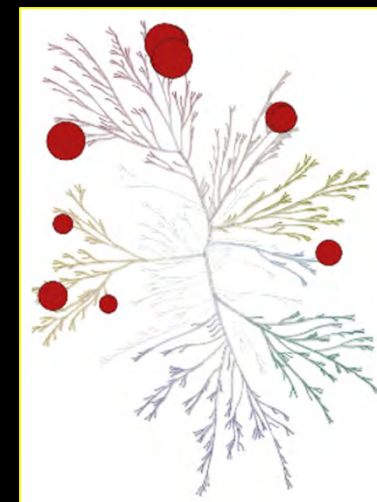


## KINOME<sup>LHM</sup>

Virtual screening  
of the human  
kinome

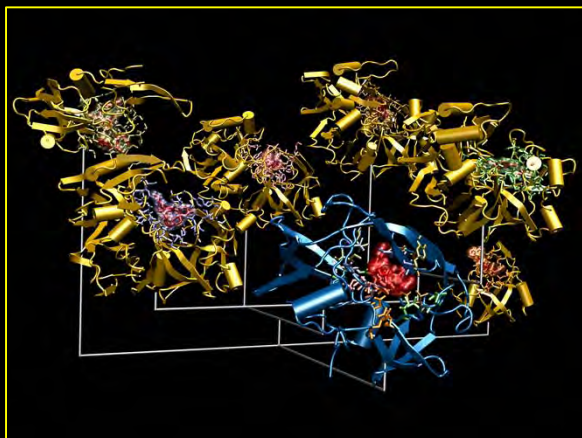
## X-React<sup>KIN</sup>

*In silico* drug  
profiling



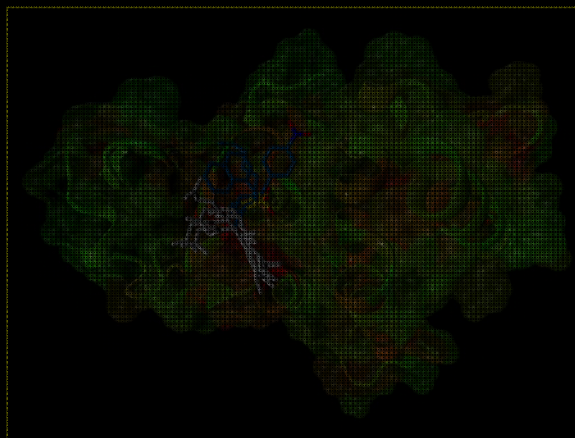
# LIGAND HOMOLOGY MODELING: FINDSITE

## FINDSITE



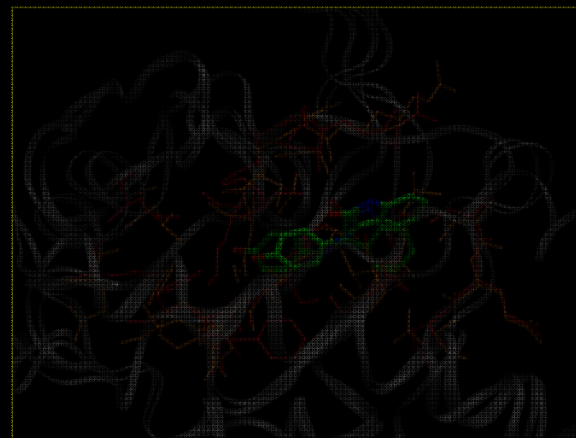
Ligand binding site  
prediction

## FINDSITE<sup>LHM</sup>



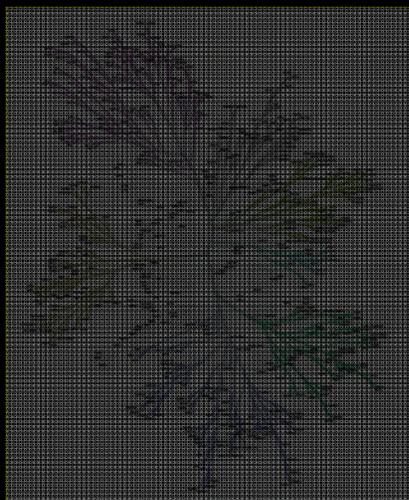
Similarity-based  
ligand docking

## Q-Dock<sup>LHM</sup>



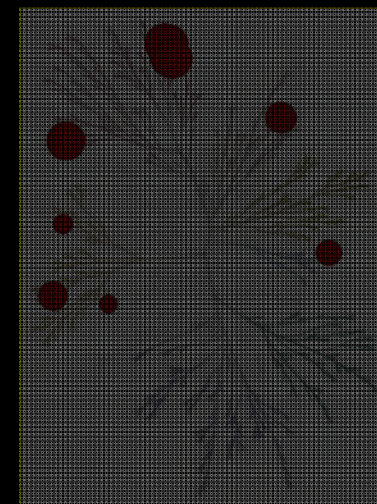
Low-resolution ligand  
docking/refinement

## KINOME<sup>LHM</sup>



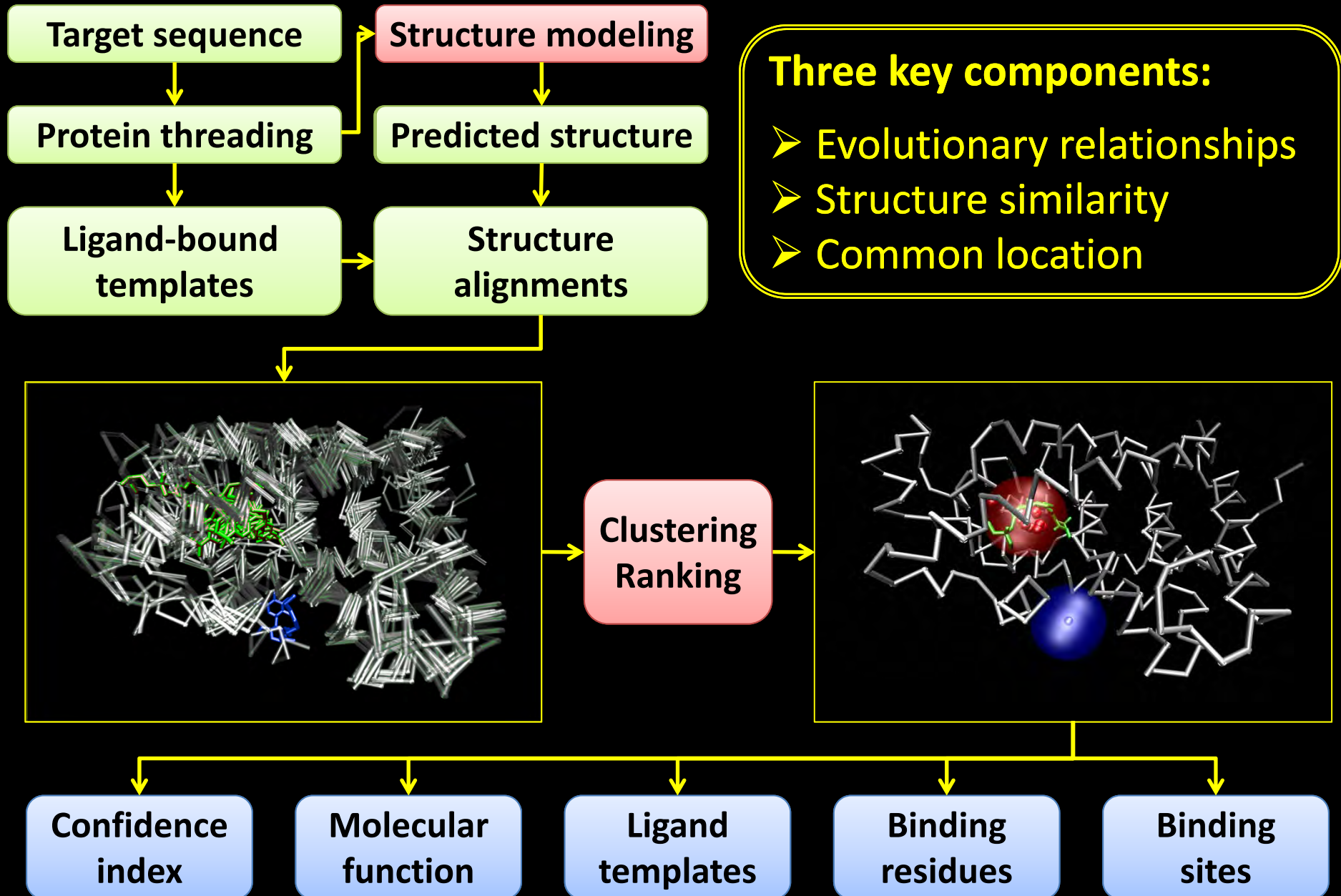
Virtual screening  
of the human  
kinome

## X-React<sup>KIN</sup>



*In silico* drug  
profiling

# LIGAND HOMOLOGY MODELING: FINDSITE



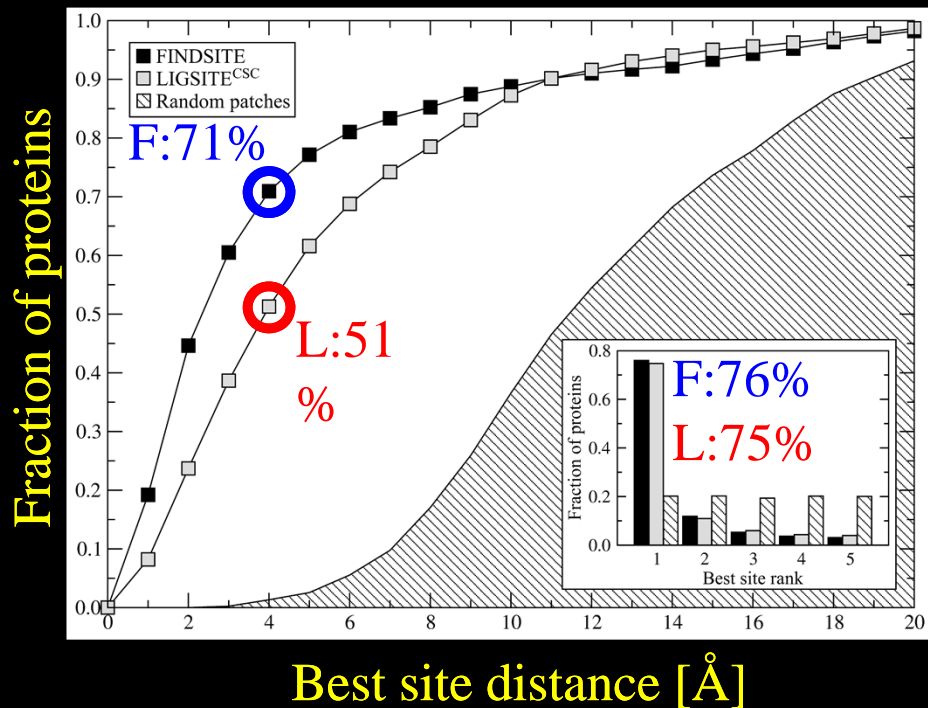
# LIGAND HOMOLOGY MODELING: FINDSITE

Benchmarks carried out for a set of 901 proteins:

- Crystal structures

FINDSITE is compared to LIGSITE<sup>CSC</sup>

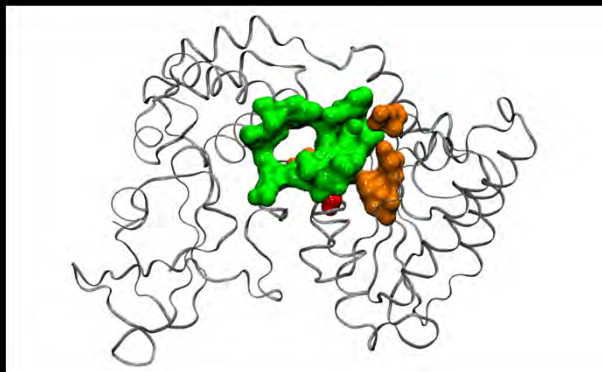
Crystal structures



# LIGAND HOMOLOGY MODELING: FINDSITE

## Performance of FINDSITE in CASP8

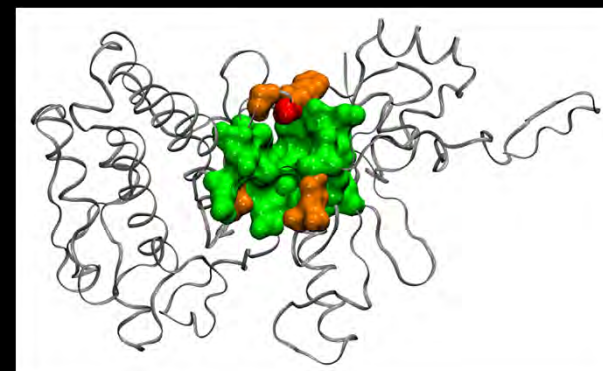
T0422



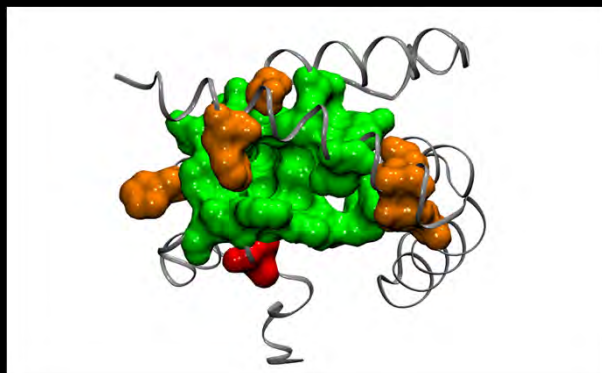
*BLIND  
PREDICTION*

Correct (TP)  
Overpredicted (FP)  
Missed (FN)

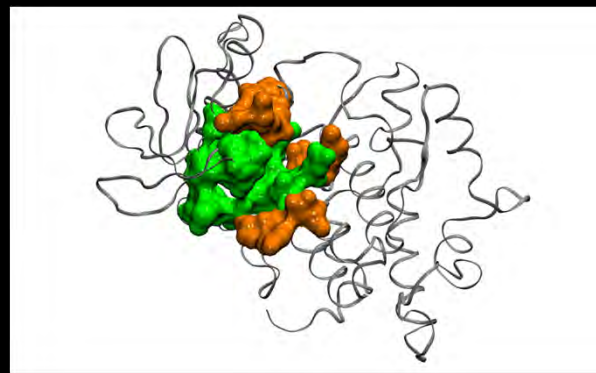
T0483



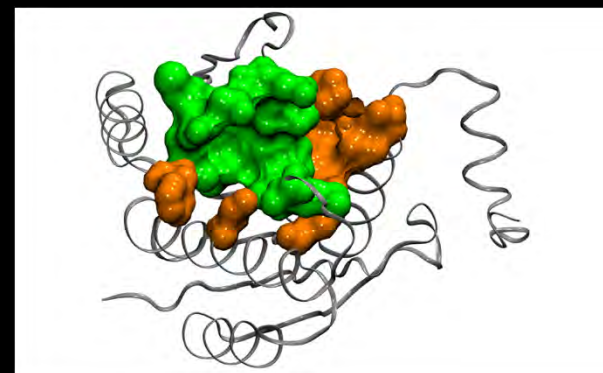
T0485



T0494



T0508



# Why does FINDSITE WORK?

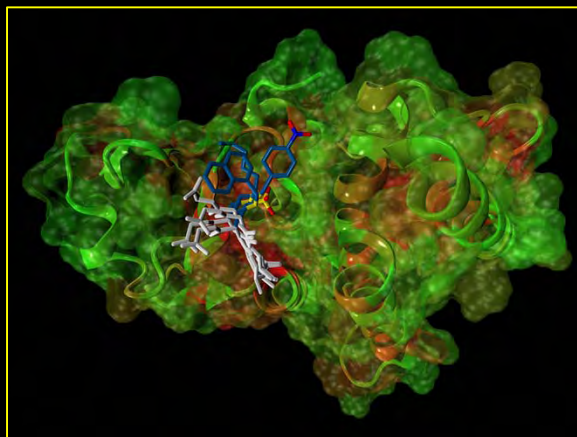
# LIGAND HOMOMOLOGY MODELING: FINDSITE<sup>LHM</sup>

FINDSITE



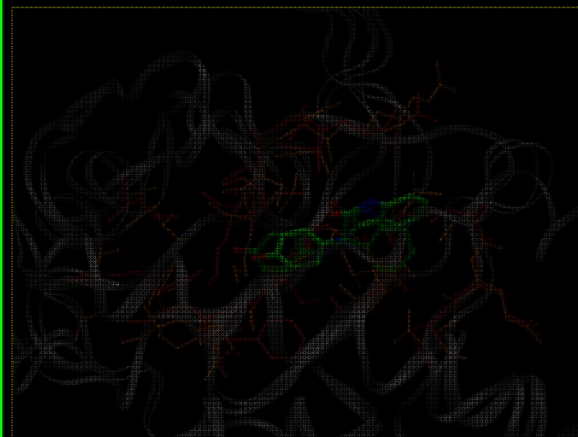
Ligand binding site prediction

FINDSITE<sup>LHM</sup>



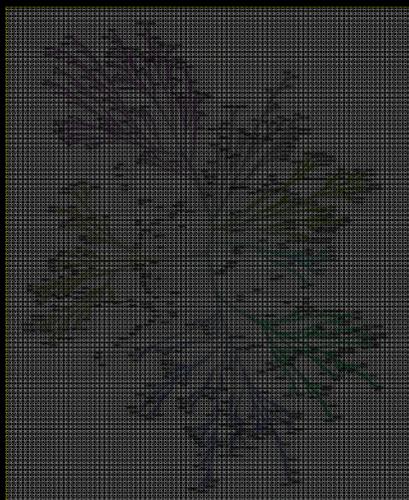
Similarity-based ligand docking

Q-Dock<sup>LHM</sup>



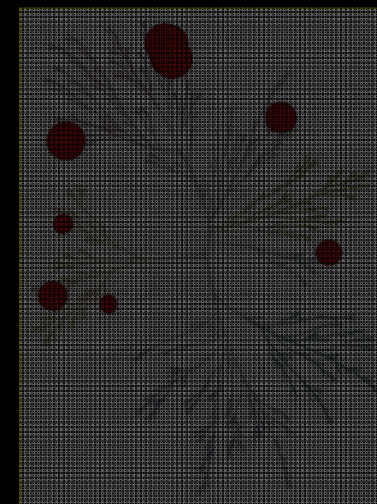
Low-resolution ligand docking/refinement

KINOME<sup>LHM</sup>



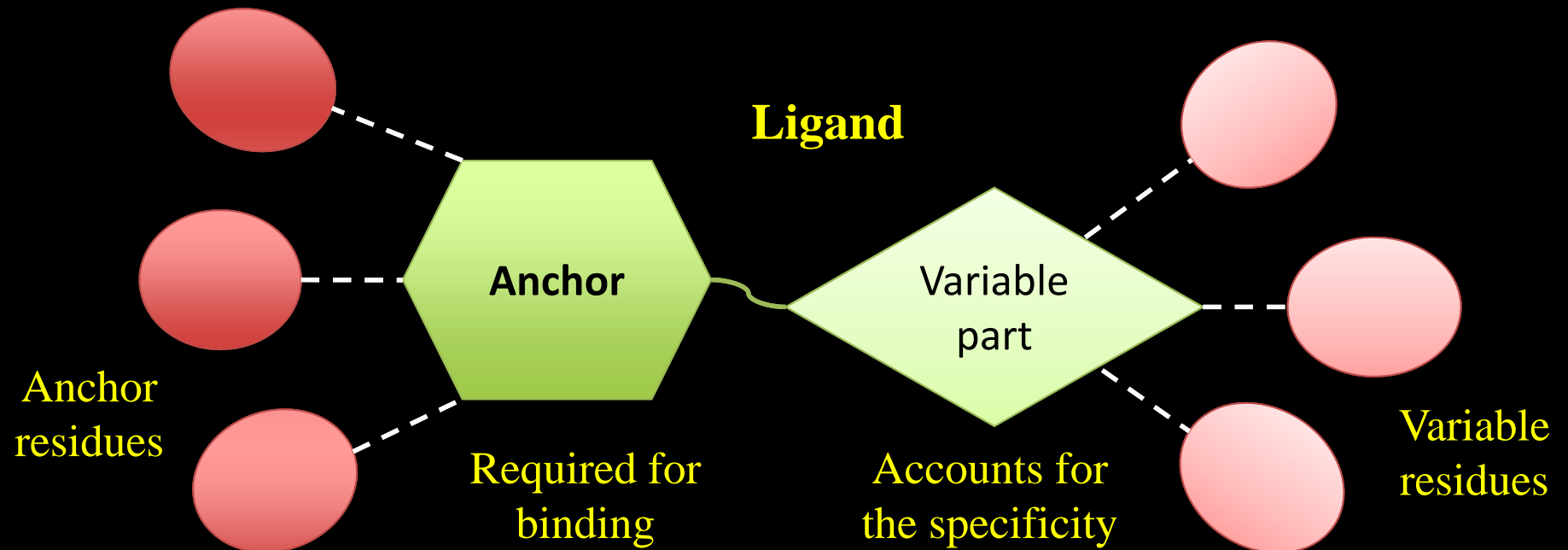
Virtual screening of the human kinome

X-React<sup>KIN</sup>



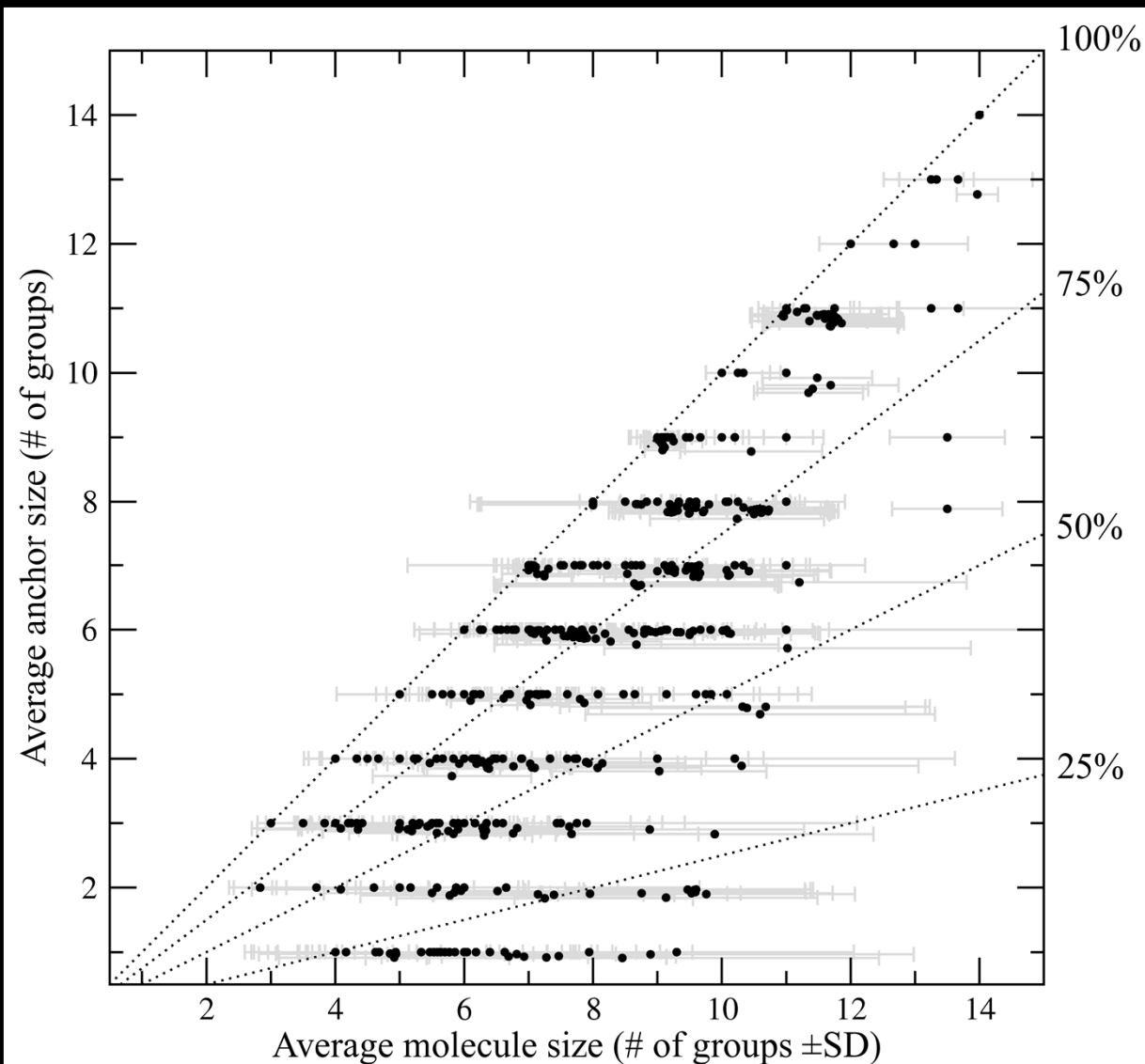
*In silico* drug profiling

# LIGAND HOMOLOGY MODELING: FINDSITE<sup>LHM</sup>



- Can an anchor be identified in ligands bound to evolutionarily related proteins?
- What is the sequence/structure conservation of the anchor and variable regions?
- Can the consensus binding mode be used for ligand docking into the predicted pockets?

# LIGAND HOMOLOGY MODELING: FINDSITE<sup>LHM</sup>



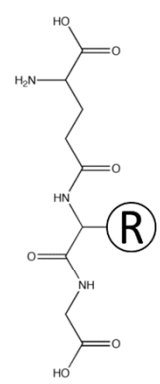
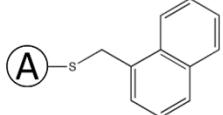
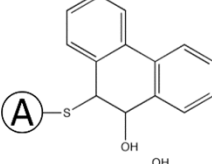
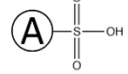
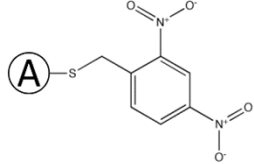
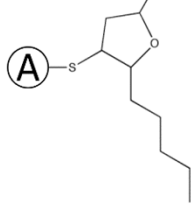
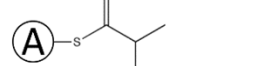
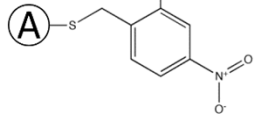
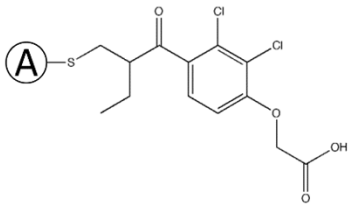
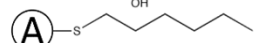
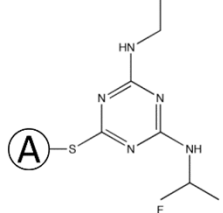
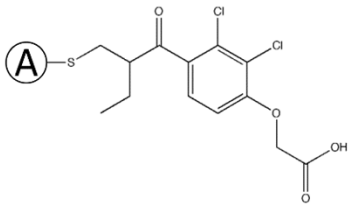
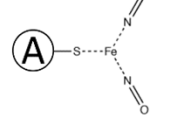
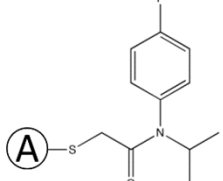
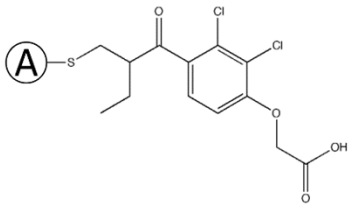
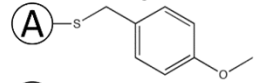
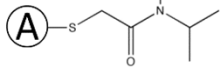
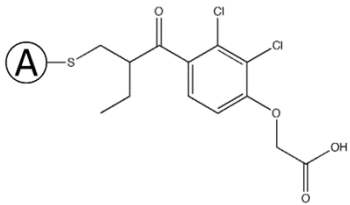
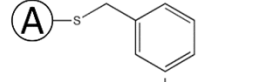
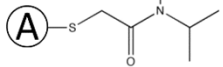
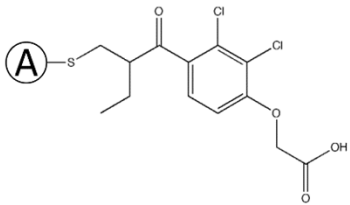
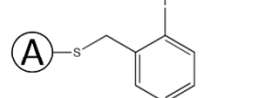
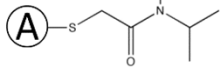
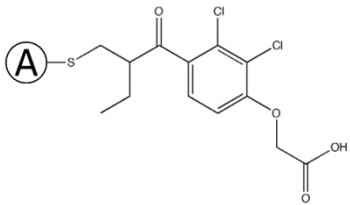
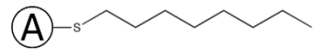
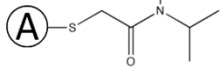
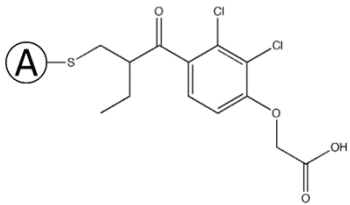
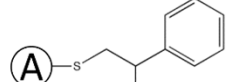
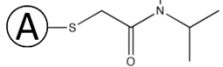
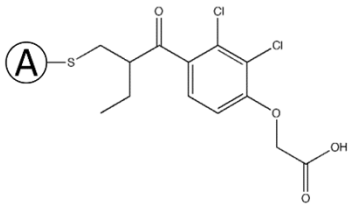
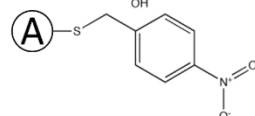
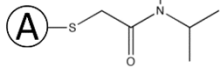
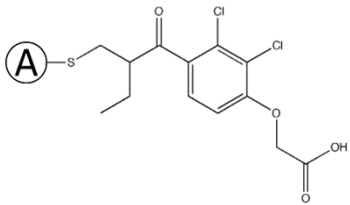
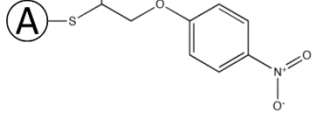
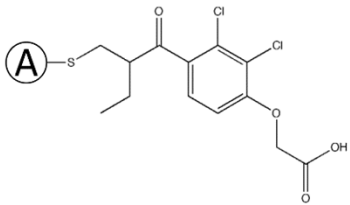
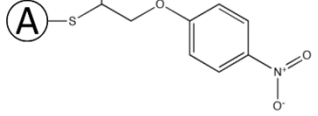
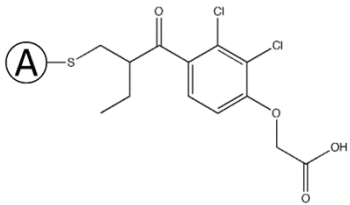
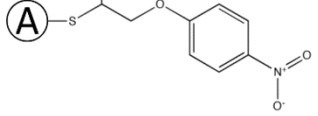
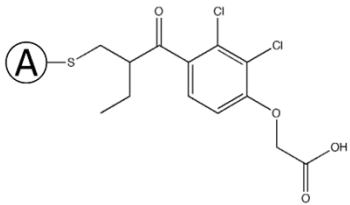
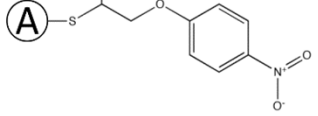
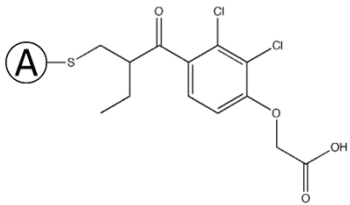
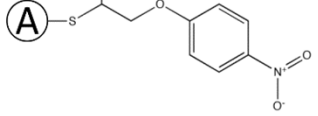
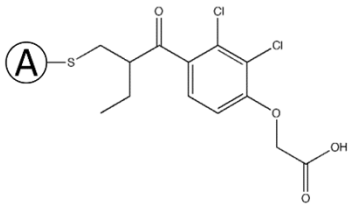
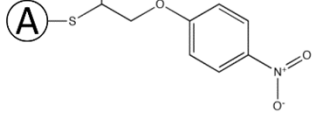
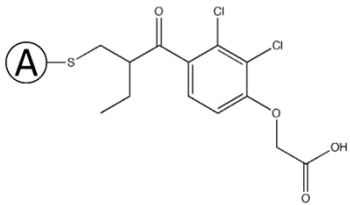
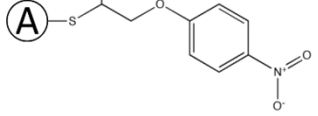
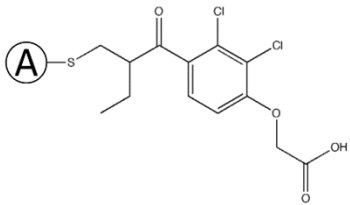
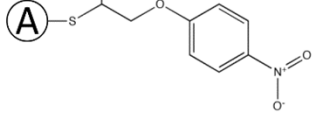
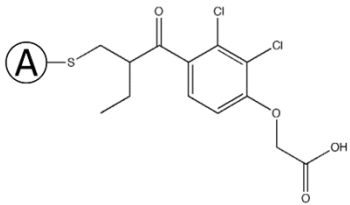
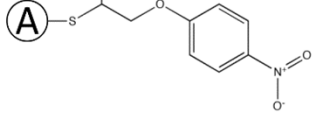
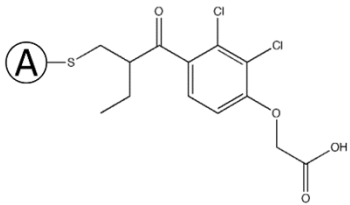
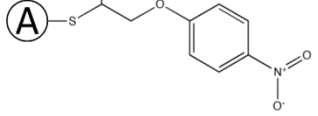
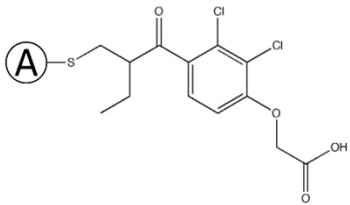
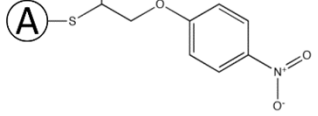
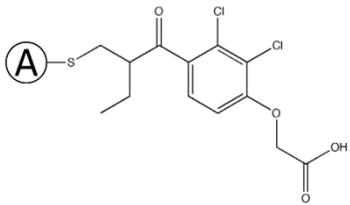
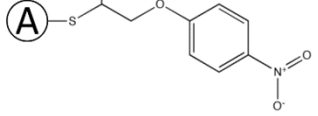
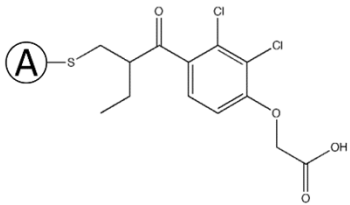
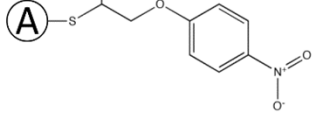
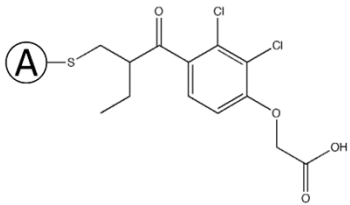
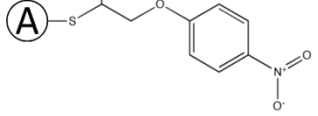
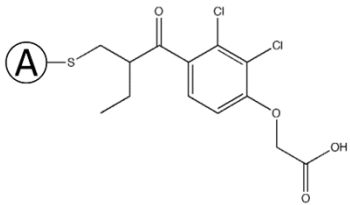
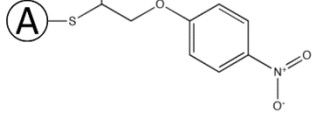
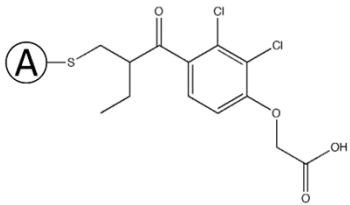
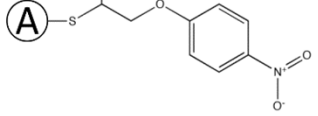
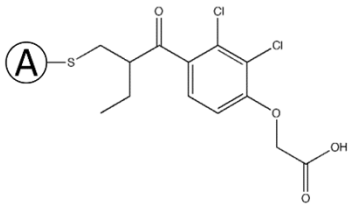
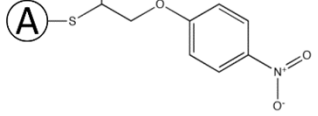
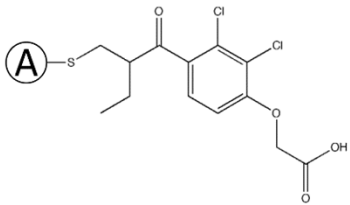
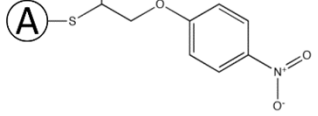
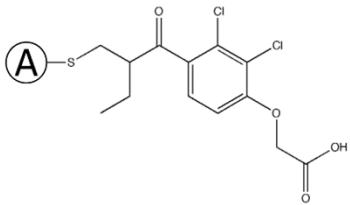
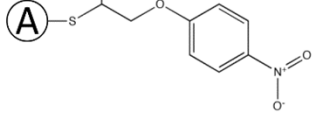
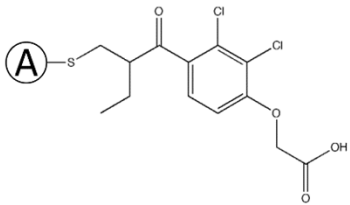
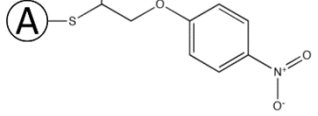
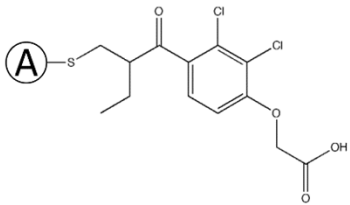
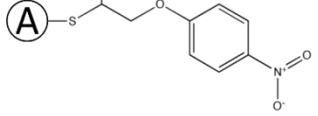
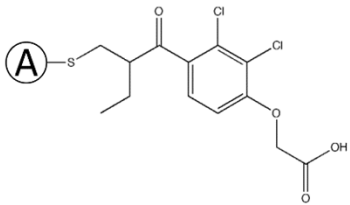
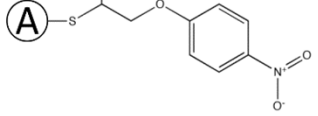
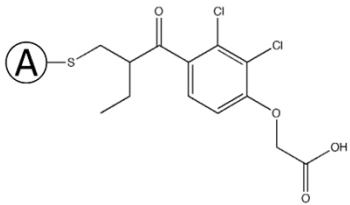
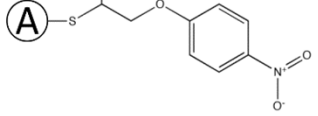
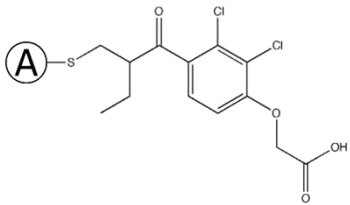
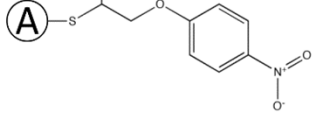
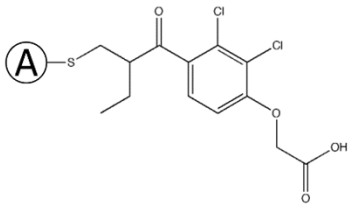
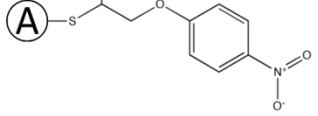
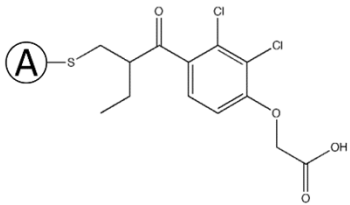
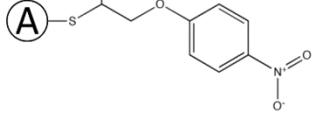
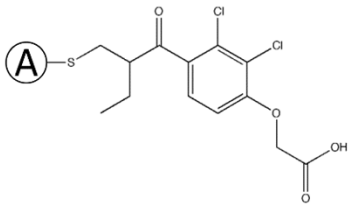
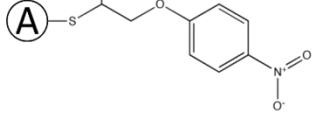
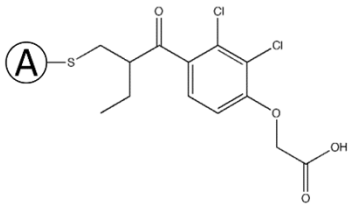
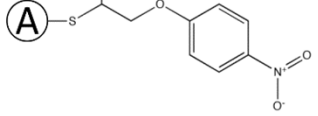
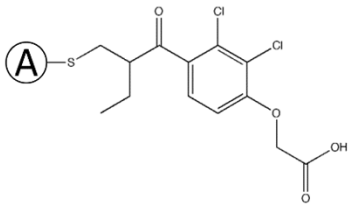
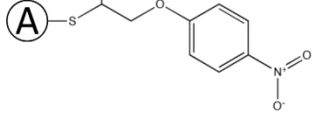
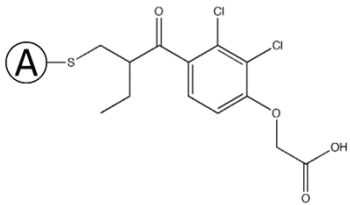
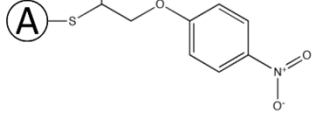
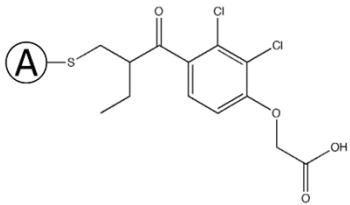
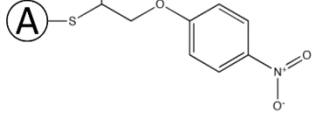
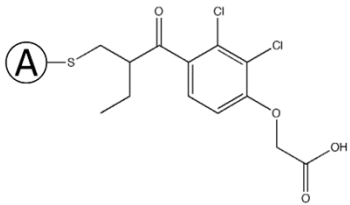
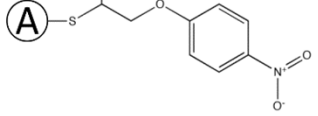
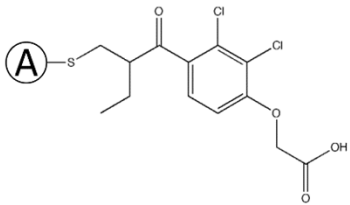
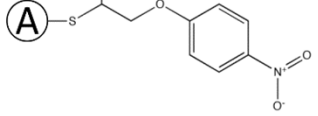
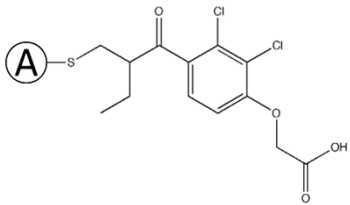
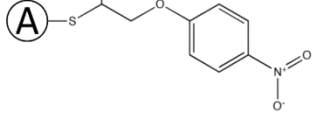
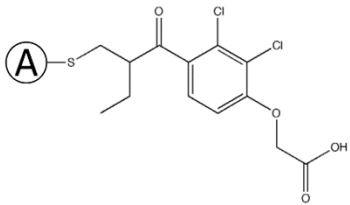
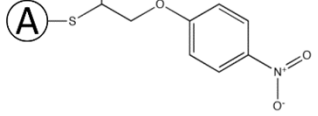
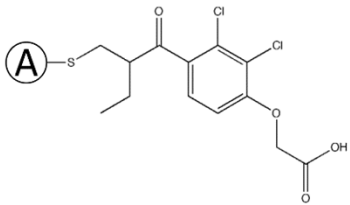
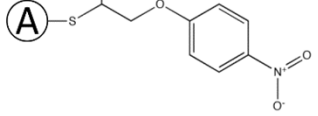
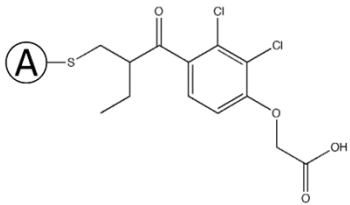
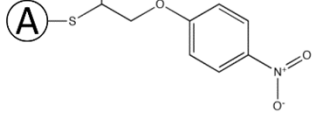
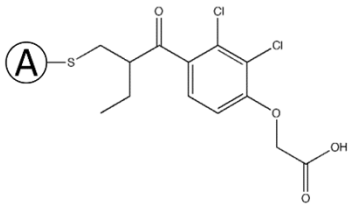
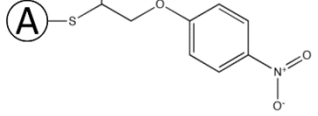
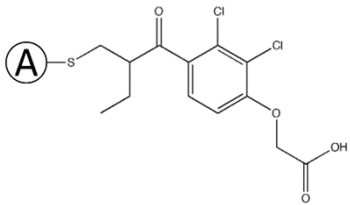
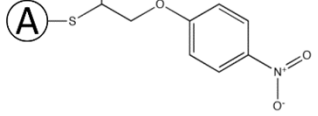
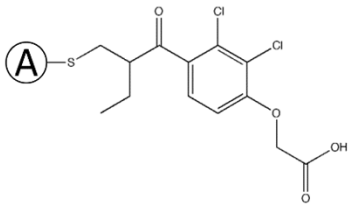
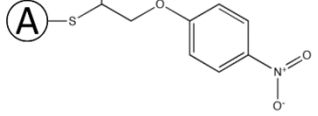
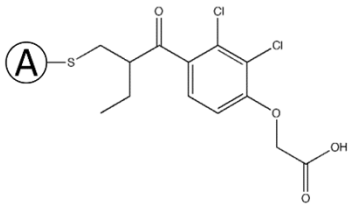
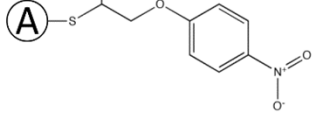
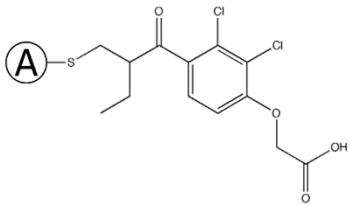
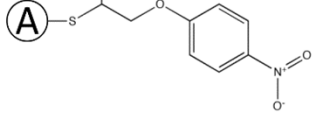
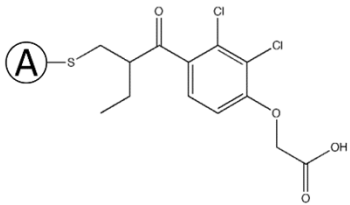
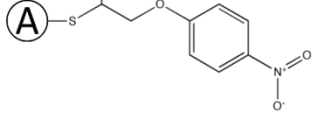
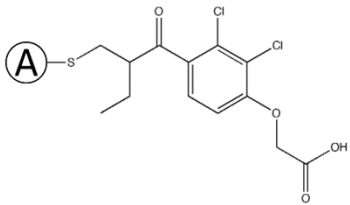
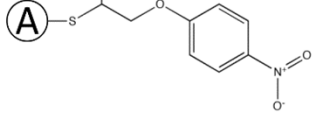
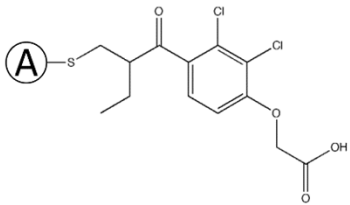
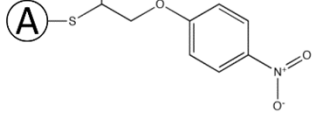
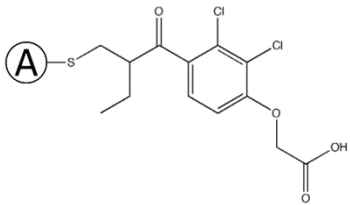
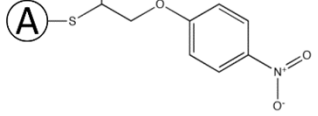
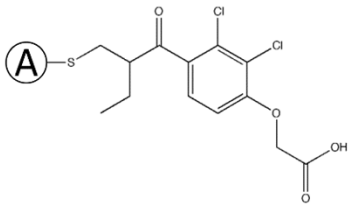
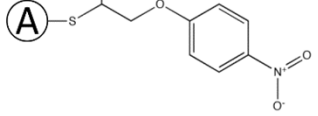
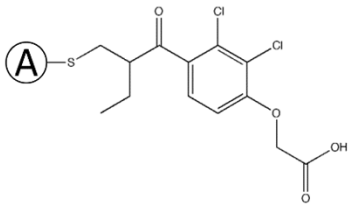
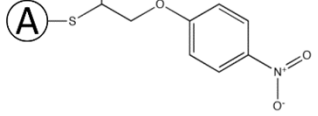
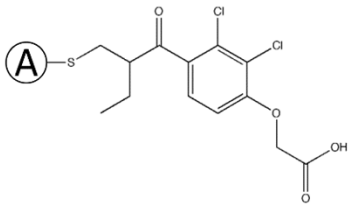
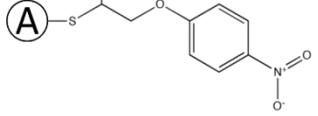
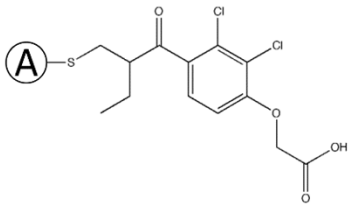
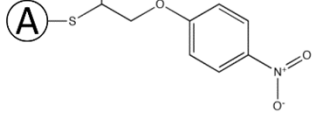
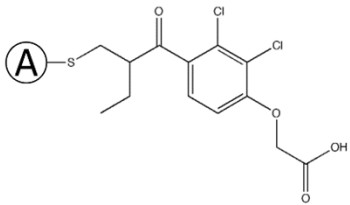
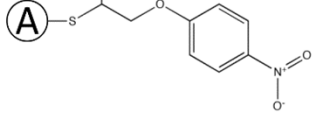
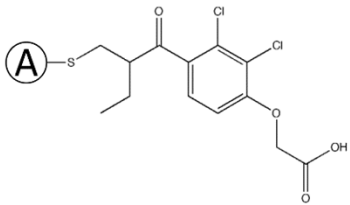
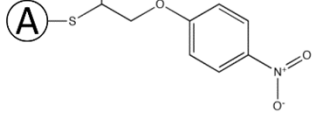
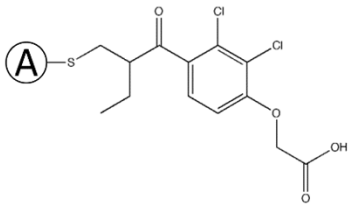
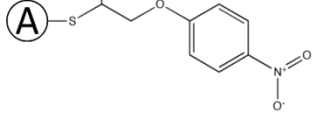
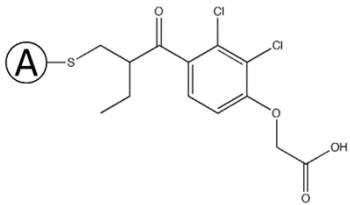
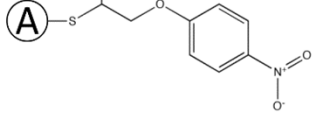
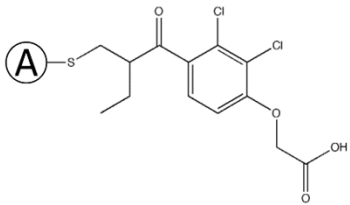
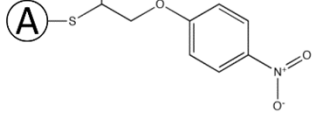
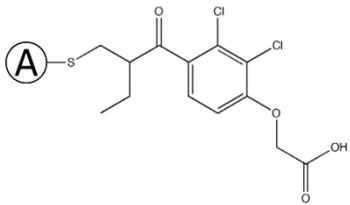
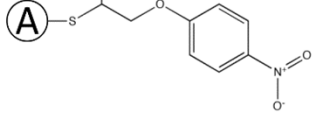
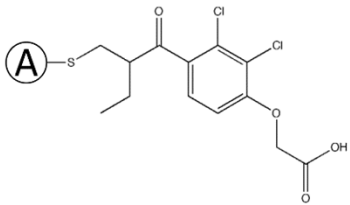
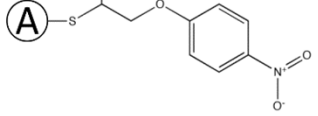
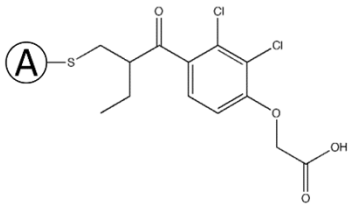
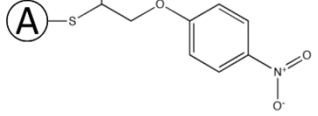
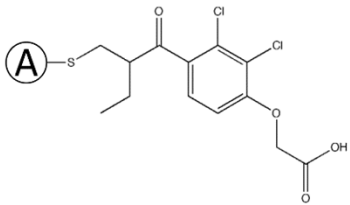
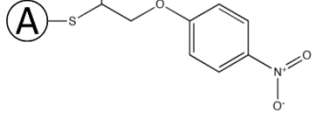
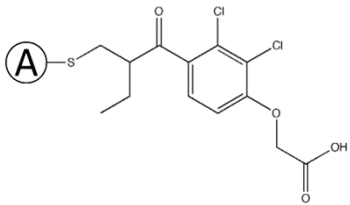
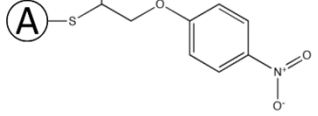
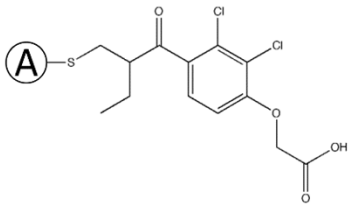
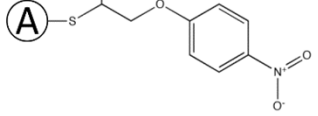
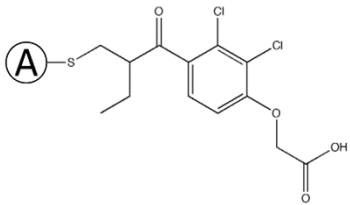
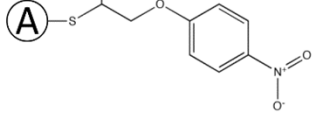
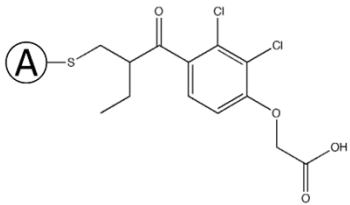
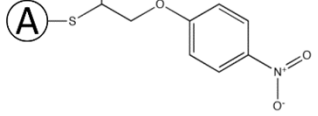
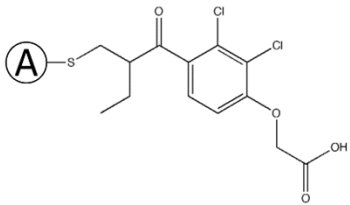
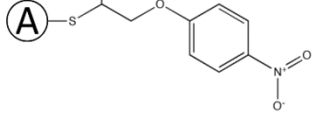
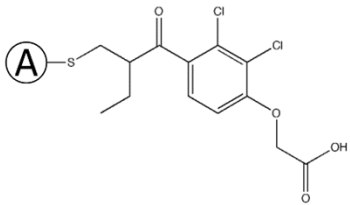
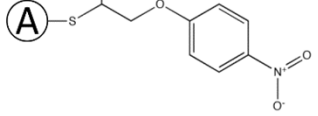
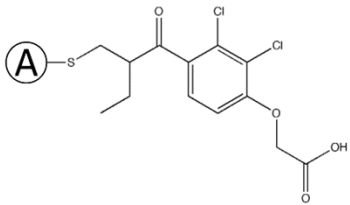
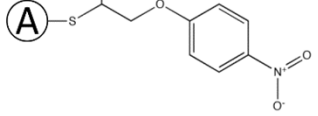
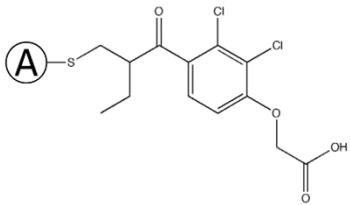
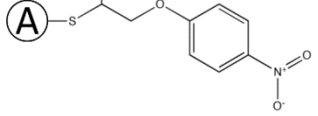
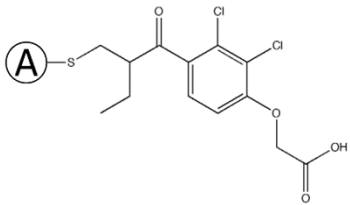
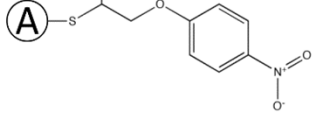
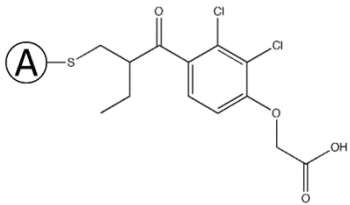
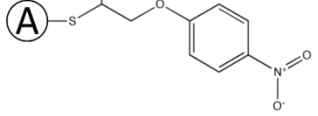
Average  
molecule size  
vs. average  
anchor size

Inset: average  
pairwise RMSD of  
the anchor groups

# LIGAND HOMOMOLOGY MODELING: FINDSITE<sup>LHM</sup>

## Glutathione S-transferase from *E. Coli* complexed with glutathionesulfonic acid (PDB-ID: 1a0f)

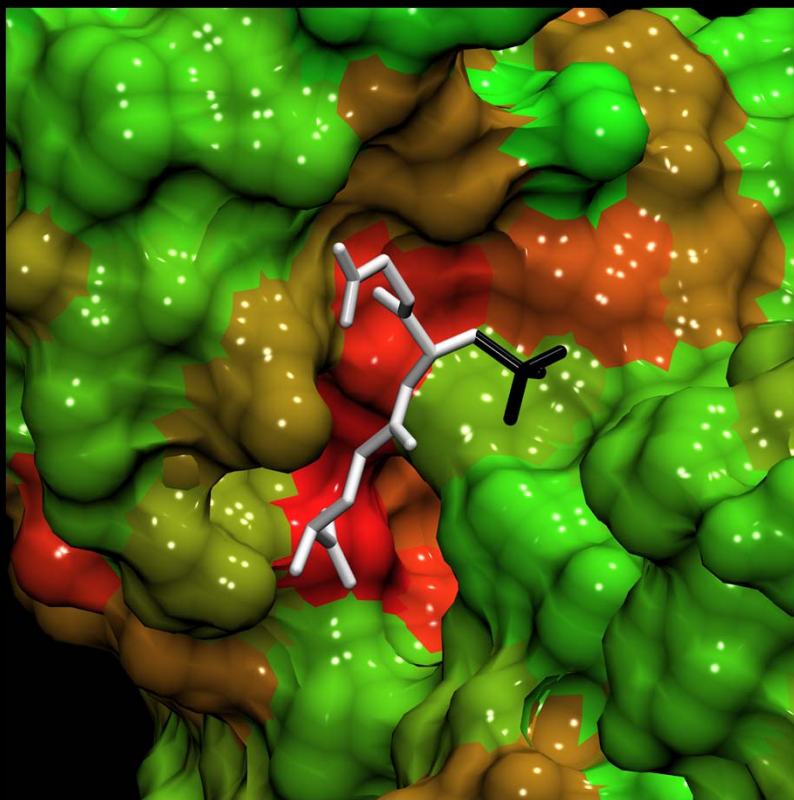
### Variable parts (extracted from remote templates)

Anchor (A)	Variable part (R)	PDB ID	Variable part (R)	PDB ID	Variable part (R)	PDB ID
		2AB6		3LJR		1B4P
		1EV4		18GS		1B48
		1AXD		1BYE		11GS
		17GS		1BX9		11GS
		1ZGN		1C72		11GS
		1PL1				11GS
		1GUH				11GS
		1M9B				11GS
		1U88				11GS
		2C4J				11GS
	1GLQ				11GS	
				1C72		11GS
				1C72		11GS
				1C72		11GS
				1C72		11GS
				1C72		11GS
				1C72		11GS
				1C72		11GS
				1C72		11GS
				1C72		11GS
				1C72		11GS
				1C72		11GS
				1C72		11GS
				1C72		11GS
				1C72		11GS
				1C72		11GS
				1C72		11GS
				1C72		11GS
				1C72		11GS
				1C72		11GS
				1C72		11GS
				1C72		11GS
				1C72		11GS
				1C72		11GS
				1C72		11GS
				1C72		11GS
				1C72		11GS
				1C72		11GS
				1C72		11GS
				1C72		11GS
				1C72		11GS
				1C72		11GS
				1C72		11GS
				1C72		11GS
				1C72		11GS
				1C72		11GS
				1C72		11GS
				1C72		11GS
				1C72		11GS
				1C72		11GS
				1C72		11GS
				1C72		11GS
				1C72		11GS
				1C72		11GS
				1C72		11GS
				1C72		11GS
				1C72		11GS
				1C72		11GS
				1C72		11GS
				1C72		11GS
				1C72		11GS
				1C72		11GS
				1C72		11GS
				1C72		11GS
				1C72		11GS
				1C72		11GS
				1C72		11GS
				1C72		11GS
				1C72		11GS
				1C72		11GS
				1C72		11GS
				1C72		11GS
				1C72		11GS
				1C72		11GS
				1C72		11GS
				1C72		11GS
				1C72		11GS
				1C72		11GS
				1C72		11GS
				1C		

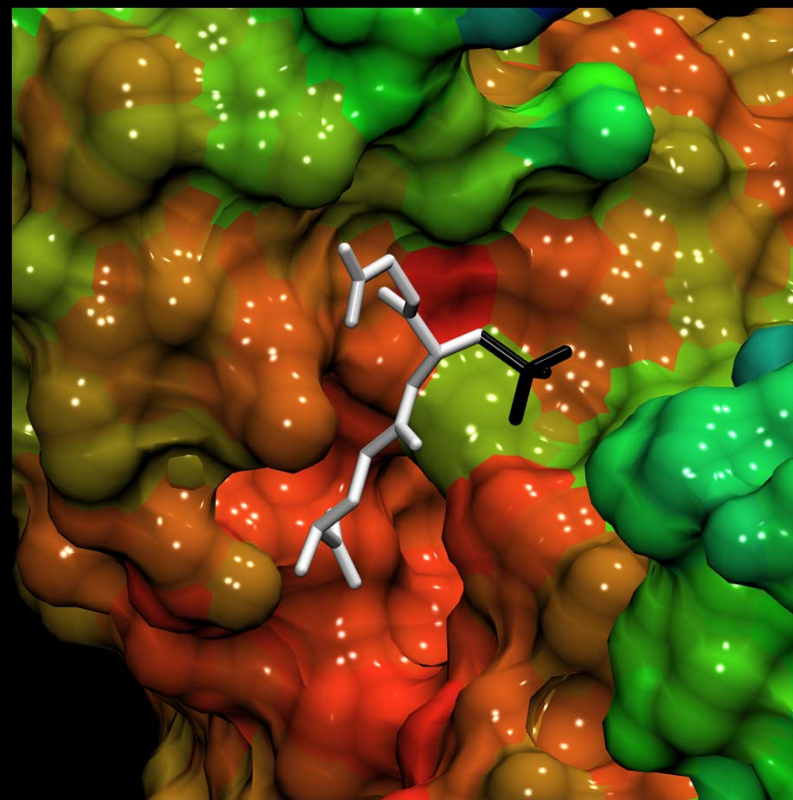
# LIGAND HOMOLOGY MODELING: FINDSITE<sup>LHM</sup>

Glutathione S-transferase from *E. Coli* complexed with glutathionesulfonic acid (PDB-ID: 1a0f)

**Conserved substructure** – white, **Variable region** – black



Sequence entropy  
(red – low, green – high)

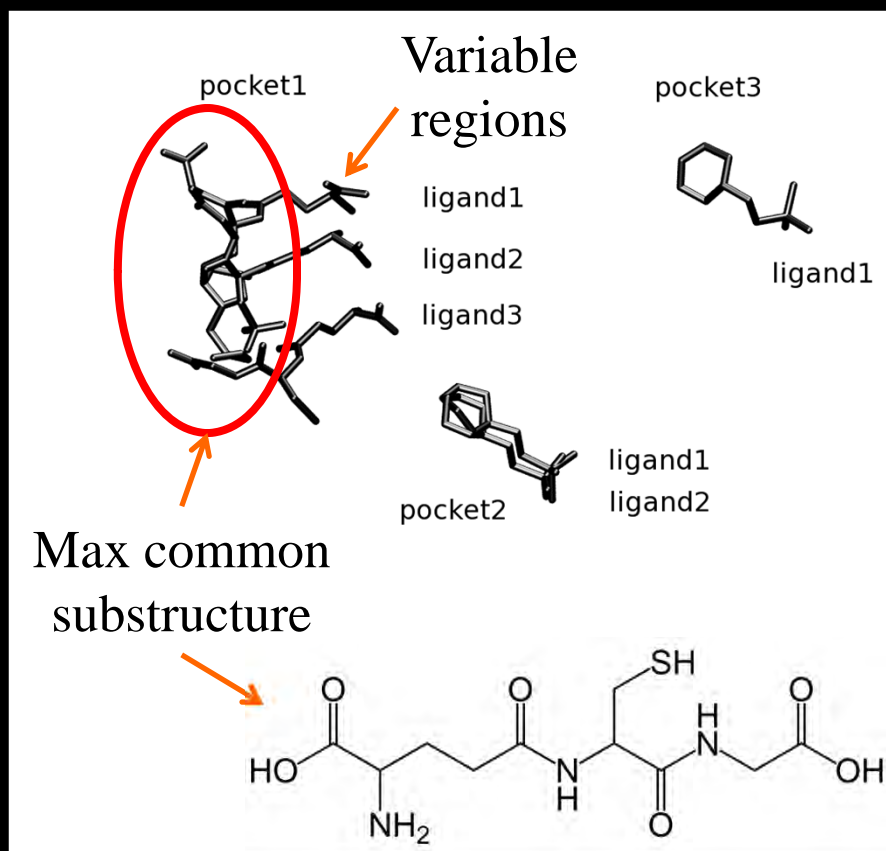
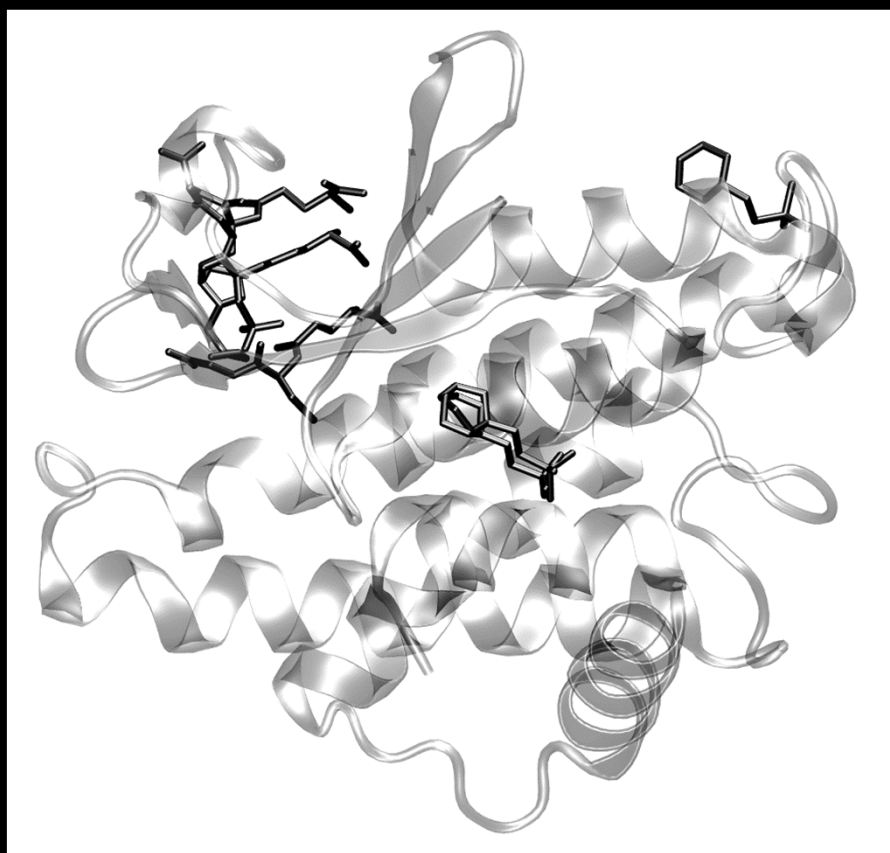


Experimental B-factors  
(red – low, green – high)

# LIGAND HOMOLOGY MODELING: FINDSITE<sup>LHM</sup>

## FINDSITE<sup>LHM</sup>

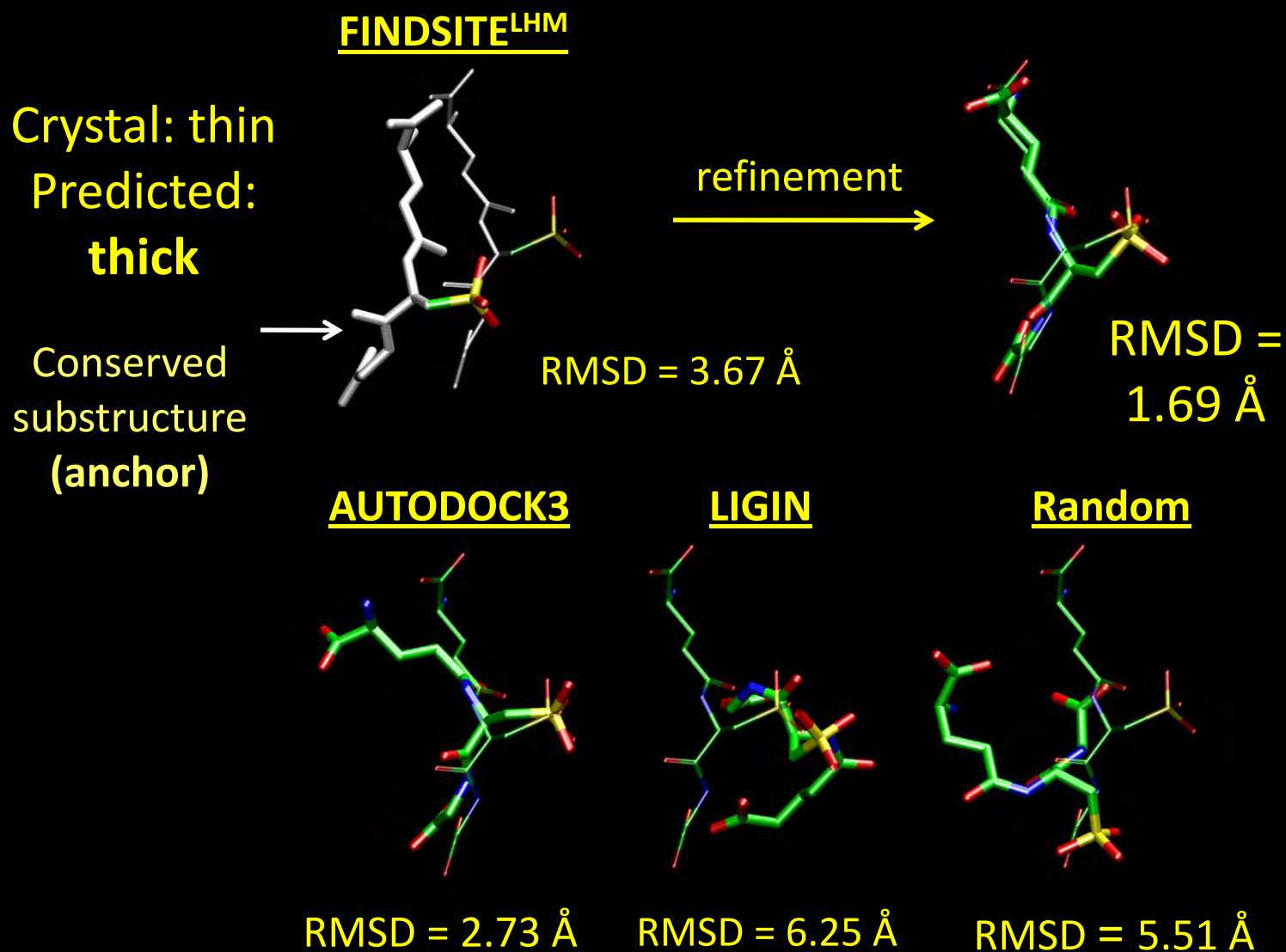
- A fast, similarity-based docking approach
- Uses conserved common ligand substructures



# LIGAND HOMOLOGY MODELING: FINDSITE<sup>LHM</sup>

Glutathione S-transferase from *E. Coli* (PDB-ID: 1a0f)

## Similarity-based docking by FINDSITE<sup>LHM</sup>



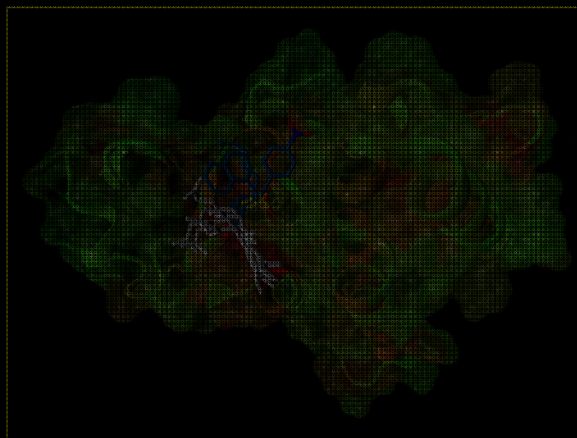
# LIGAND HOMOMOLOGY MODELING: Q-DOCK<sup>LHM</sup>

## FINDSITE



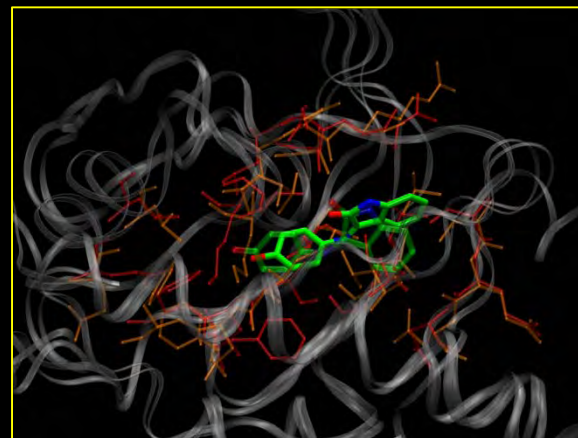
Ligand binding site prediction

## FINDSITE<sup>LHM</sup>



Similarity-based ligand docking

## Q-Dock<sup>LHM</sup>



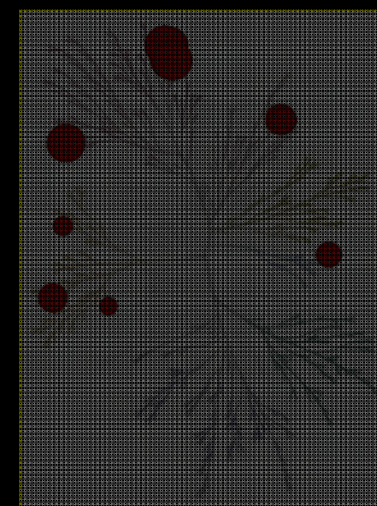
Low-resolution ligand docking/refinement

## KINOME<sup>LHM</sup>

Virtual screening of the human kinome

## X-React<sup>KIN</sup>

*In silico* drug profiling

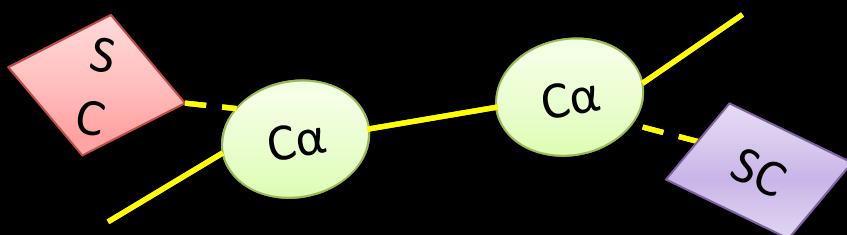


# LIGAND HOMOLOGY MODELING: Q-DOCK<sup>LHM</sup>

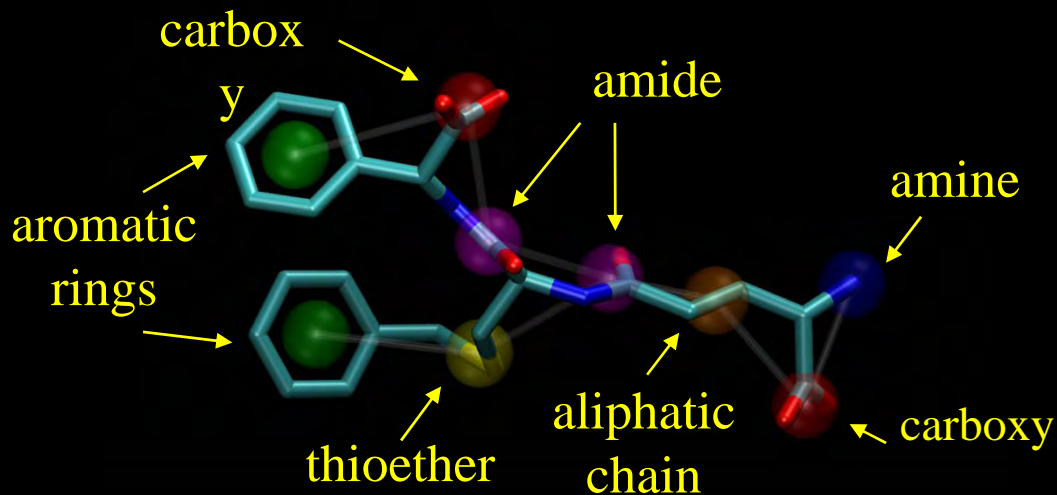
## Q-Dock<sup>LHM</sup>:

### Low-resolution modeling

**RECEPTOR**: C $\alpha$  and side chain centers of mass



**LIGANDS**: quasichemical building blocks (functional groups)



<i>Description</i>	<i>Symbol/formula</i>
Aromatic rings	mono-, heterocyclic
Ether	-C-O-C-
Thioether	-C-S-C-
Carbonyl	>C=O
Thiocarbonyl	>C=S
Halogene	-Cl; -Br; -F; -I
Guanidine	-NHC(NH <sub>2</sub> )NH
Amide	-CONH-
Carboxyl	-COOH
Amine (1°,2°,3°)	-NH <sub>2</sub> ; >NH; >N-
Phosphate	-PO <sub>4</sub>
Sulphate	-SO <sub>4</sub>
Nitro group	-NO <sub>2</sub>
Metals	Fe; Zn; Mg; Ca
Hydroxyl group	-OH
Thiol group	-SH
Aliphatic chain	-(C-C) <sub>x</sub> -

# LIGAND HOMOLOGY MODELING: Q-DOCK<sup>LHM</sup>

## Q-Dock<sup>LHM</sup>

➤ Combined knowledge-based potentials:

Docking  
accuracy

• Generic energy terms (derived from PDB)

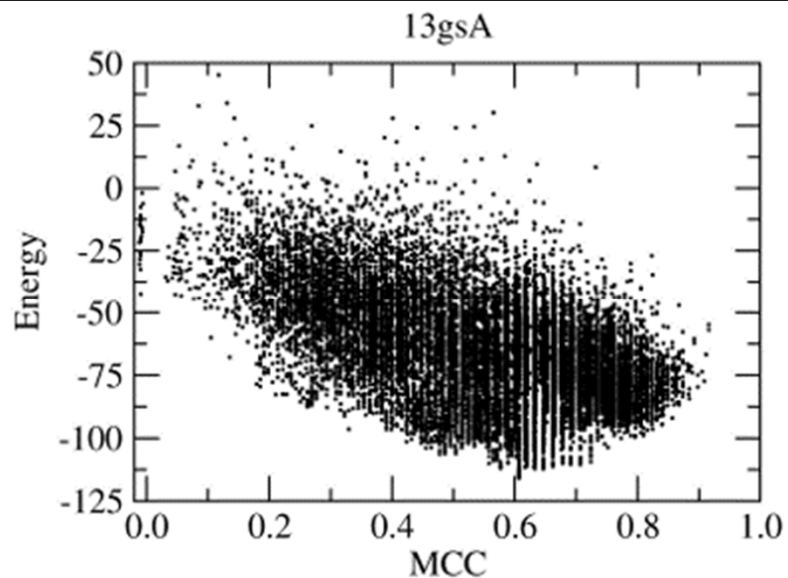
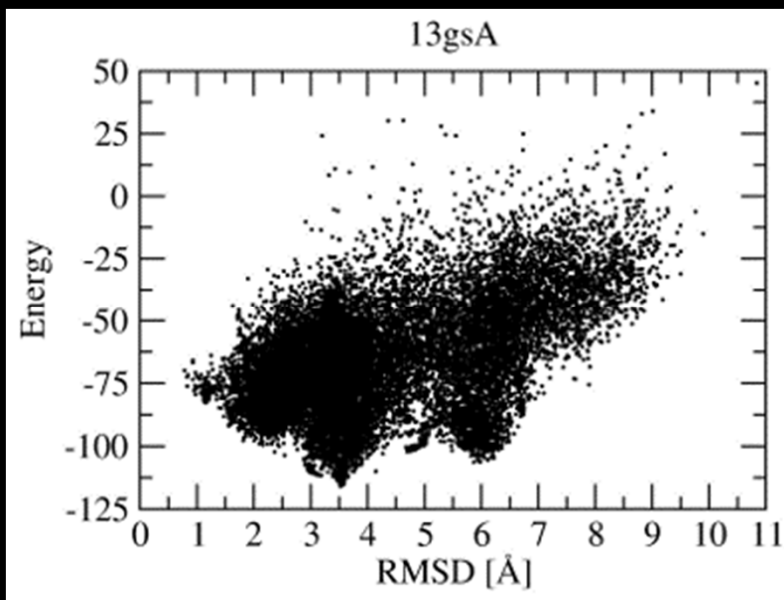
• Harmonic restraints on conserved ligand groups

• Pocket specific contact potential

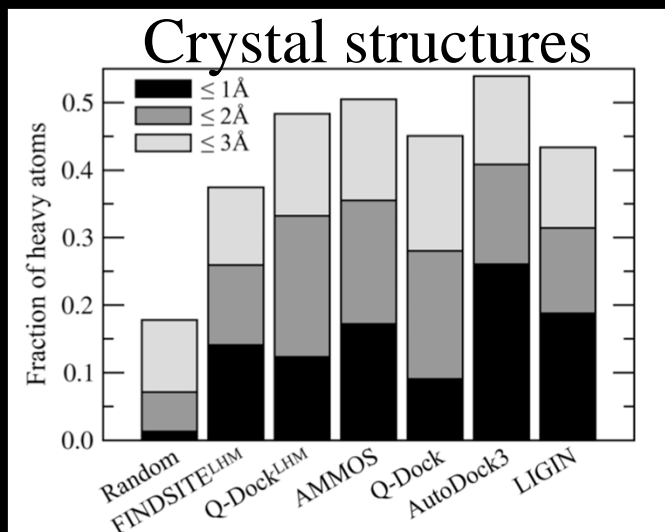
• Optimized weight factors

Ligand ranking

➤ Replica Exchange Monte Carlo sampling



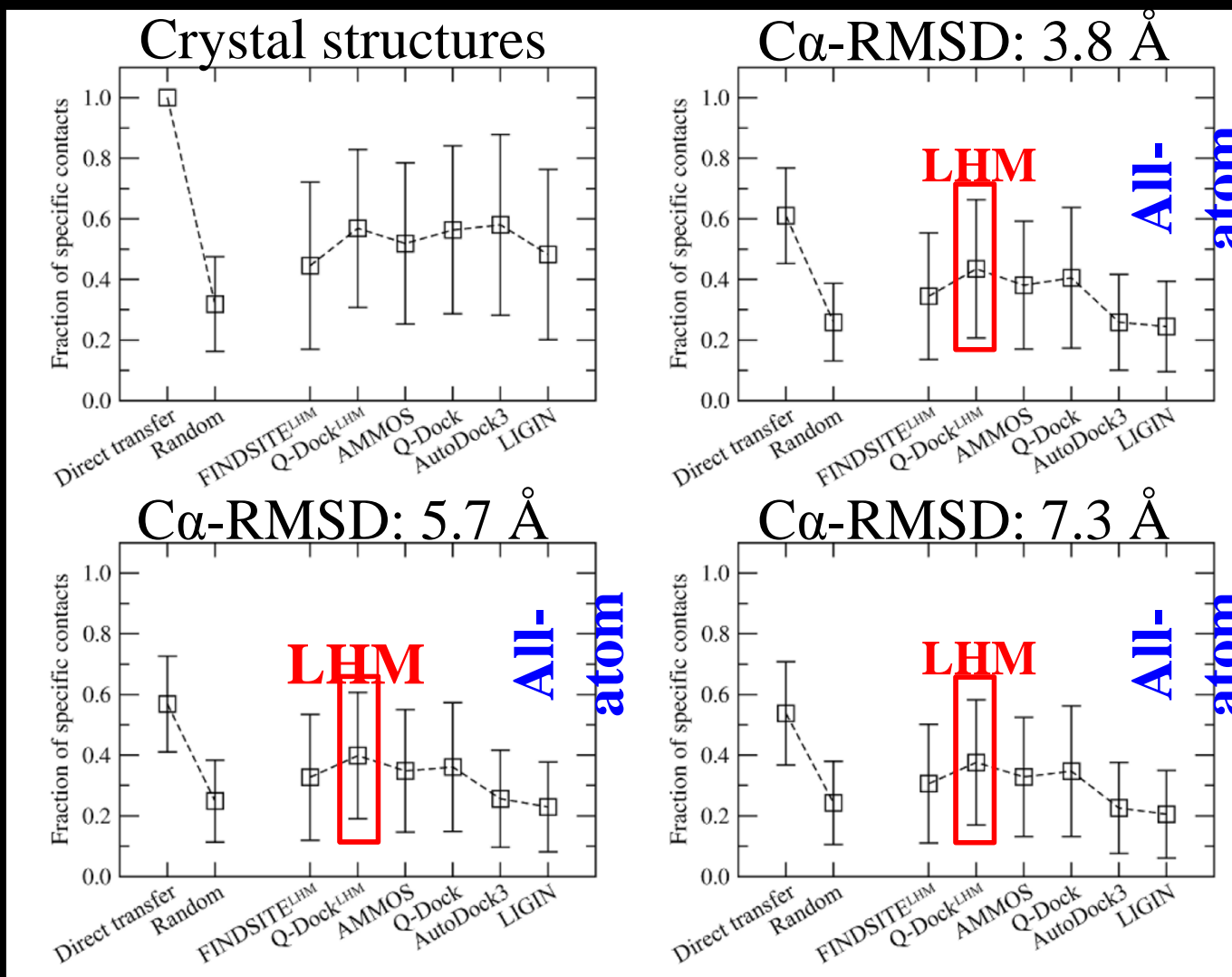
## 204 pharmacologically relevant targets from CCDC/Astex dataset



Average fraction of ligand heavy atoms predicted within 1, 2 and 3 Å

# LIGAND HOMOLOGY MODELING: Q-DOCK<sup>LHM</sup>

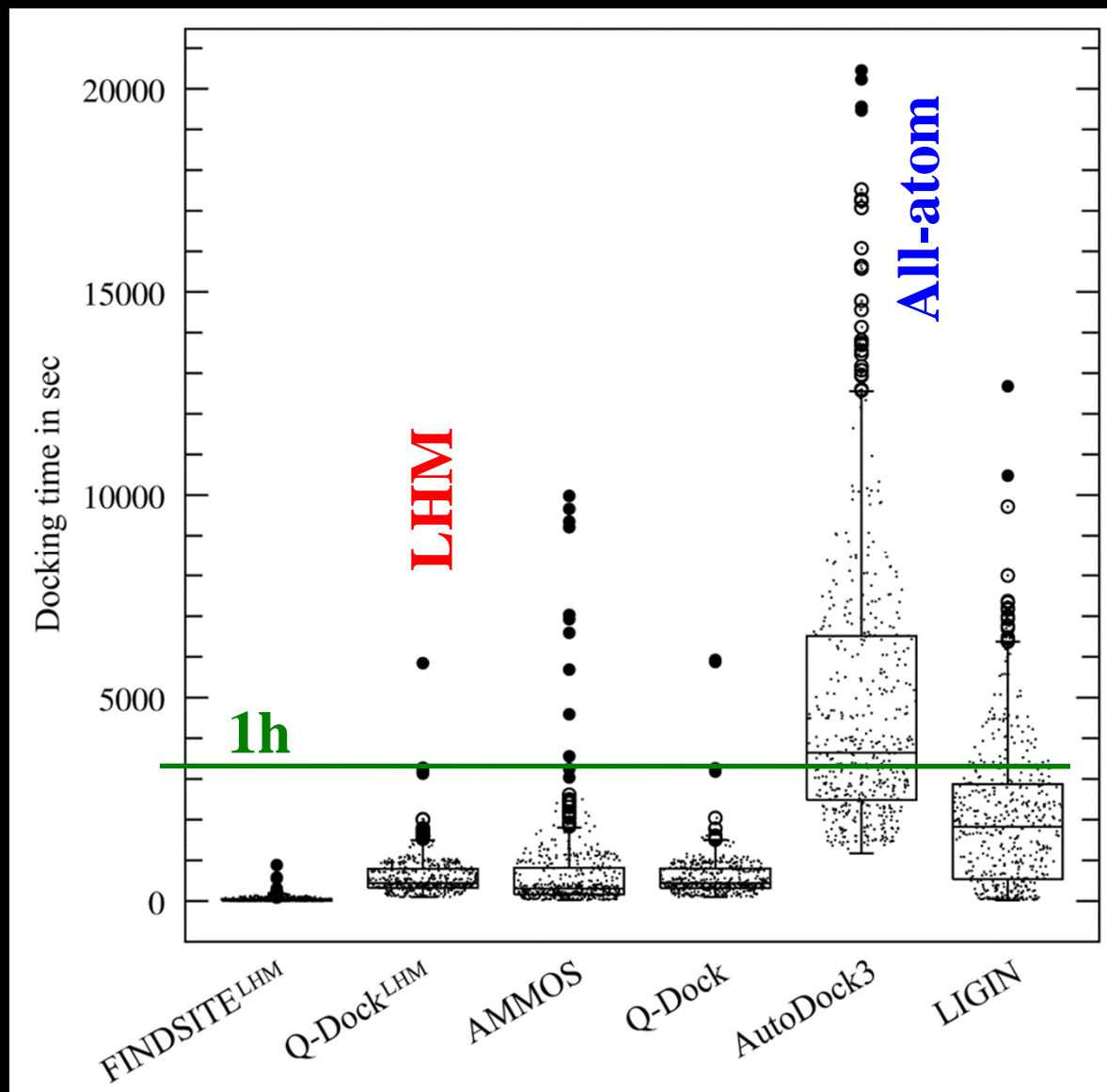
204 pharmacologically relevant targets from CCDC/Astex dataset



Average fraction of correctly predicted specific protein-ligand contacts

# LIGAND HOMOLOGY MODELING: Q-DOCK<sup>LHM</sup>

## Docking times on 2.0 GHz AMD Opteron processor

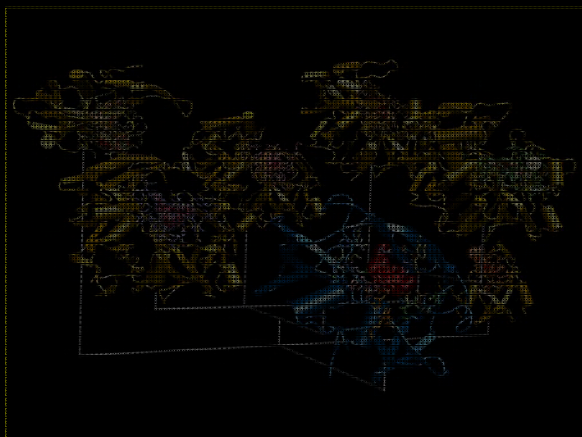


LHM is more accurate and much faster

*For AMMOS, AutoDock3 and LIGIN, the default sets of parameters were used and the docking protocols have not been optimized with respect to the accuracy and simulation time.*

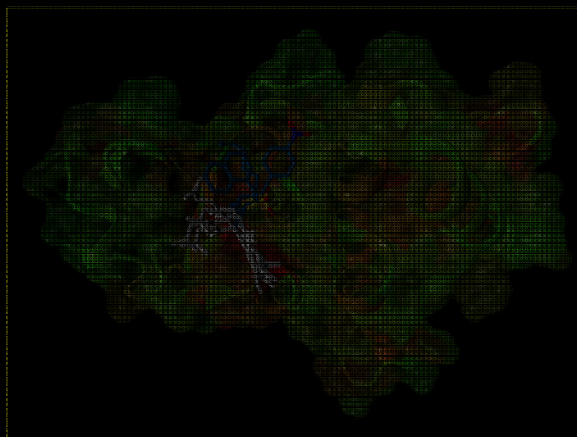
# LIGAND HOMOLOGY MODELING: KINOME<sup>LHM</sup>

FINDSITE



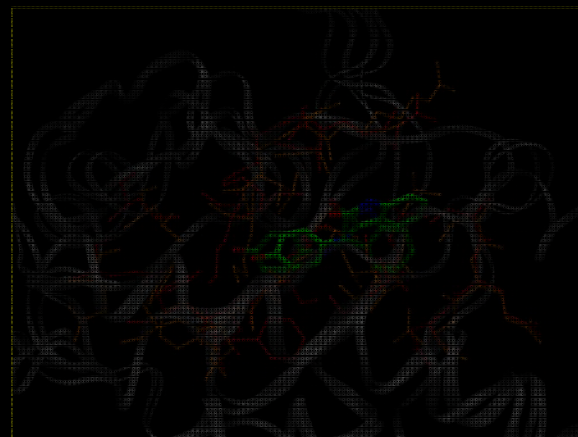
Ligand binding site prediction

FINDSITE<sup>LHM</sup>



Similarity-based ligand docking

Q-Dock<sup>LHM</sup>



Low-resolution ligand docking/refinement

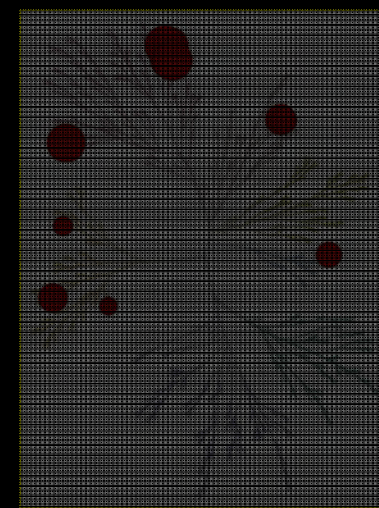


KINOME<sup>LHM</sup>

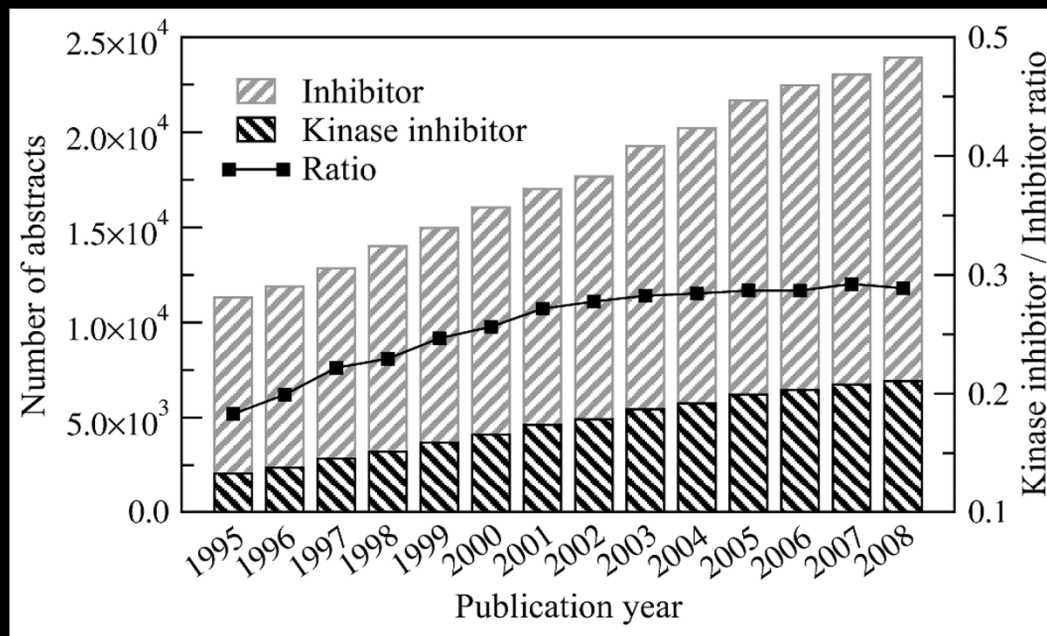
Virtual screening of the human kinome

X-React<sup>KIN</sup>

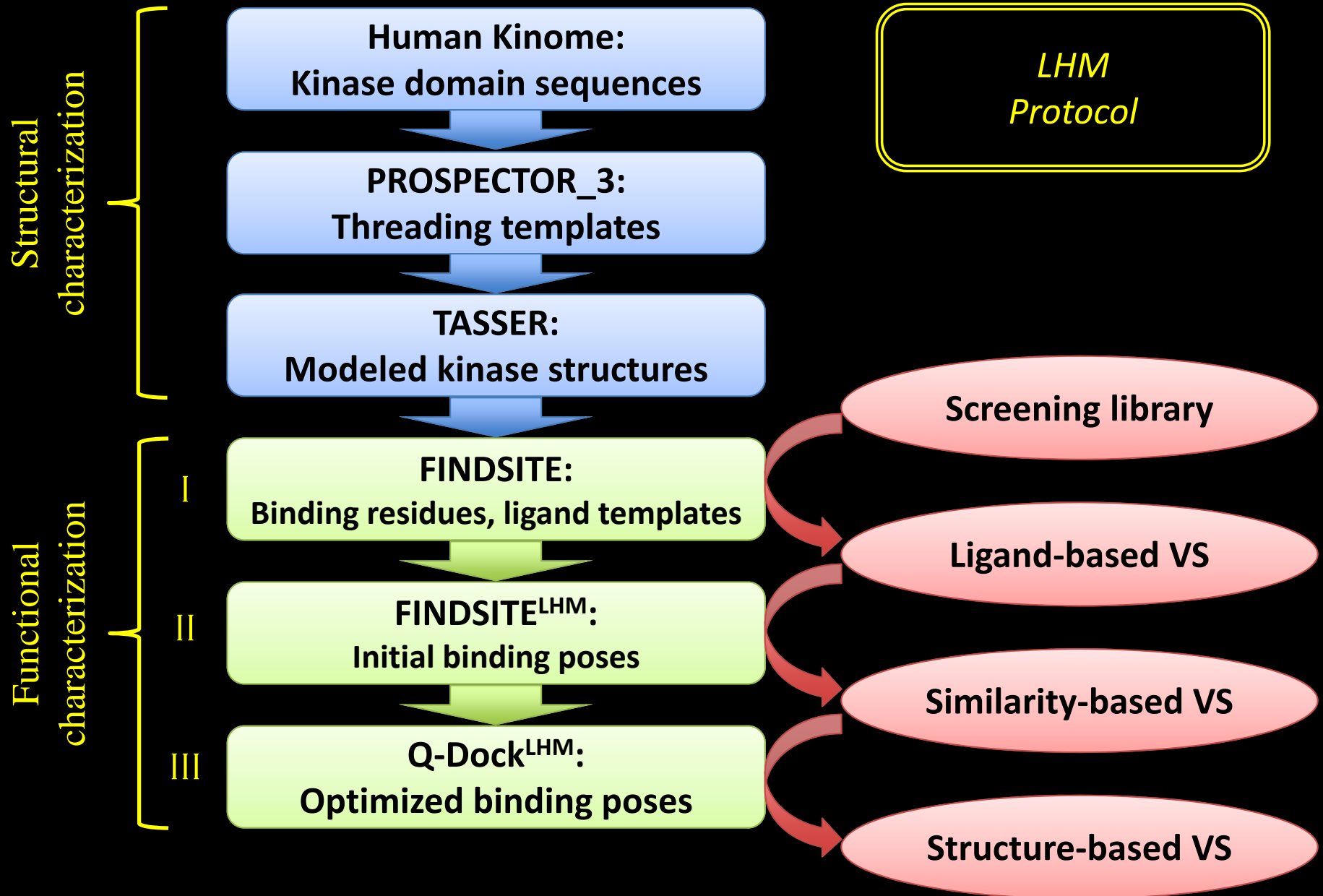
*In silico* drug profiling



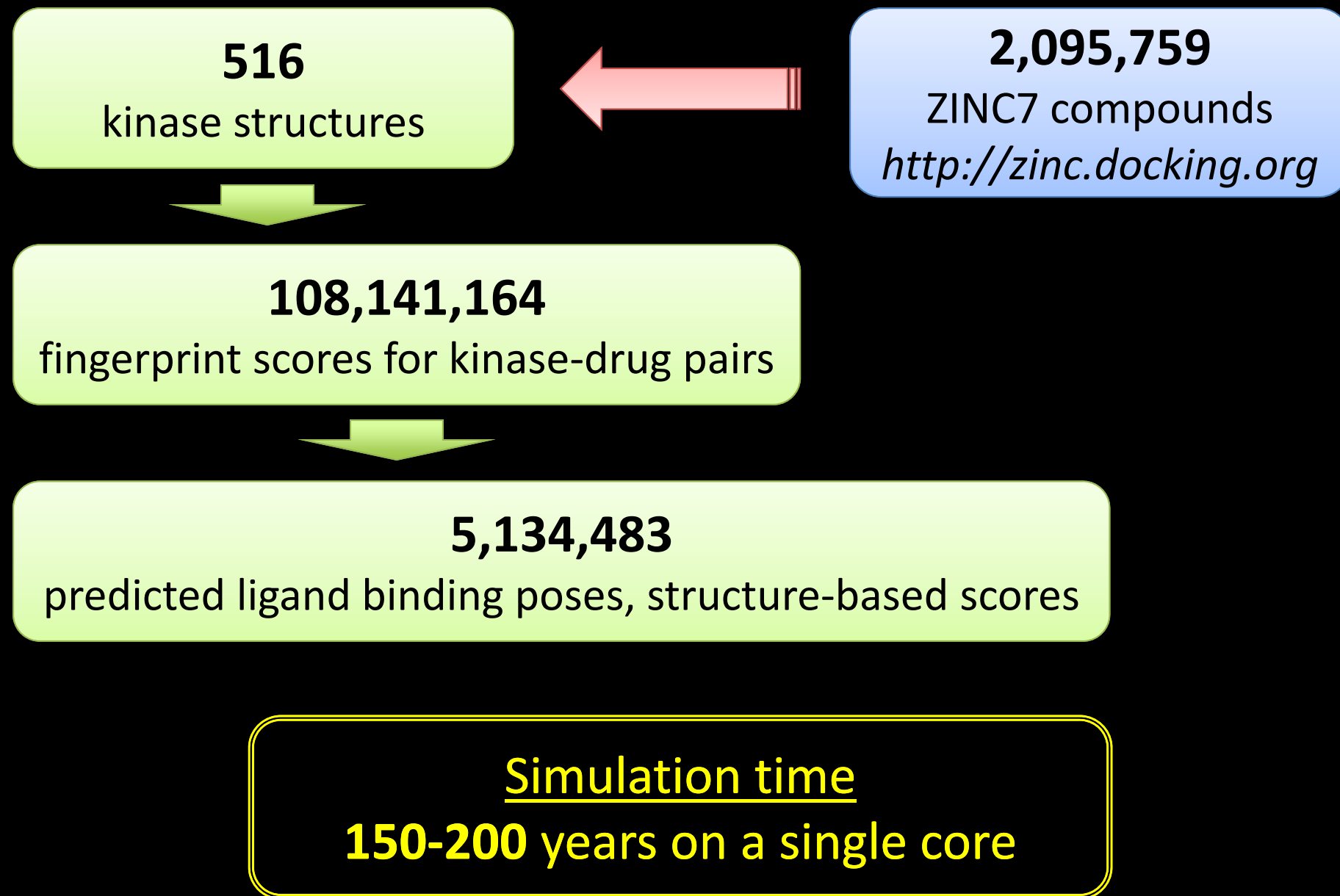
# Availability of high-resolution crystal structures for the human kinome



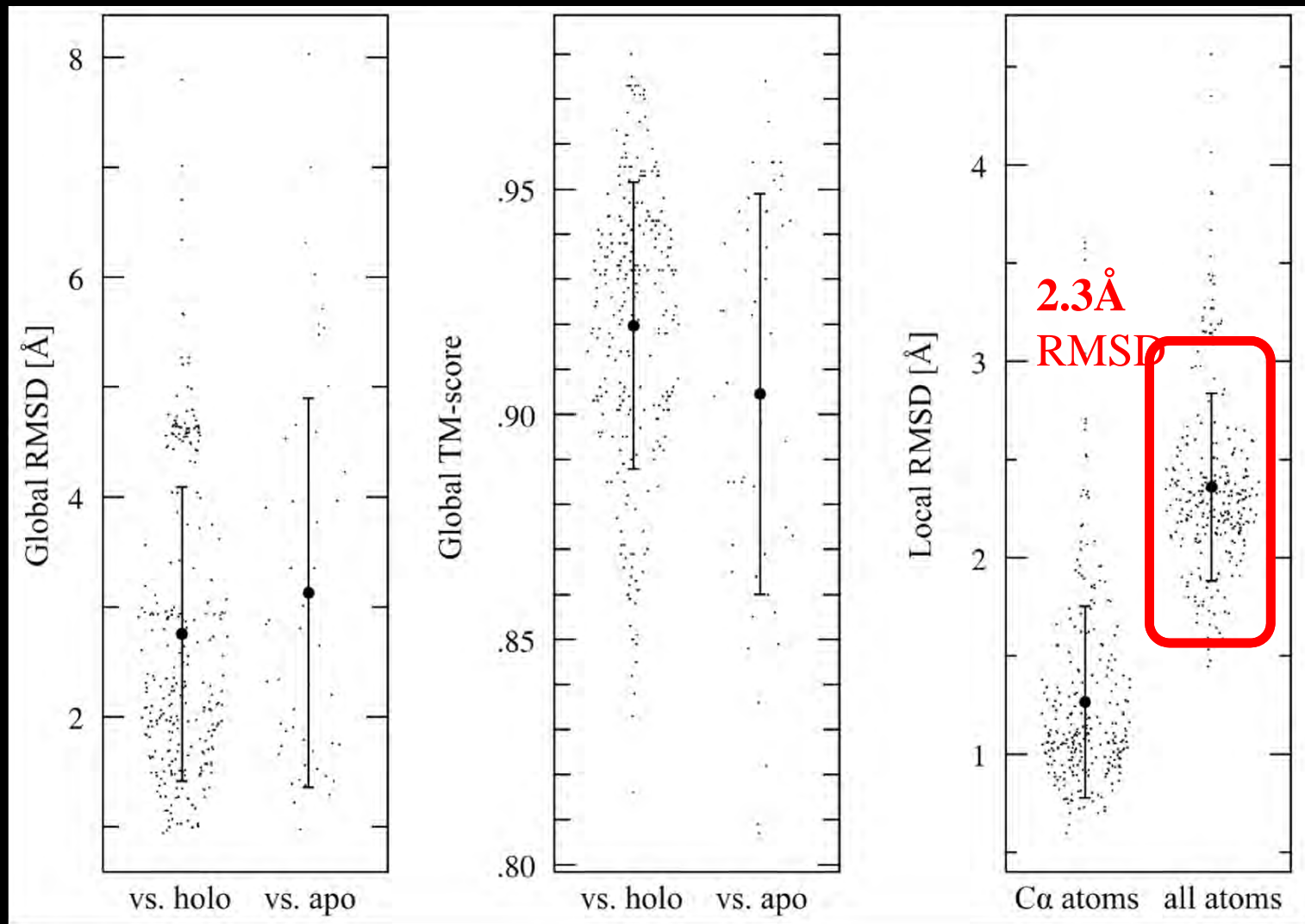
# LIGAND HOMOLGY MODELING: KINOME<sup>LHM</sup>



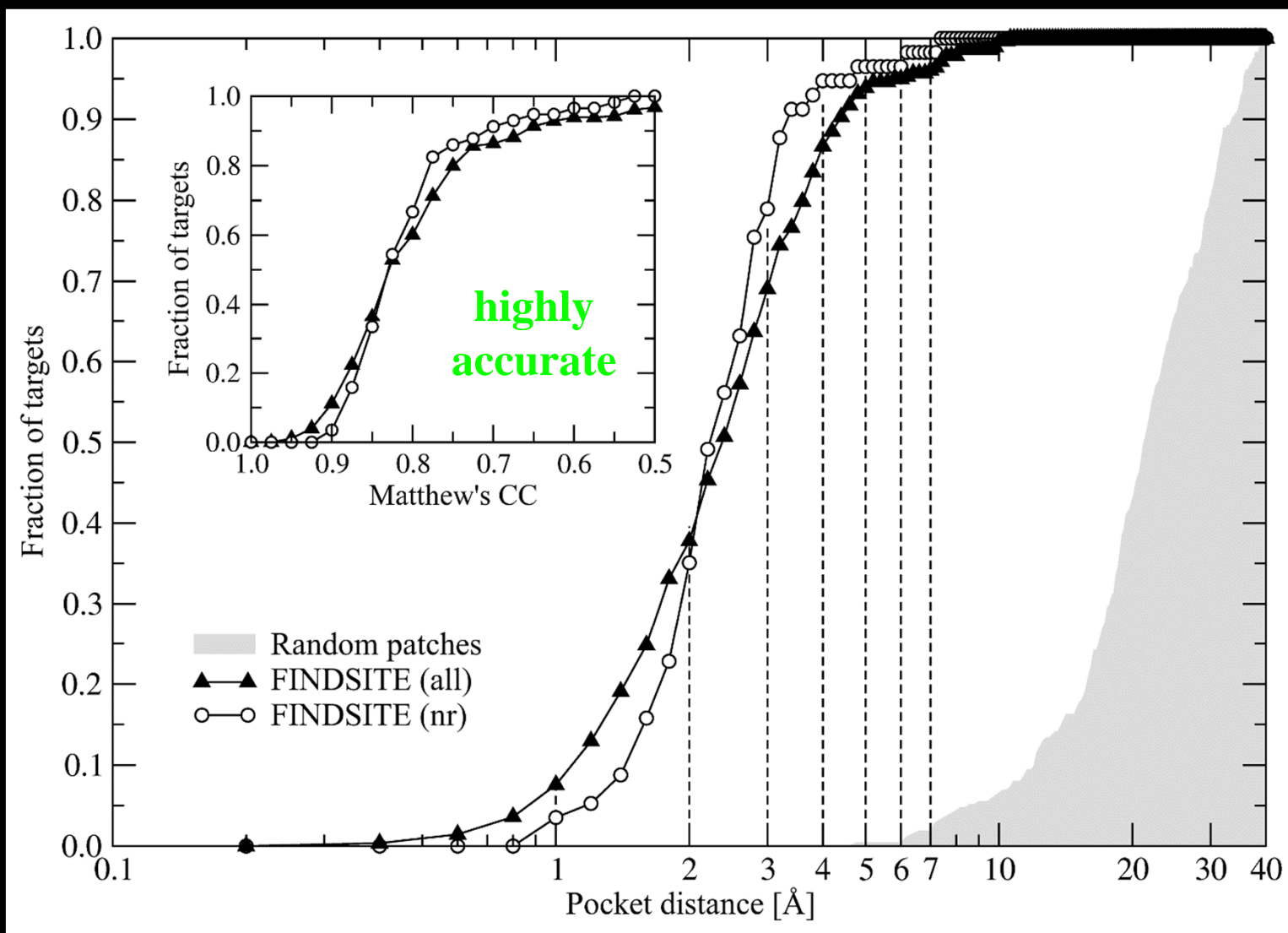
# LIGAND HOMOMOLOGY MODELING: KINOME<sup>LHM</sup>



## Structure modeling of kinase domains

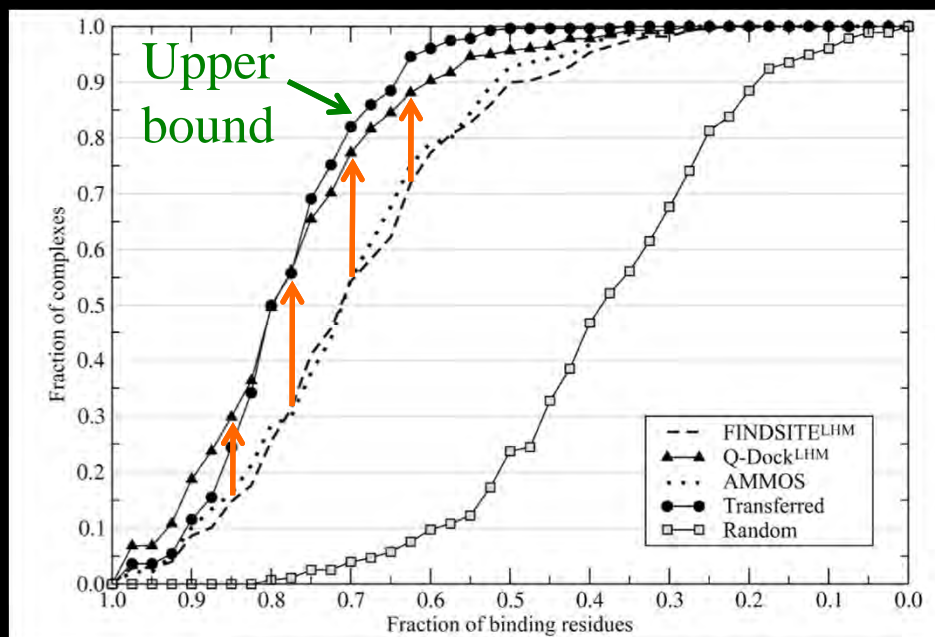


## Binding site/residue prediction



## Docking accuracy for kinase inhibitors

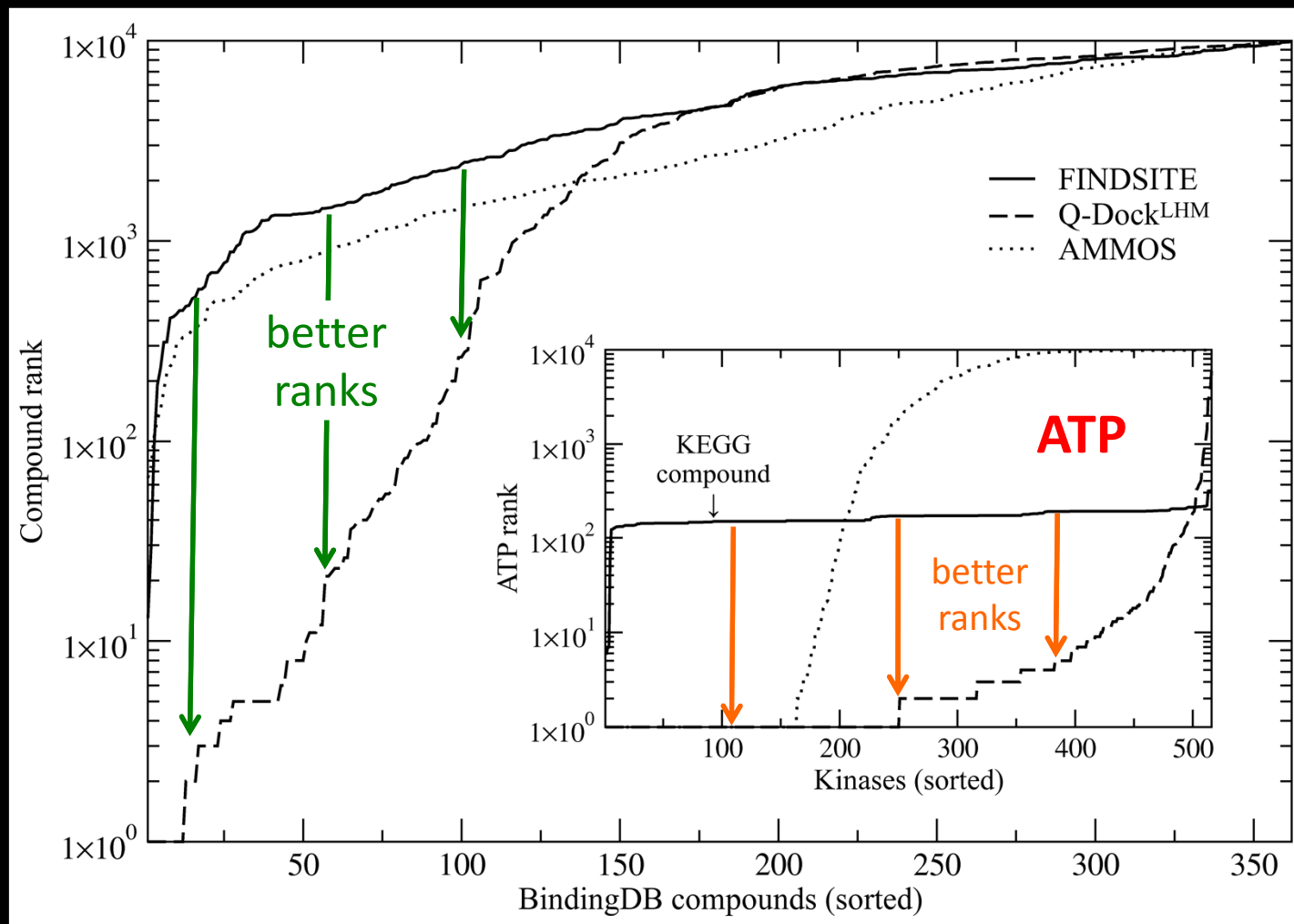
*Non-specific contacts*



↑ Low-resolution refinement by Q-Dock<sup>LHM</sup> ↑  
 improves binding poses over FINDSITE<sup>LHM</sup> ↑

# LIGAND HOMOLOGY MODELING: KINOME<sup>LHM</sup>

Virtual screening benchmarks using **362** kinase inhibitors from BindingDB (<http://www.bindingdb.org>)

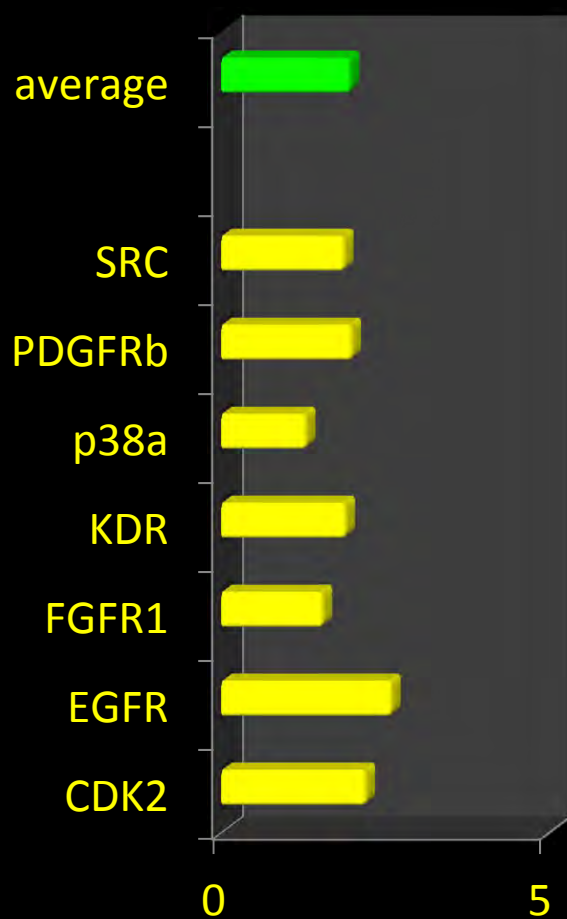


# Virtual screening against 7 protein kinases from DUD

DUD: Huang *et al.* (2006) *J Med Chem* **49**, 6789-6801

## DOCK6

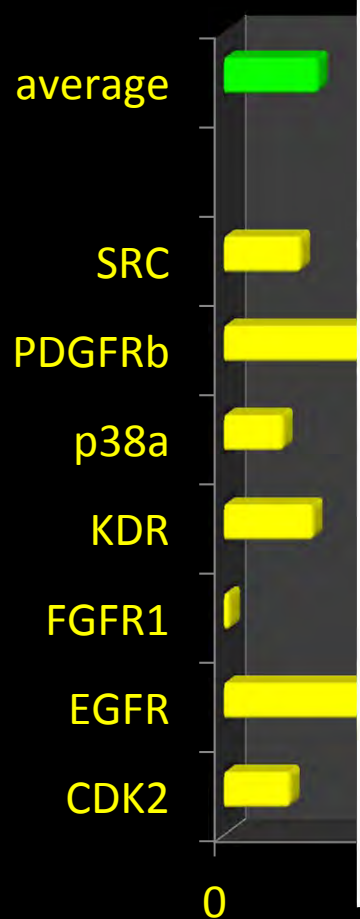
*Crystal structures*



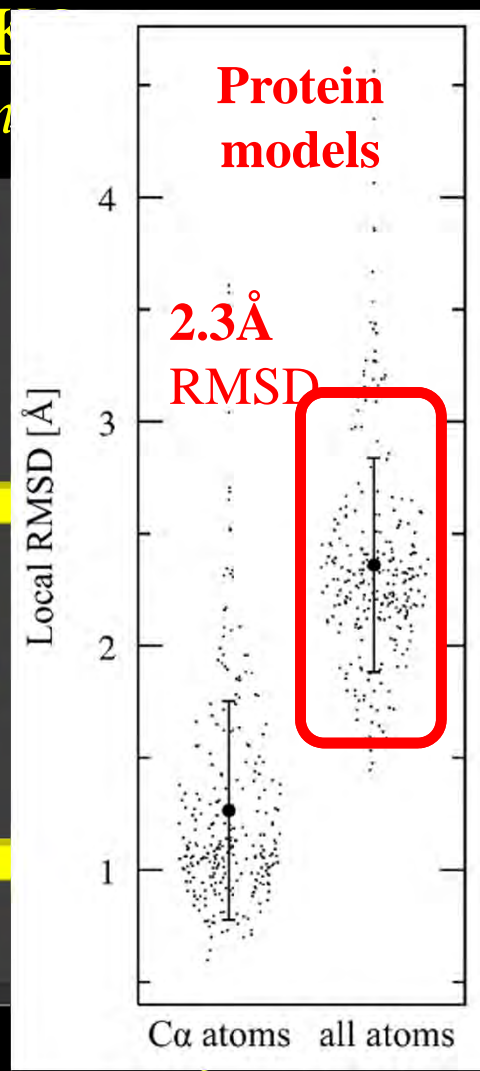
*EF-10*

## DOCK6

*Protein models*



*EF-10*



## LHM

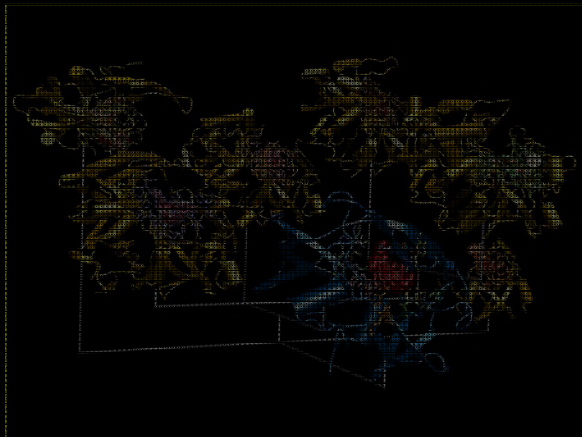
*Protein models*



*EF-10*

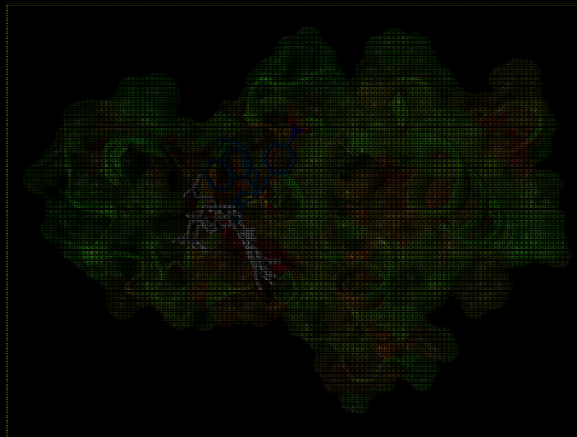
# LIGAND HOMOMOLOGY MODELING: X-REACT<sup>KIN</sup>

## FINDSITE



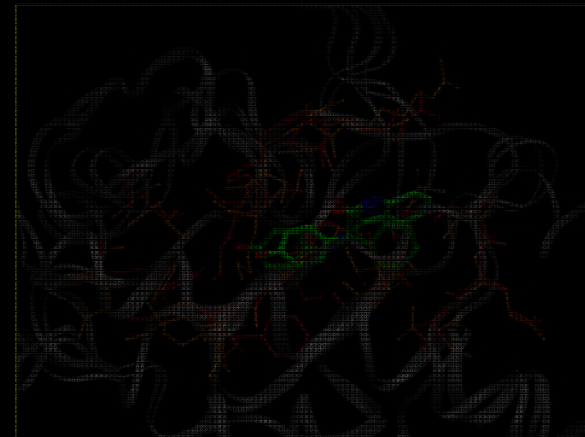
Ligand binding site  
prediction

## FINDSITE<sup>LHM</sup>



Similarity-based  
ligand docking

## Q-Dock<sup>LHM</sup>



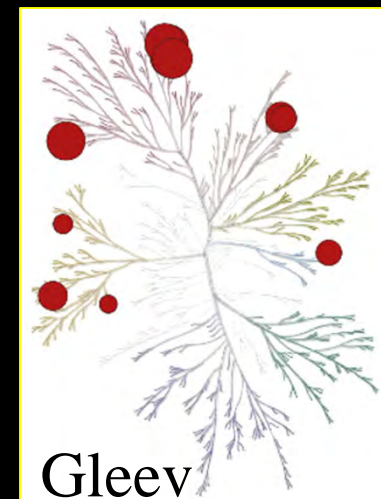
Low-resolution ligand  
docking/refinement

## KINOME<sup>LHM</sup>

Virtual screening  
of the human  
kinome

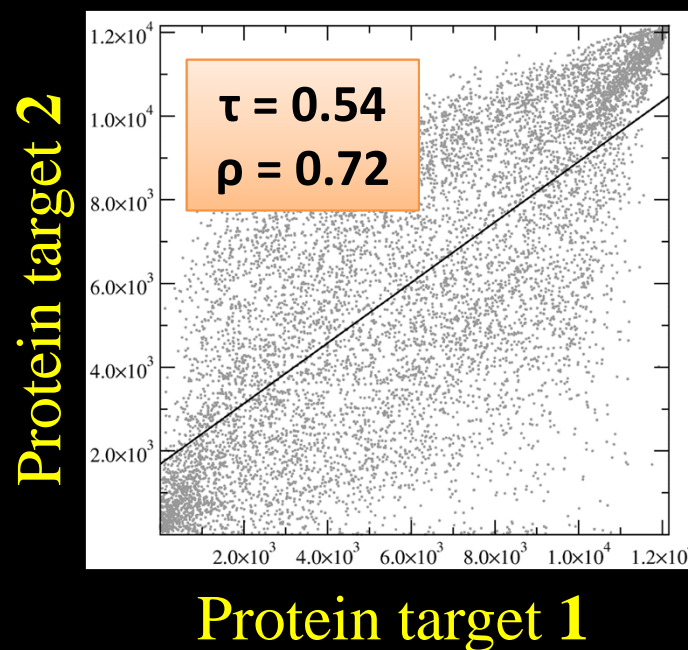
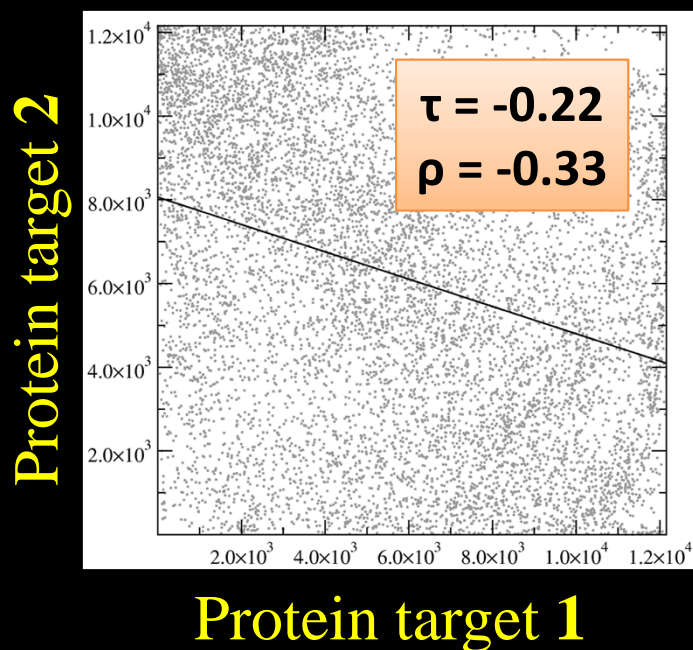
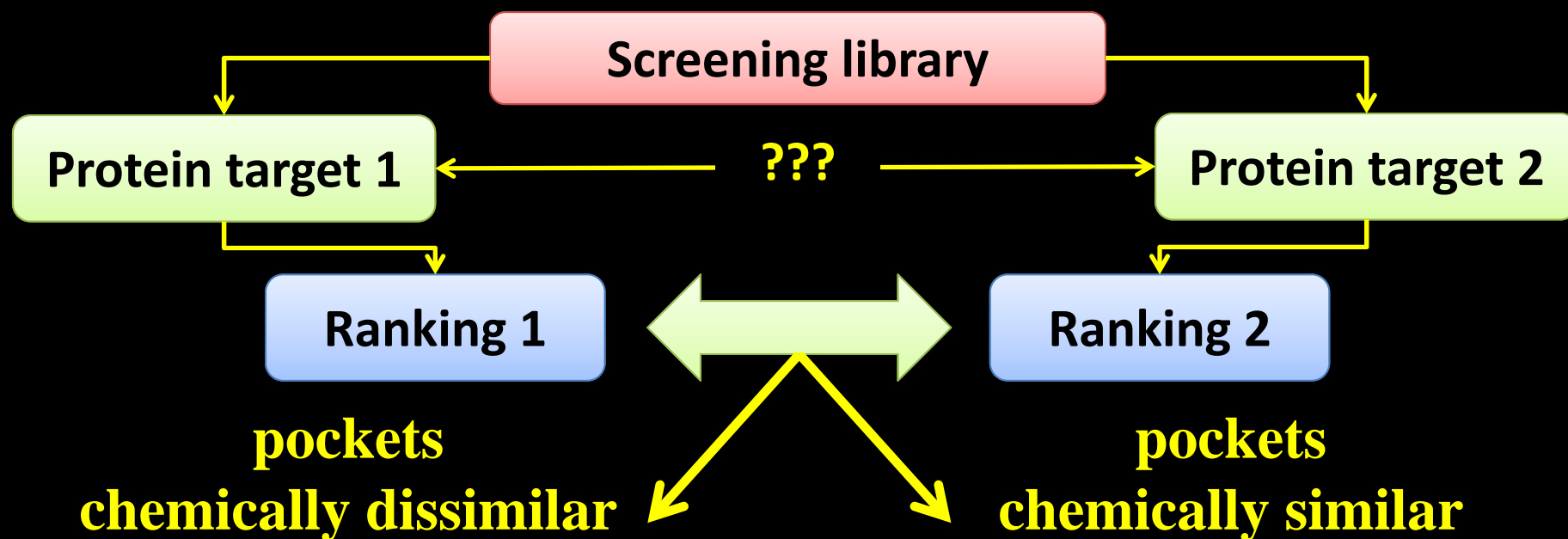
## X-React<sup>KIN</sup>

*In silico* drug  
profiling



Gleev

# LIGAND HOMOMOLOGY MODELING: X-REACT<sup>KIN</sup>



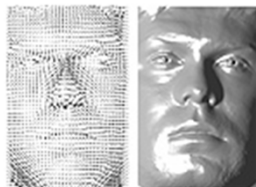
# LIGAND HOMOLOGY MODELING: X-React<sup>KIN</sup>

## Sequence-based

```
VDIYSSGVILYALCGT
```

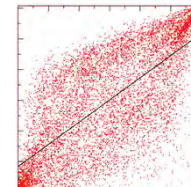
*Pocket SID*

## Structure-based



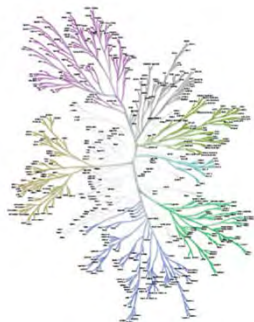
*Geometric hashing*

## Ligand-based



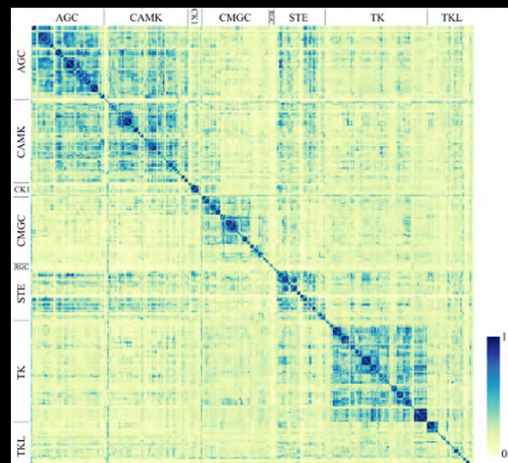
*Chemical correlation*

## Human Kinome<sup>LHM</sup>



## X-React<sup>KIN</sup> Machine learning

## Bioassay data

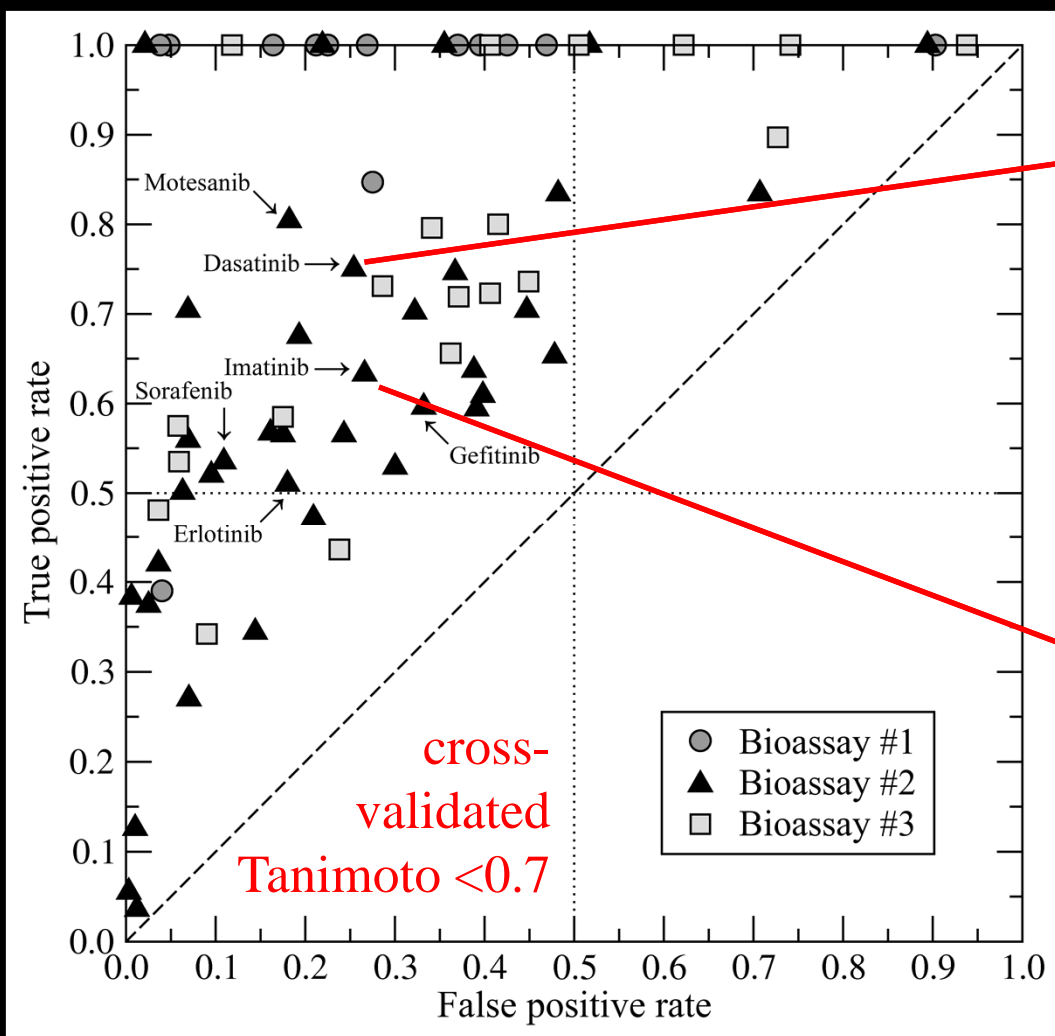


**Off-target identification**

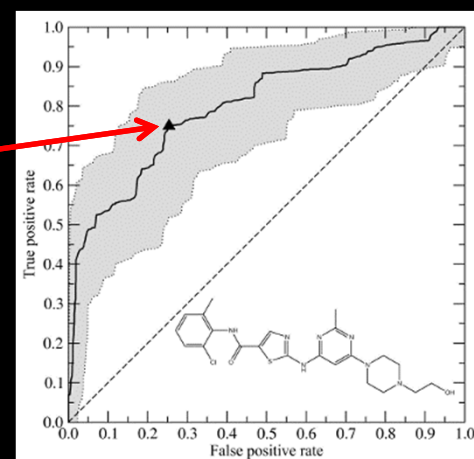
# LIGAND HOMOMOLOGY MODELING: X-REACT<sup>KIN</sup>

## Prediction of inhibitor cross-reactivity for the human kinome

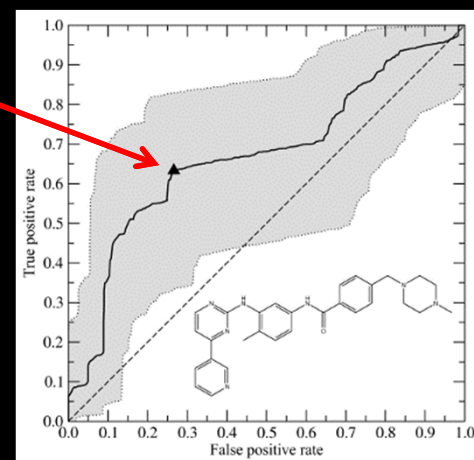
21 (#1), 112 (#2), 275 (#3) kinases



### Dasatinib



### Imatinib



# LIGAND HOMOMOLOGY MODELING: X-React<sup>KIN</sup>

## Comparison to experimental SAR profiles

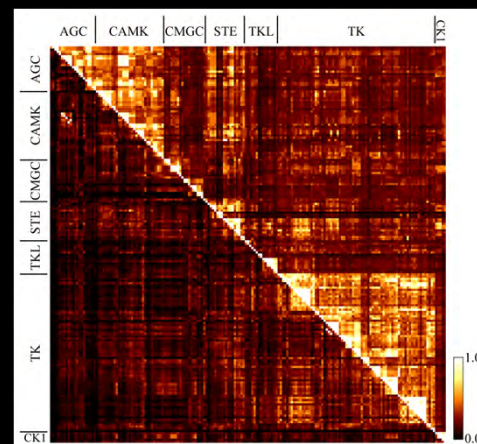
577 cmps

203 kinases

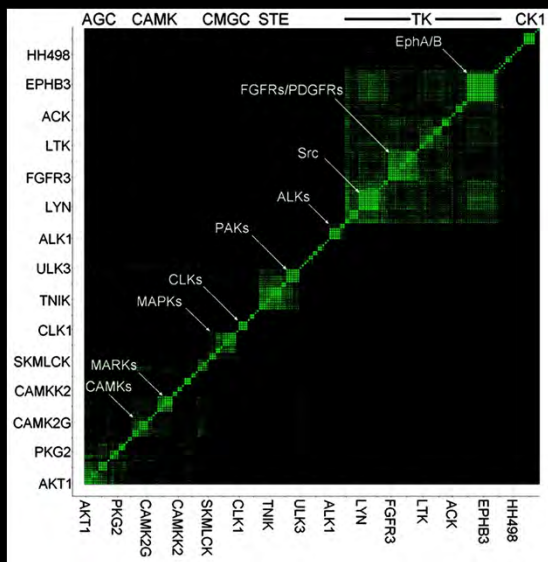


SAR similarity

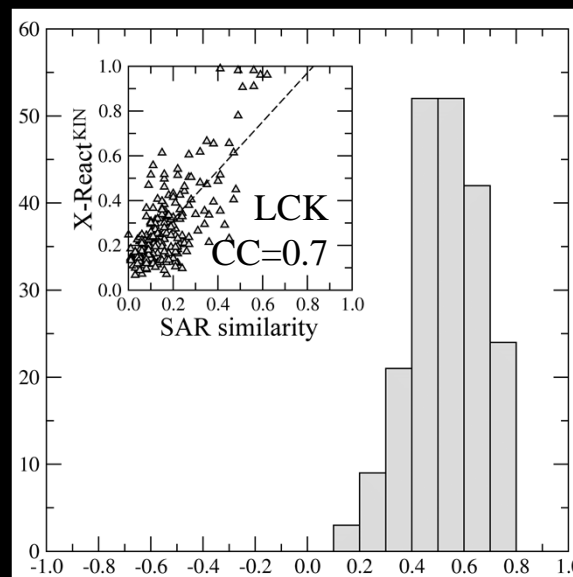
X-React<sup>KIN</sup>



SAR similarity



Number of kinases



CC (SAR/X-React<sup>KIN</sup>)

Bamborough *et al.* (2008) *J Med Chem* **51**, 7898-7914

## LIGAND HOMOLOGY MODELING: SUMMARY OF FINDSITE

- FINDSITE is a powerful threading based approach for the prediction of protein function, binding site location and ligand screening.
- Based on the insight that across evolution the location of the binding site is conserved as well as common features of the bound ligands.
- Method does not require a crystal structure, but also works for low resolution predicted models; tolerates inaccuracies up to a global RMSD of 8-10Å because the binding site is often  $< 2 \text{ \AA}$ .
- For approximate models, predicts the binding site within 4 Å for 67% of target proteins.
- Have also demonstrated promising results for GO-based functional inference. Average MCC=0.64

## LIGAND HOMOMOLOGY MODELING: SUMMARY OF FINDSITE<sup>LHM</sup>

- Have developed FINDSITE<sup>LHM</sup>, an automated approach to the prediction of the ligand anchor and variable regions, ligand binding pose and virtual ligand screening that is applicable to experimental structures and lower resolution predicted models.
- Has significant implications as to how protein function evolves. Have conserved anchor region and variable region that imparts specificity.
- For binding pose prediction, method works acceptably for protein models with a RMSD from native of 4-5 Å.
- Encouraging results shown for the use of low resolution models in virtual ligand screening.
- Ligand ranking is not simply correlated with its molecular weight. Unfortunately, many ligand docking algorithms give results that are strongly correlated with molecular weight.

## LIGAND HOMOLOGY MODELING: SUMMARY KINOME<sup>LHM</sup>/X-REACT<sup>KIN</sup>

- Have provided structure predictions for the entire human kinome
- For each KINASE, have screened ZINC7 library of ~2 million compounds. Have ranking and binding pose predictions for each compound.
- Can exploit these screening results to prioritize ligands that might be specific or general kinase inhibitors.
- Have predicted the structure and cross-reactivity of all proteins in the Human Kinome, results are strongly correlated with experimental SAR results.
- A database of all predictions of the entire human kinome is at Kinome<sup>LHM</sup> is at <http://cssb.biology.gatech.edu/kinomelhm>.

# LIGAND HOMOLOGY MODELING: PUBLICATIONS

## FINDSITE

Brylinski M, Skolnick J (2008) *PNAS* **105**:129

Skolnick J, Brylinski M (2009) *Brief Bioinform* **10**:378

Brylinski M, Skolnick J (2010) *Proteins* **78**:118

## FINDSITE<sup>LHM</sup>

Brylinski M, Skolnick J (2009) *PLoS Comput Biol* **5**:e405

**F1000**

FACULTY of 1000  
POST-PUBLICATION PEER REVIEW



Evaluated by **Rainer Merkl & Reinhard Sterner**

## Q-Dock<sup>LHM</sup>

Brylinski M, Skolnick J (2008) *J Comput Chem* **29**:1574

Brylinski M, Skolnick J (2010) *J Comput Chem* **31**:1093

## Kinome<sup>LHM</sup> / X-React<sup>KIN</sup>

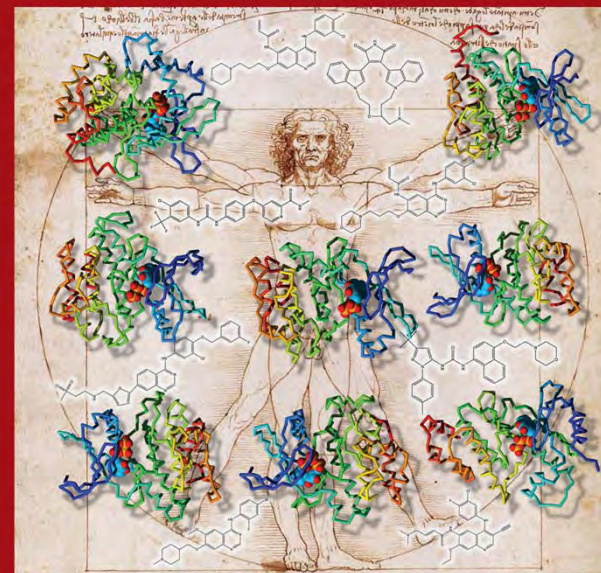
Brylinski M, Skolnick J (2010) *J Chem Inf Model* **50**:1839

Brylinski M, Skolnick J (2010) *Mol Pharm* **7**:2324

## Kinome<sup>LHM</sup> October 2010

JOURNAL OF  
CHEMICAL INFORMATION  
AND MODELING

OCTOBER 2010  
Volume 50  
Number 11  
10.1021/ni100110a



50TH  
ANNIVERSARY

ACS Publications  
High quality. High impact.

www.acs.org

# LIGAND HOMOMOLOGY MODELING: AVAILABILITY

<http://cssb.biology.gatech.edu>

User-friendly  
webservers

Software &  
databases

Manuals &  
documentation

## SERVICES

**PSIFR** PSIFR

### Protein Structure Prediction



chunk-TASSER  
MetaTASSER  
pro-sp3-TASSER  
TASSER  
BSR

### Protein Structure Alignment



Fr-TM-align  
iAlign

### DNA-binding Prediction



DBD-Threader  
DBD-Hunter  
DP-dock

### Protein Function Prediction



FINDSITE  
FINDSITE-metal  
EFICAz<sup>2</sup>

### Ligand Docking/Screening



FINDSITE<sup>LHM</sup>  
Q-Dock<sup>LHM</sup>

## SOFTWARE

EFICAz<sup>2</sup>

FINDSITE



FINDSITE<sup>LHM</sup>

FINDSITE-metal

Fr-TM-align

iAlign

PULCHRA

TASSER-Lite

## Databases

### Structure Prediction Libraries



Human GPCRs

E. coli Proteome

PDB-like Structures

### Function Prediction Libraries

Kinome<sup>LHM</sup>



X-React<sup>KIN</sup>

Human Proteome

Human DNA Binders

### Reference Libraries



Active Site

Templates

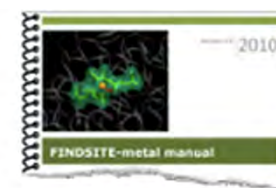
Apo/Holo Pairs

## MANUALS

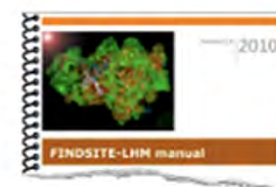
### FINDSITE



### FINDSITE-metal



### FINDSITE<sup>LHM</sup>

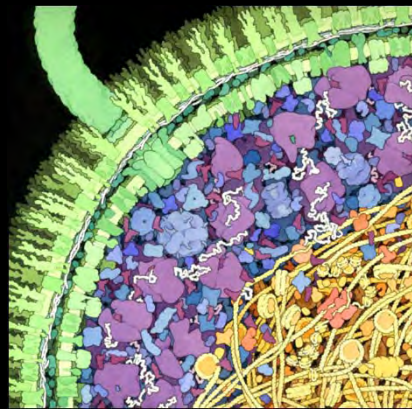


A grayscale electron micrograph showing a dense, complex network of biological structures, likely a cell's internal organelles or cytoskeleton. The structures are interconnected and form a highly textured, porous-looking network. A bright yellow rectangular box is superimposed over the center of the image, containing text.

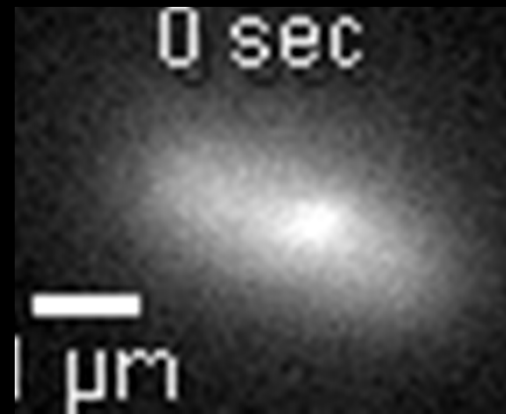
CROWDING AND HYDRODYNAMIC INTERACTIONS LIKELY DOMINATE  
*IN VIVO*  
MACROMOLECULAR MOTION

## INTRODUCTION

The total concentration of macromolecules inside an *E. coli* cell is in the range of 300-400 mg/ml. This crowding greatly affects both the kinetics and equilibria of biochemical reactions in living systems.



(Illustrated by D. Goodsell)



Motion of a tagged RNA inside an *E. coli* cell (Golding and Cox, 2006)

To improve our understanding of a living cell, development of computational methods that can provide reliable predictions of crowding effects on biological reactions is necessary.

Need to develop and apply simulation methods, e.g. Brownian Dynamics

What are the features dominating macromolecular diffusion within an *E. coli* cell?

- Crowding alone?
- How important is macromolecular shape?
- Are hydrodynamic interactions important?
- What are the differences in dynamic behavior when HI or attractive interactions dominate?
- What is needed to reproduce experiment?

## PRELIMINARY PROTOCELL STUDY

The “crowded environment” inside a cell can alter and modify the overall behavior of biological systems.



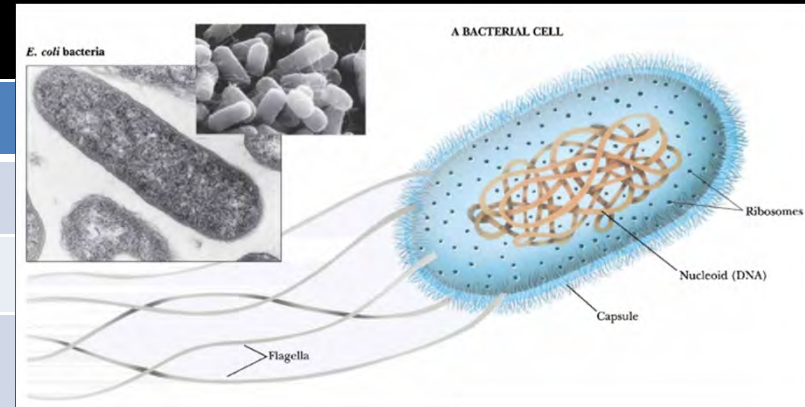
Modeling the crowded cellular environment is an important first step toward whole cell simulation.



We have developed a Brownian dynamics method for simulating the motion of molecules in a cell that can include HI .

# PROPERTIES OF AN *E. COLI* CELL

Description	Data
Cell total volume	1 fL
Cytoplasm volume	0.67 fL
Nucleoid (DNA + protein) volume	0.16 fL
# of cytoplasmic proteins (excluding ribosomal proteins):	1,000,000 (3 mM) <sup>†</sup>
# of ribosomes	18,000 (58 μM) <sup>†</sup>
# of tRNAs	200,000 (650 μM) <sup>†</sup>
# of mRNAs	4,000 (13 μM) <sup>†</sup>
Volume occupancy of macromolecules	~30% (300 – 400 mg/mL)

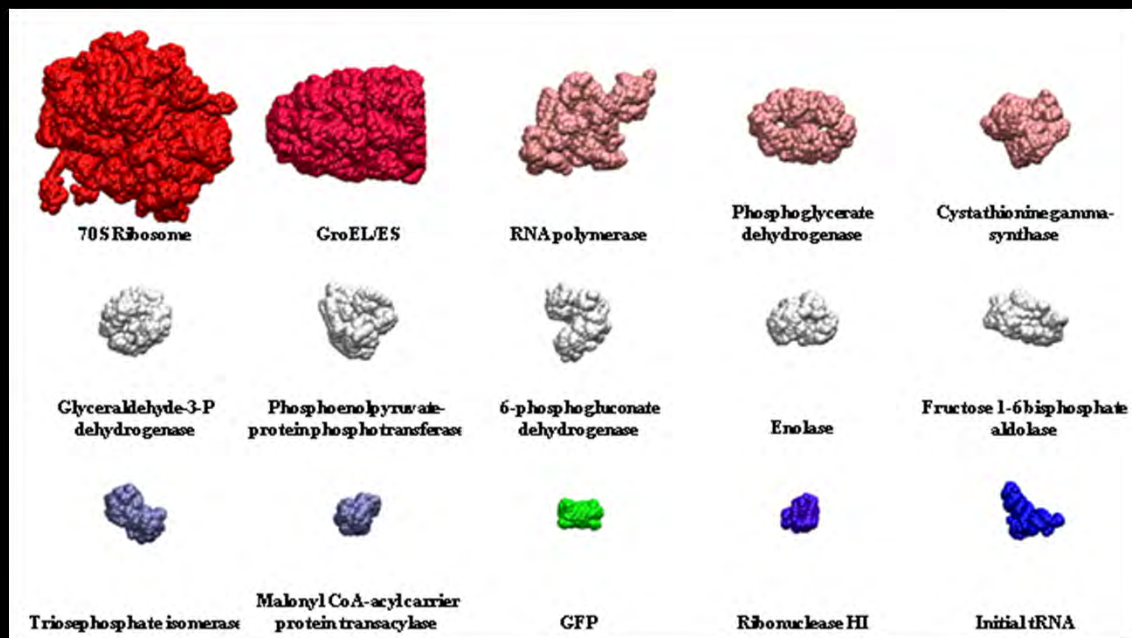


(R. H. Garrett and C. M. Grisham, *Biochemistry*, 1999)

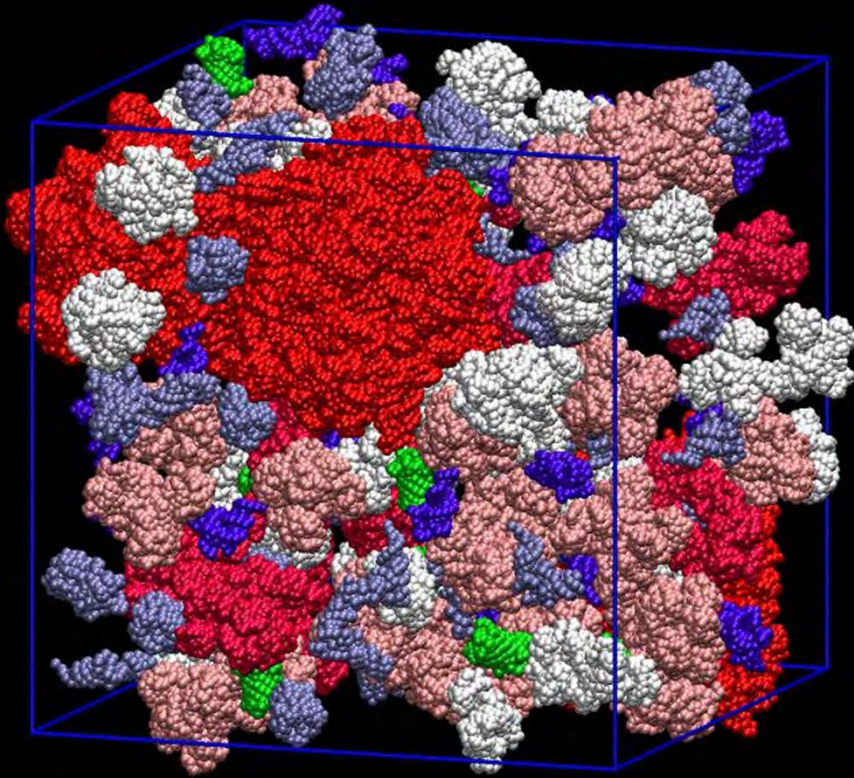
(From the CyberCell database, CCDB)

<sup>†</sup>The value of [(Cytoplasmic volume) – (Nucleoid volume)] was used as the volume for the denominator of the concentration calculation.

# 15 TYPES OF MACROMOLECULES IN VIRTUAL CELL



## VIRTUAL CYTOPLASMIC SYSTEM



- Proteins are represented by  $\alpha$  beads. For nucleic acids, C4 and P atoms were used to describe each nucleotide.
- Box size is 100 nm x 50 nm x 50 nm ( $1.25 \times 10^{-4}$  fL).
- This system contains 29 ribosomes, 528 glycolytic enzymes, 299 tRNA's, and 113 GFP's. Total concentration is 300 mg/mL.
- The macromolecules were placed within the box by random translation and rotation without any steric clashes.

## STOKES-EINSTEIN RELATIONSHIPS

- Stokes-Einstein relationships for spherical particles:

$$D^T = \frac{k_B T}{6\pi\eta a} \quad \text{and} \quad D^R = \frac{k_B T}{8\pi\eta a^3},$$

where  $\eta$  is the viscosity of the solvent and  $a$  is the Stokes radius of the sphere.

## FOR NONSPHERICAL PARTICLES,

An arbitrarily shaped object undergoing Brownian motion is expressed by a  $6 \times 6$  diffusion tensor,  $\mathbf{D}$ , which is related to a resistance tensor,  $\mathbf{R}$ , through the generalized Einstein relationship. The translational diffusion tensor  $\mathbf{D}_{tt}$  is related to the translational diffusion coefficient,  $D_o$  by

$$D_o = 1/3 \text{Tr}(\mathbf{D}_{tt})$$

For a system with hydrodynamic interactions, the hydrodynamic interaction tensor is calculated using the Rotne, Prager, Yamakawa formalism:

$$\mathbf{T}_{ij} = \begin{cases} \frac{1}{8\pi\eta r_{ij}} \left[ \left( \mathbf{I} + \frac{\mathbf{r}_{ij}\mathbf{r}_{ij}}{r_{ij}^2} \right) + \frac{2a^2}{r_{ij}^2} \left( \frac{1}{3}\mathbf{I} - \frac{\mathbf{r}_{ij}\mathbf{r}_{ij}}{r_{ij}^2} \right) \right] & r_{ij} \geq 2a, \\ \frac{1}{6\pi\eta a} \left[ \left( 1 - \frac{9}{32} \frac{r_{ij}}{a} \right) \mathbf{I} + \frac{3}{32} \frac{\mathbf{r}_{ij}\mathbf{r}_{ij}}{r_{ij}a} \right] & r_{ij} < 2a. \end{cases}$$

With  $\eta$  the viscosity of the solvent and  $\mathbf{r}_{ij}$  is the distance vector between beads  $i$  and  $j$ . Note that the radius of bead is the only parameter to be optimized to reproduce hydrodynamic properties in dilute conditions.

Now, consider a  $3N \times 3N$  supermatrix,  $\mathbf{B}$ , consisting of  $N \times N$   $\mathbf{B}_{ij}$  blocks at an arbitrary origin  $O$

$$\mathbf{B} = \begin{pmatrix} \mathbf{B}_{11} & \mathbf{L} & \mathbf{B}_{1N} \\ \mathbf{M} & \mathbf{O} & \mathbf{M} \\ \mathbf{B}_{N1} & \mathbf{L} & \mathbf{B}_{NN} \end{pmatrix},$$

$$\mathbf{B}_{ij} = \delta_{ij} \frac{1}{6\pi\eta a} + (1 - \delta_{ij}) \mathbf{T}_{ij}.$$

Here,  $\delta_{ij}$  is the Kronecker delta function. This supermatrix is then inverted to obtain a  $3N \times 3N$  supermatrix,  $\mathbf{C}$ ,

$$\mathbf{C} = \mathbf{B}^{-1} = \begin{pmatrix} \mathbf{C}_{11} & \mathbf{L} & \mathbf{C}_{1N} \\ \mathbf{M} & \mathbf{O} & \mathbf{M} \\ \mathbf{C}_{N1} & \mathbf{L} & \mathbf{C}_{NN} \end{pmatrix},$$

and

$$\bar{\mathbf{E}}_{tt} = \sum_i \sum_j \mathbf{C}_{ij}$$

For  $N$  particles system in a Newtonian fluid and in absence of an external shear flow, the hydrodynamic forces acting on particles,  $\mathbf{F}$ , are related to the particle velocities,  $\mathbf{U}$ , through the Stokes equation

$$\mathbf{F} = \mathbf{R} \cdot \mathbf{U}$$

where  $\mathbf{R}$  is the resistance matrix and is the inverse of the mobility matrix,  $\mathbf{M}$ .

When torque-angular velocity is not considered, the so-called “F version” in Ref. (11),  $\mathbf{F}$  and  $\mathbf{U}$  are  $3N \times 1$  vectors and  $\mathbf{R}$  and  $\mathbf{M}$  are  $3N \times 3N$  matrices. Then, the diffusion matrix of the system is simply given by

$$\mathbf{D} = k_B T \mathbf{M}$$

The resistance tensor  $\mathbf{R}$ , which contains both near-field lubrication effects and far-field many-body interactions, is calculated as

$$\mathbf{R} = \left(\mathbf{M}^\infty\right)^{-1} + \mathbf{R}_{2B} - \mathbf{R}_{2B}^\infty$$

- $\left(\mathbf{M}^\infty\right)^{-1}$ , represents the contribution of many-body, far-field interactions.
- $\mathbf{R}_{2B}$  represents the exact two-body HI, which includes both near-field and far-field interactions.
- $\mathbf{R}_{2B}^\infty$  is the resistance tensor that represents two-body far-field interactions. The far-field part has already been included on  $\left(\mathbf{M}^\infty\right)^{-1}$ . Thus, in order not to count these interactions twice, we must subtract off the two-body interactions. This is the standard method to correct for the lubrication effects in the resistance tensor.

## BROWNIAN DYNAMICS (BD) OF ARBITRARILY SHAPED OBJECTS WITHOUT HI

$$\mathbf{x}_i = \mathbf{x}_i^0 + \frac{\Delta t}{k_B T} \mathbf{D}_i \cdot \mathbf{F}_i^p + \mathbf{G}_i(\Delta t)$$

where  $\Delta t$  is the time step and  $\mathbf{x}_i$  is the vector describing the position of the center of diffusion and orientation of the  $i$ -th object.  $\mathbf{F}^p$  is a generalized force and  $\mathbf{G}_i(\Delta t)$  is a  $6 \times 1$  random displacement vector during time step  $\Delta t$  due to the Brownian noise, which satisfies

$$\langle \mathbf{G}_i(\Delta t) \rangle = 0, \langle \mathbf{G}_i(\Delta t) \mathbf{G}_j(\Delta t) \rangle = 2\mathbf{D}_i \Delta t \delta_{ij}$$

## BD WITH HYDRODYNAMIC INTERACTIONS: MIDPOINT ALGORITHM

When HI are considered, the diffusion tensor depends in principle on the configuration of the entire system. The propagation eq is

$$\begin{aligned}\mathbf{r} &= \mathbf{r}^0 + (\nabla \cdot \mathbf{D})\Delta t + \frac{\mathbf{D} \cdot \mathbf{F}^p}{k_B T} \Delta t + \mathbf{G}(\Delta t) \\ &= \mathbf{r}^0 + k_B T (\nabla \cdot \mathbf{M})\Delta t + (\mathbf{M} \cdot \mathbf{F}^p)\Delta t + \mathbf{G}(\Delta t),\end{aligned}$$

Where  $\mathbf{r}$  is the particle's position vector and  $\mathbf{G}(\Delta t)$  is the random displacement due to Brownian motion, which has the following properties

$$\langle \mathbf{G}(\Delta t) \rangle = 0, \langle \mathbf{G}(\Delta t) \mathbf{G}(\Delta t) \rangle = 2k_B T \mathbf{M} \Delta t$$

In contrast to a BD algorithm with constant diffusion tensors, we need to evaluate the spatial gradient of the mobility tensor in the BD simulation with HI, in which the explicit computation of is a  $O(N^3)$  task. To avoid this, we used a method introduced by Banchio and Brady, based on Fixman's idea, the so-called "mid-point scheme".

$$\langle \mathbf{F}^B \rangle = 0, \langle \mathbf{F}^B(0) \mathbf{F}^B(t) \rangle = 2k_B T \mathbf{R} / \Delta t$$

Here,  $\mathbf{F}^B$  is the Brownian force, obtained by the Cholesky decomposition method. The procedure is the following:

(1) Compute the velocity  $\mathbf{U}^0$  using an initial configuration  $\mathbf{r}^0$

$$\mathbf{U}^0 = \left( \mathbf{R}^0 \right)^{-1} \cdot \left( \mathbf{F}^{p,0} + \mathbf{F}^{B,0} \right)$$

(2) Move the particles to intermediate positions  $\mathbf{r}'$  by a small fraction of a time step,  $\Delta t/m$

where  $m$  is 100.

$$\mathbf{r}' = \mathbf{r}^0 + \frac{\Delta t}{m} \mathbf{U}^0$$

(3) Calculate a new velocity  $\mathbf{U}'$  at the intermediate positions using the forces evaluated at  $\mathbf{r}^0$

$$\mathbf{U}' = (\mathbf{R}')^{-1} \cdot (\mathbf{F}^{\text{p},0} + \mathbf{F}^{\text{B},0})$$

(4) Calculate the drift velocity,  $\mathbf{U}^{\text{drift}}$ ,

$$\mathbf{U}^{\text{drift}} = \frac{m}{2} (\mathbf{U}' - \mathbf{U}^0)$$

(5) Finally, update the positions of the particles for time step  $\Delta t$ .

$$\mathbf{r} = \mathbf{r}^0 + (\mathbf{U}^0 + \mathbf{U}^{\text{drift}}) \Delta t$$

## DIFFUSION CONSTANT CALCULATION

For short times, the mean square displacement is linear and the short time diffusion constant is defined as

$$D_i^S = \frac{1}{3N_i} \sum_{\alpha \in i}^{N_i} \text{tr} (\mathbf{D}^{\alpha\alpha})$$

$N_i$  is the number of type  $i$  particles in the system and  $\mathbf{D}^{\alpha\alpha}$  is the  $3 \times 3$  matrix of the self part of the diffusion tensor.

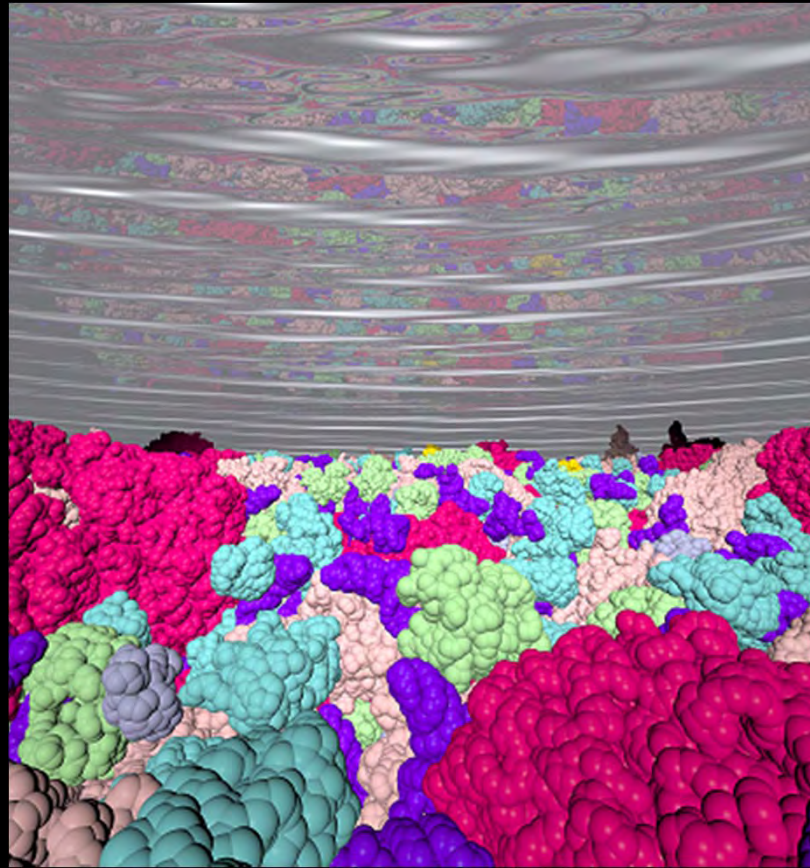
Similarly, the long time diffusion constant is given by

$$D^L = \lim_{t \rightarrow \infty} \frac{\langle |\mathbf{r}(t) - \mathbf{r}(0)|^2 \rangle}{6t}$$

## SIMULATION CONDITIONS

- Periodic boundary conditions were used.
- Simulation temperature was 298 K.
- Generated ten different random configurations of the system.
- 30 independent simulations were done.
- For BD simulations of repulsive and non-specific, attractive binding models without HI, 30 and 50  $\mu\text{s}$  simulations were performed with a time step of 0.5 and 0.1 ps, respectively.
- For BD simulations with HI, we ran 15  $\mu\text{s}$  simulations with a time step of 2 ps.
- The first 5, 30, and 5  $\mu\text{s}$  of simulations of repulsive, non-specific binding models, and HI models were ignored entirely. To estimate the long-time diffusion coefficients, MSD values after a relative time interval of 5  $\mu\text{s}$  was used.

## RESULTS

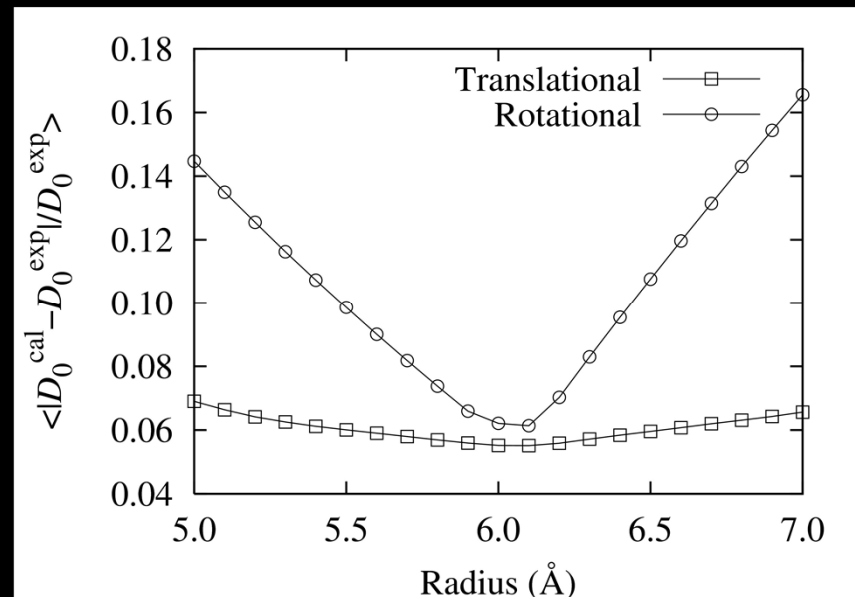


See: T. Ando and J. Skolnick. Crowding and hydrodynamic interactions likely dominate *in vivo* macromolecular motion. Proc Natl Acad Science 2010:**107**: 18457-18462.

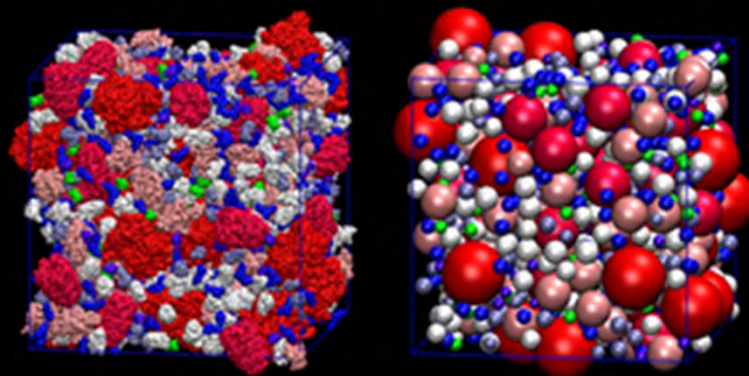
# ESTIMATION OF INFINITE DILUTION MACROMOLECULAR DIFFUSION CONSTANT FROM ATOMIC STRUCTURE

Fit to infinite dilution diffusion constant of a representative set of proteins and t-RNA using the rigid-particle formalism (see Garcia De La Torre J, Huertas ML, & Carrasco B (2000) *Biophys J* 78(2):719-730). Fit the data with a bead radius of 6.1 Å

Gives GFP diffusion constant of 8.9 Å<sup>2</sup> vs experiment of 8.7 Å<sup>2</sup>.

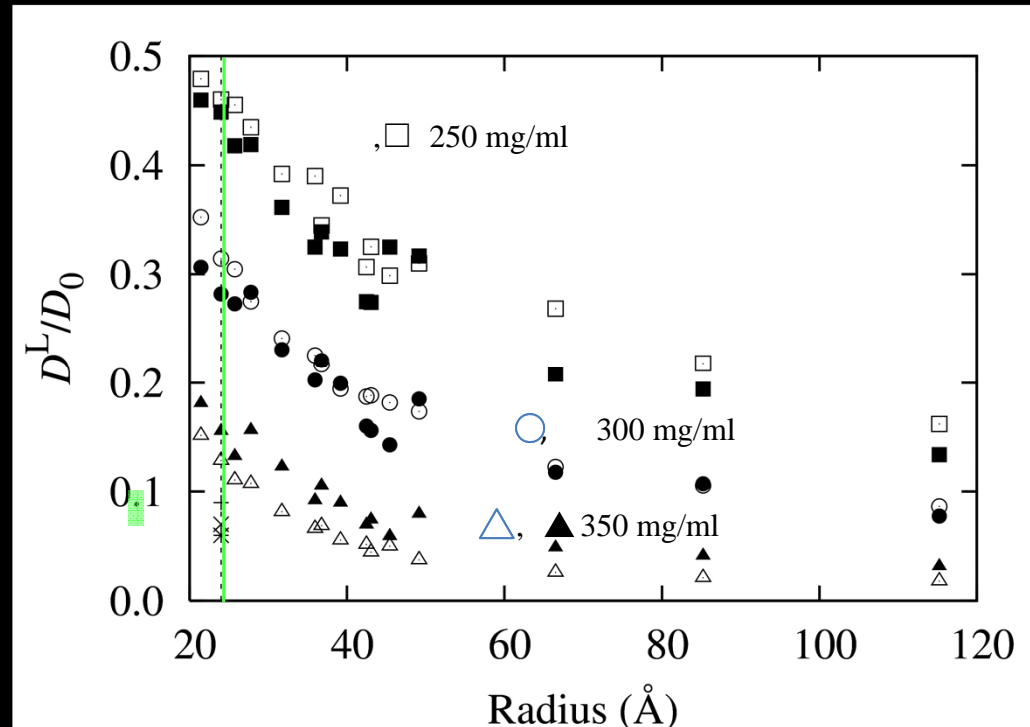


## EFFECT OF MOLECULAR SHAPE IN DIFFUSION OF DENSE HARD SPHERE SYSTEMS



Molecular-shaped (*left*) and sphere (*right*) systems at 300 mg/ml.  
Macromolecules are represented in different colors.

# DIFFUSION CONSTANTS IN DENSE SYSTEMS OF MOLECULES AND EQUIVALENT SPHERE SYSTEMS

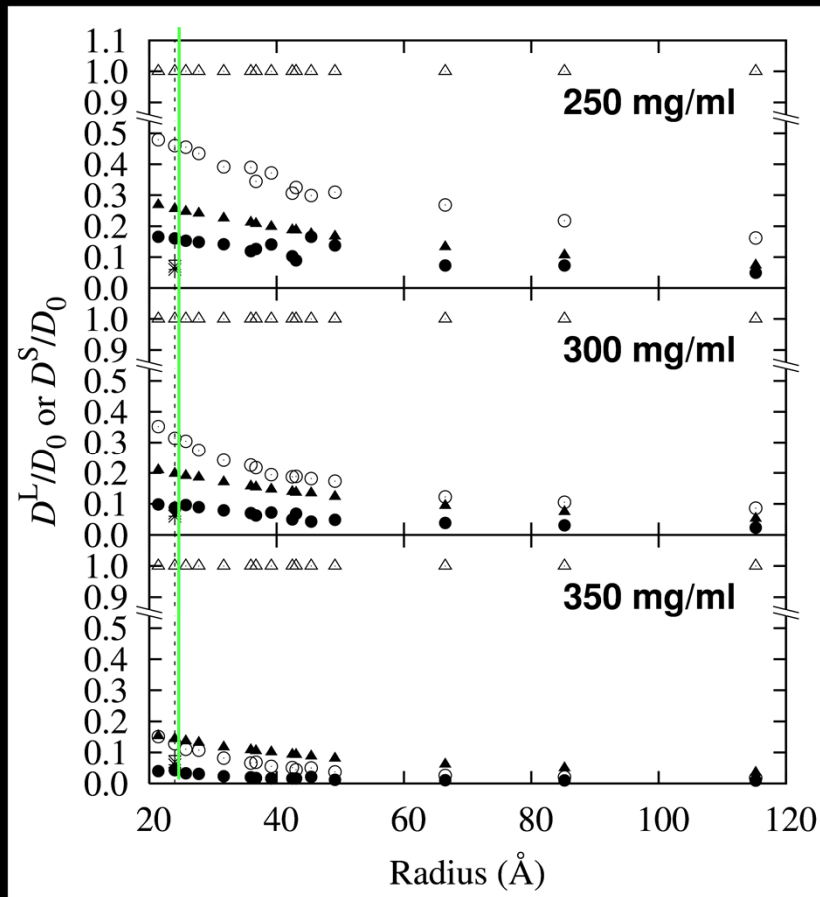


Long time diffusion constant ratio as a function of macromolecule radius in the sphere (open symbols) and molecular-shaped systems (filled symbols). Reduction in diffusion constant of GFP measured *in vivo* of DH5 $\alpha$ , BL21(DE3), and K-12 *E. coli*. are shown by plus, cross, and asterisk, respectively. Green line is GFP's radius.

## SPHERE VERSUS ACTUAL SHAPE RESULTS:

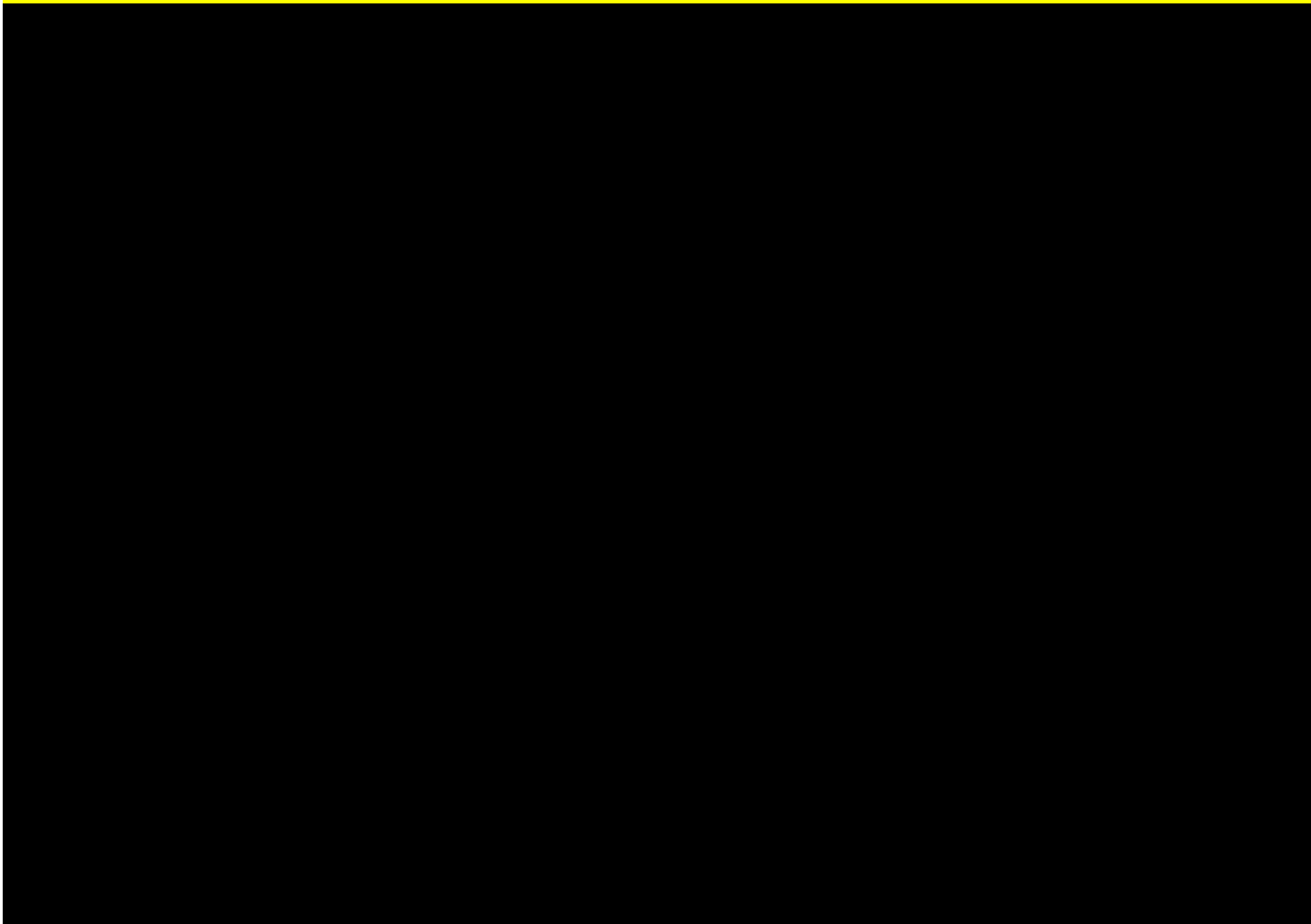
- Below 350 mg/ml, the results of explicit shape and equivalent sphere systems are very close.
- At 350 mg/ml,  $D_L$  is somewhat smaller for the sphere systems.
- So we can use the equivalent sphere approximation to explore the role of HI.
- But for both representations, crowding cannot explain the  $D_L/D_o$  of 0.06-0.09 for GFP. For example, at 300 mg/ml, simulated  $D_L/D_o = 0.31$ .
- Something is missing!

# COMPARISON OF SPHERICAL SYSTEM WITH HYDRODYNAMIC INTERACTIONS VS JUST REPULSIVE INTERACTIONS



Reduction in diffusivity as a function of radius at three different concentrations. Triangles and circles represent  $D^S/D_0$  and  $D^L/D_0$ . Open (filled) symbols are values in the sphere model with repulsive (HI) interactions. Plus, cross, and asterisk symbols exp. Green line is GFP's radius.

## COMPARISON OF HARD SPHERE AND HI SIMULATIONS:



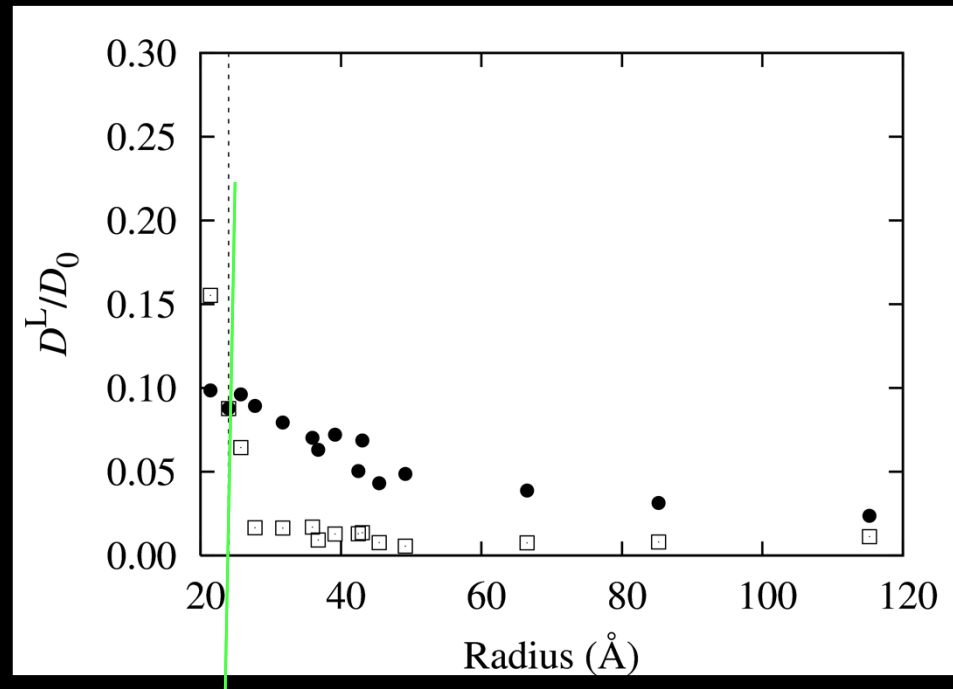
## HI RESULTS

- HI greatly reduces the short time diffusion constant,  $D^S$  from the infinite dilution value,  $D_0$ . In contrast,  $D^S = D_0$  when HI are ignored.
- For GFP, without adjustable parameters, simulations reproduce the experimental reduction in  $D_L$ .
- Implies that crowding and HI are major factors responsible for the slow down in diffusion in intracellular environments.

## EFFECT ON NONSPECIFIC ATTRACTIVE INTERACTIONS ON DIFFUSION

- Consider each macromolecule to be a rough sphere filled with van der Waals particles with a 3 Å diameter.
- Surface roughness is estimated as the difference between the Stokes radius and the radius of gyration of the macromolecule.
- Ignore HI and adjust the strength of the van der Waals attraction to give the experimentally observed reduction in GFP's diffusion constant.

## COMPARISON OF $D^L/D_0$ IN NONSPECIFIC ATTRACTION MODEL WITH HI MODEL



At 300 mg/ml, long-time diffusion constant ratio,  $D^L/D_0$ , as a function of radius in the non-specific, van der Waals interaction (HI) model is represented by squares (filled circles). Green line is GFP's radius.

## IMPLICATIONS

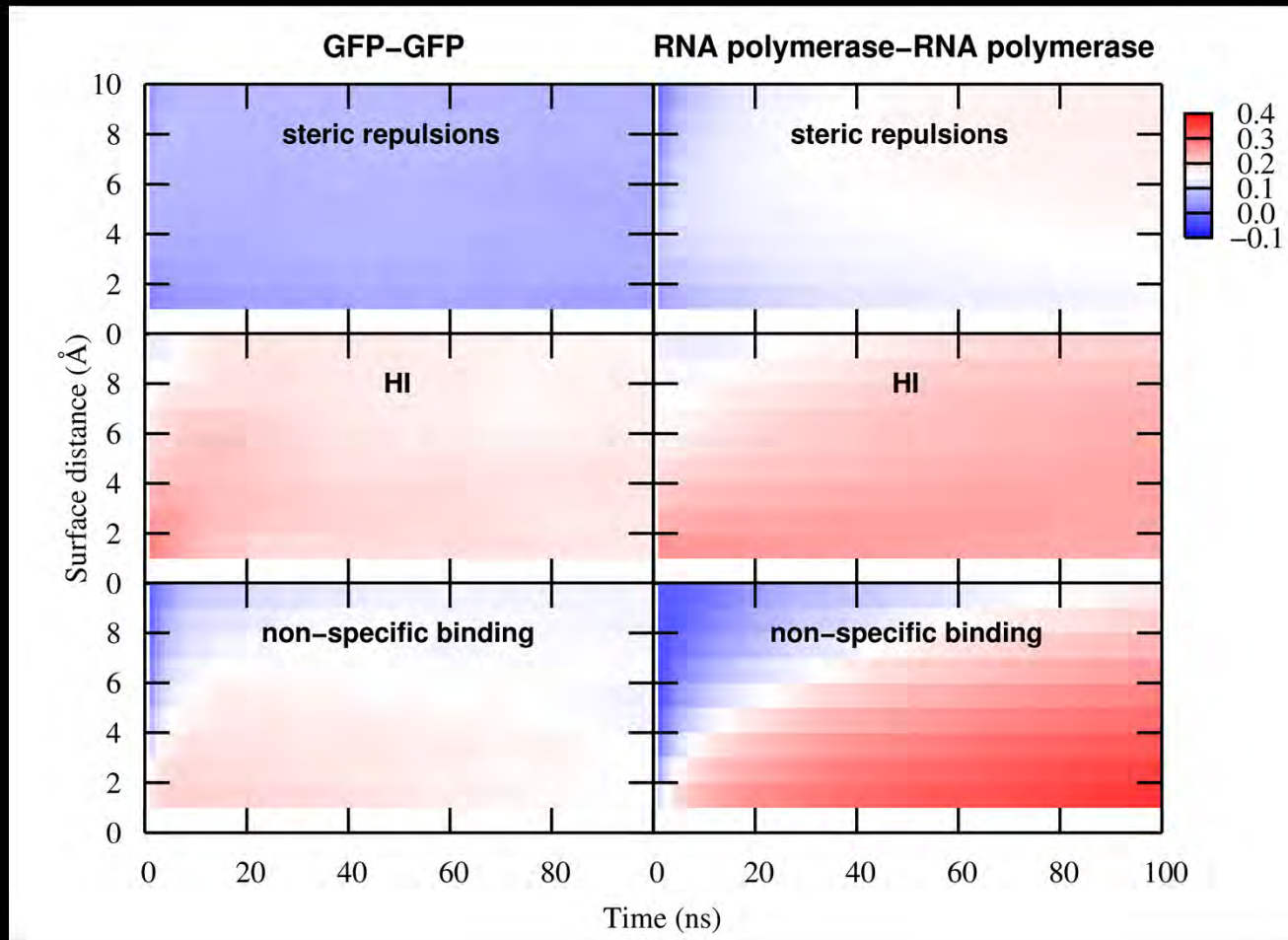
- If non specific attractions dominate *in vivo* diffusion, then reduction in diffusion constant is very strongly dependent on molecular radius.
- In contrast, if HI dominate, reduction in diffusion constant is much less sensitive to molecular radius.

- Calculate normalized pair correlation function between molecules  $i$  and  $j$ :

$$C_{ij}(d_0, \tau) = \frac{\sum \left[ \left( \Delta \mathbf{r}_i(\tau) \cdot \Delta \mathbf{r}_j(\tau) \right) \delta(d_0 - d_{ij}) \right]}{\sqrt{\sum \left| \Delta \mathbf{r}_i(\tau) \delta(d_0 - d_{ij}) \right|^2} \sqrt{\sum \left| \Delta \mathbf{r}_j(\tau) \delta(d_0 - d_{ij}) \right|^2}}$$

Where  $d_0$  is a specified the surface distance between particles  $i$  and  $j$ , and  $\tau$  is the time interval.  $\delta(d_0 - d_{ij})$  is the Dirac delta function.  $d_{ij}$  is the surface distance between particles  $i$  and  $j$  at time  $t$ .

# NORMALIZED PAIR CORRELATION FUNCTION AVERAGED OVER PAIRS OF GFP AND RNA POLYMERASE MOLECULES FOR THE THREE DIFFERENT SIMULATION MODELS AT 300 MG/ML.



## DIFFERENCES OF THE THREE MODELS

### Hard sphere model

- Little spatial or temporal correlation.
- $C_{ij} < 0.1$  even at short times.
- True for all size pairs of molecules.

### HI model

- For both small pairs and large pairs, see significant, but weak,  $C_{ij} < 0.3$ , intermolecular correlation that persists up to quite long times ( $>100$  ns) and distances (at least  $10 \text{ \AA}$ ).

### Non specific binding model

- For large molecules, see positive correlation for distances  $< 5 \text{ \AA}$  that are long lived in time. See long lived clusters.
- For small molecules, this effect is greatly reduced.

## CONCLUSIONS

- Equivalent sphere model is a good description of the motion of macromolecules in intracellular environments.
- HI dynamics likely exert a significant effect on intercellular dynamics.
- Crowding and HI can quantitatively reproduce the experimentally observed diffusion constant of GFP *without any adjustable parameters.*

# HOW TO EXPERIMENTALLY DIFFERENTIATE BETWEEN HI AND NON SPECIFIC BINDING MODELS:

## If HI dominate:

- Decay like  $1/r$ ; lubrication forces give repulsion on approach and attraction as pairs of move apart.
- Short time diffusion constant,  $D_s$  is significantly reduced from  $D_o$ .
- $D_s/D_o$  depends on molecule radius.
- Long time diffusion constant  $D_L$  has much weaker dependence on particle radius.
- Have significant spatial and temporal correlations for all size macromolecules.

## If nonspecific binding dominates:

- Decay like  $1/r^2$  for spherical macromolecules filled with small van der Waal spheres.
- Short time diffusion constant is the same as in infinite dilution,  $D_o$ .
- $D_s/D_o$  is independent of molecule radius.
- $D_L$  is strongly size dependent, with long lived clusters formed with larger macromolecules.
- Significant, radius independent spatial and temporal correlations are absent.

## OTHER FACTORS THAT COULD AFFECT INTRACELLULAR DIFFUSION:

- *Electrostatics*- but inclusion in simulations only slightly reduces GFP diffusion constant.
- *Viscosity of the cytoplasm*- *In vivo* viscosity is essentially the same as bulk water; < 2CP.
- *GFP dimerization*- GFP dimerizes at <100nm ionic strength.

But we expect these factors to be small.

## OUTLOOK

- Have a useful model to elucidate some general features of intracellular dynamics at the molecular level.
- Exploring differences in metabolic fluxes *in vivo* from that at infinite dilution.
- Have generalized this class of models to include a schematic membrane. Using this to examine very simple models of cellular division.

# ACKNOWLEDGEMENTS

Michael Baxa



Michal  
Brylinski



Aysam Guerler



Narendra Kumar



Bartosz  
Ilkowski



## Center for the Study of Systems Biology

Tadashi Ando



Jessica Forness



Mu Gao



Hongyi Zhou



# ACKNOWLEDGMENTS



**Tadashi Ando**

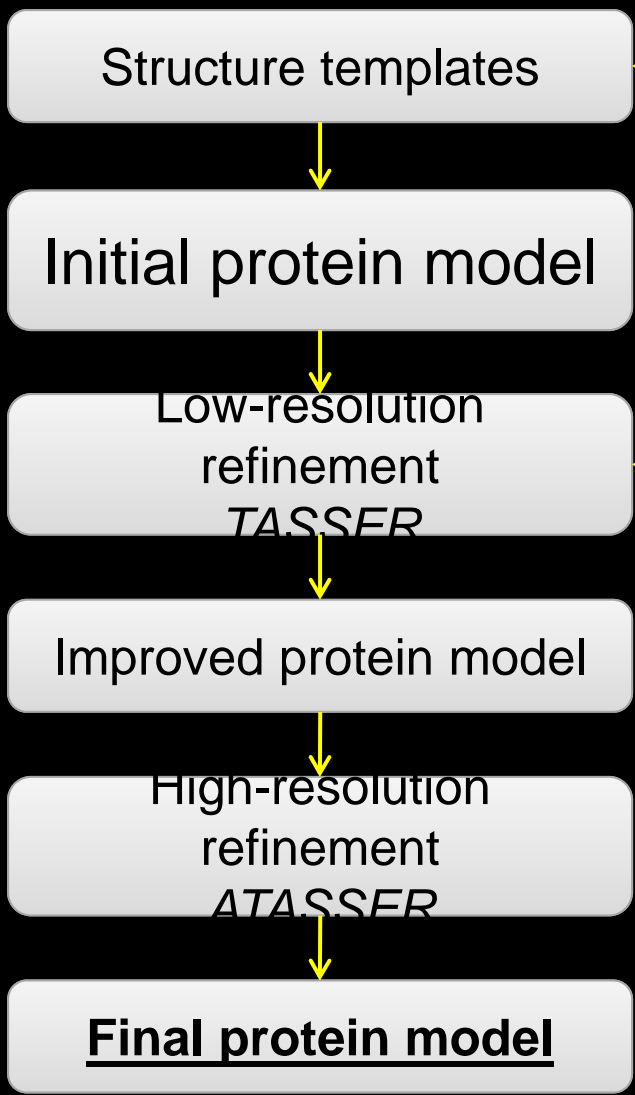


## CORRELATION BETWEEN STOKES RADIUS AND THE AVERAGE VALUE OF $R_g$ AND $R_{MAX}$

Molecule	Stokes radius (Å)	$R_g$ (Å)	$R_{max}$ (Å)	Average of $R_g$ and $R_{max}$ (Å)
Ribonuclease	18	14.2	22.4	18.3
GFP	24.7	17.0	27.6	22.3
Phe-tRNA	28.8	22.3	45.9	34.1
Ovoalbumin	31	21.7	38.5	30.1
Hemoglobin	31	23.7	33.0	28.3
Enolase	36	26.5	41.2	33.8
Aldolase	46	34.9	59.0	47.0
Ribosome	126	85.0	154.9	120.0
<b>(RMSD)</b>	<b>0</b>	<b>17.5</b>	<b>14.2</b>	<b>3.5</b>

# Ligand Homology Modeling: Overview

## Template-based protein structure prediction

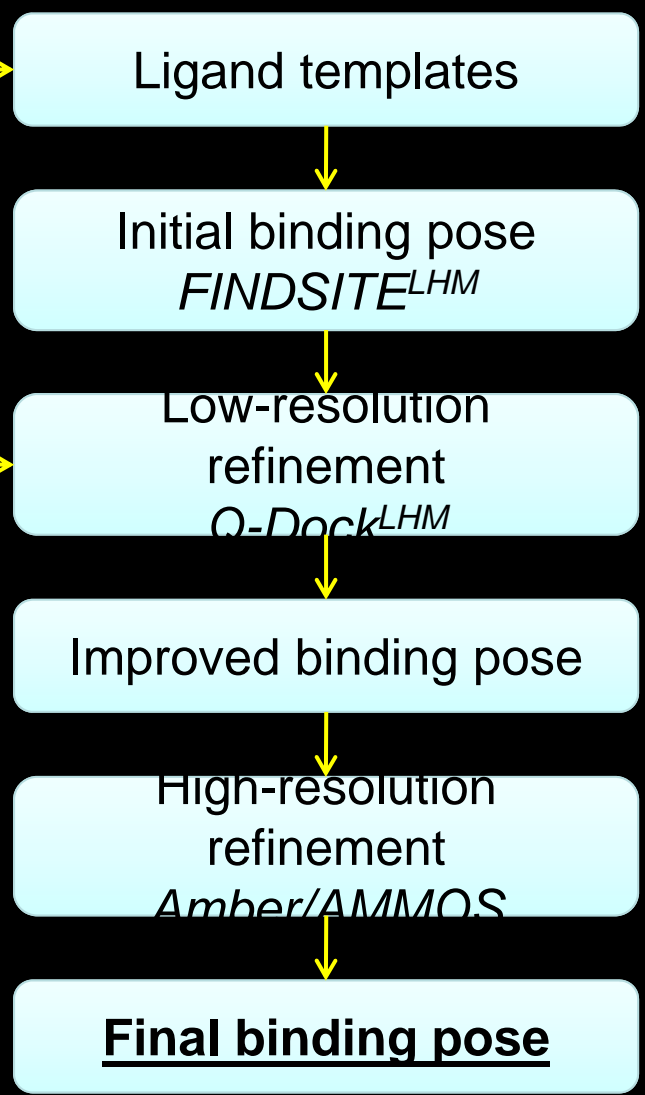


PDB

(meta) Threading  
*PROSPECTOR\_3, SP3, Sparks*

Specific potentials & restraints

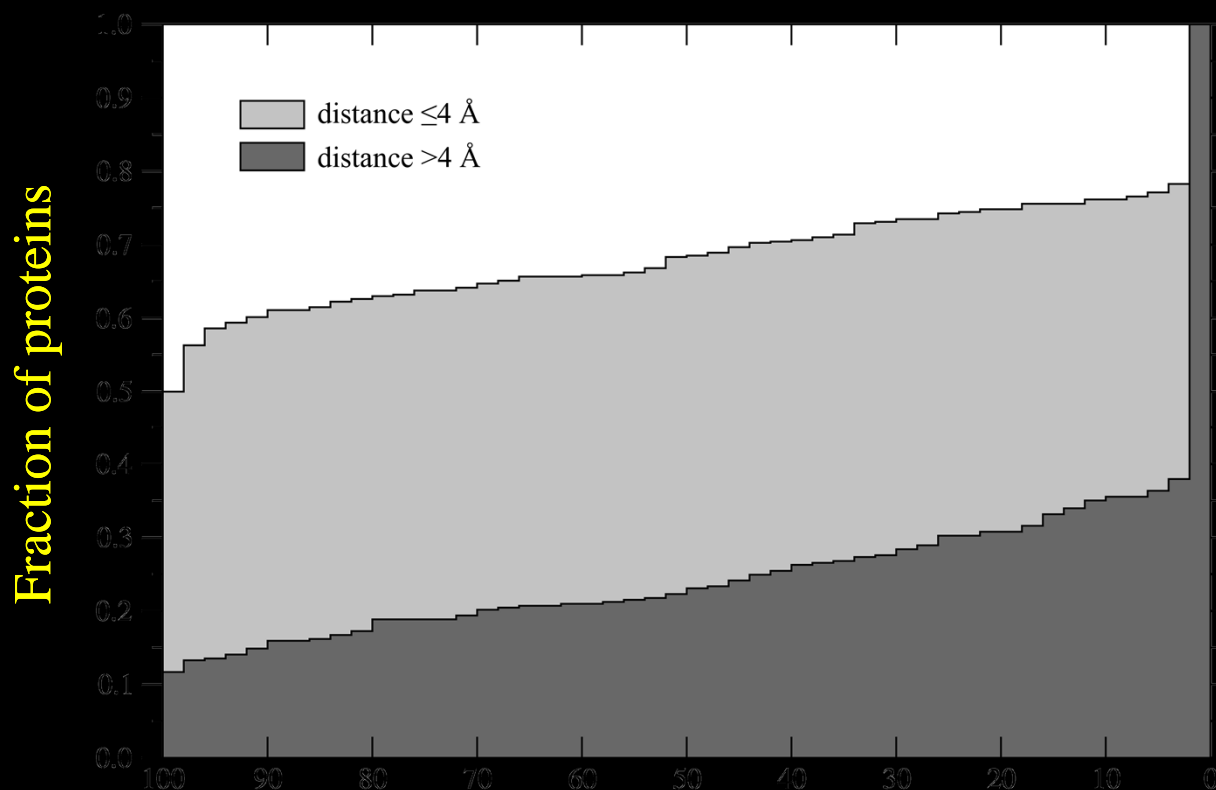
## Template-based protein-ligand modeling



# Ligand Homology Modeling:

Ligand-based virtual screening using 1024-bit fingerprints against the KEGG Compound library of 12,478 molecules

FINDSITE

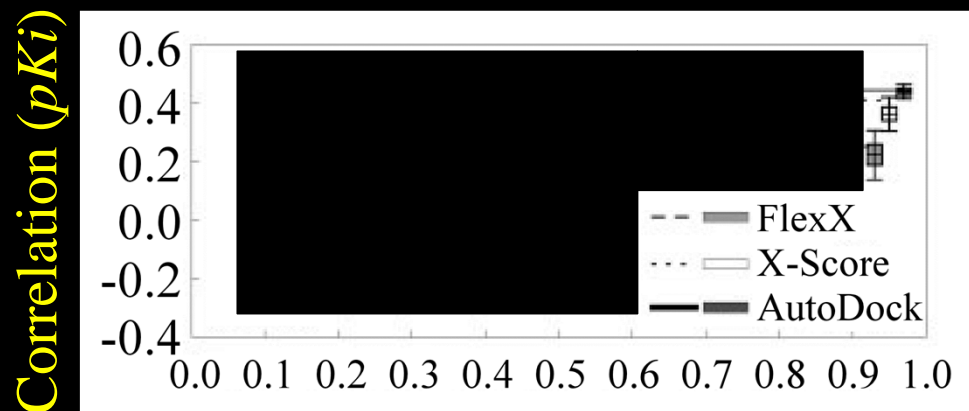


Enrichment factor for the top 1% of the screening library

# Ligand Homology Modeling: Most ligand docking/scoring algorithms lack specificity

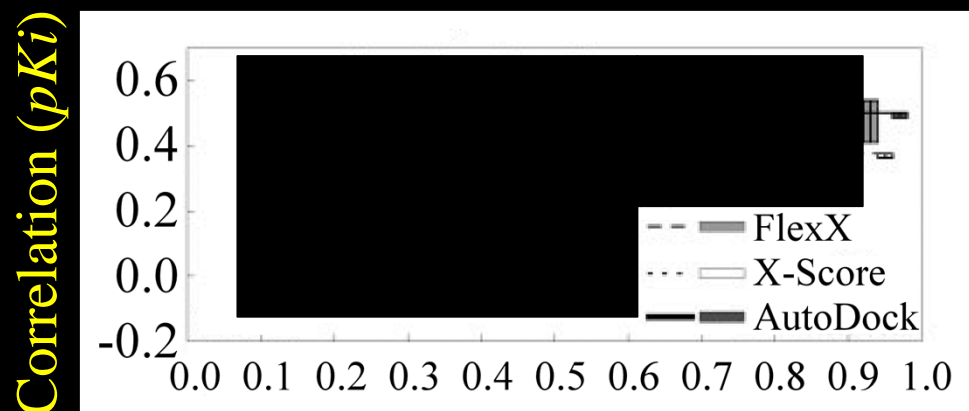
## Challenges

*HIV-1 protease*



Tanimoto coefficient

*Ribonuclease A*



Tanimoto coefficient

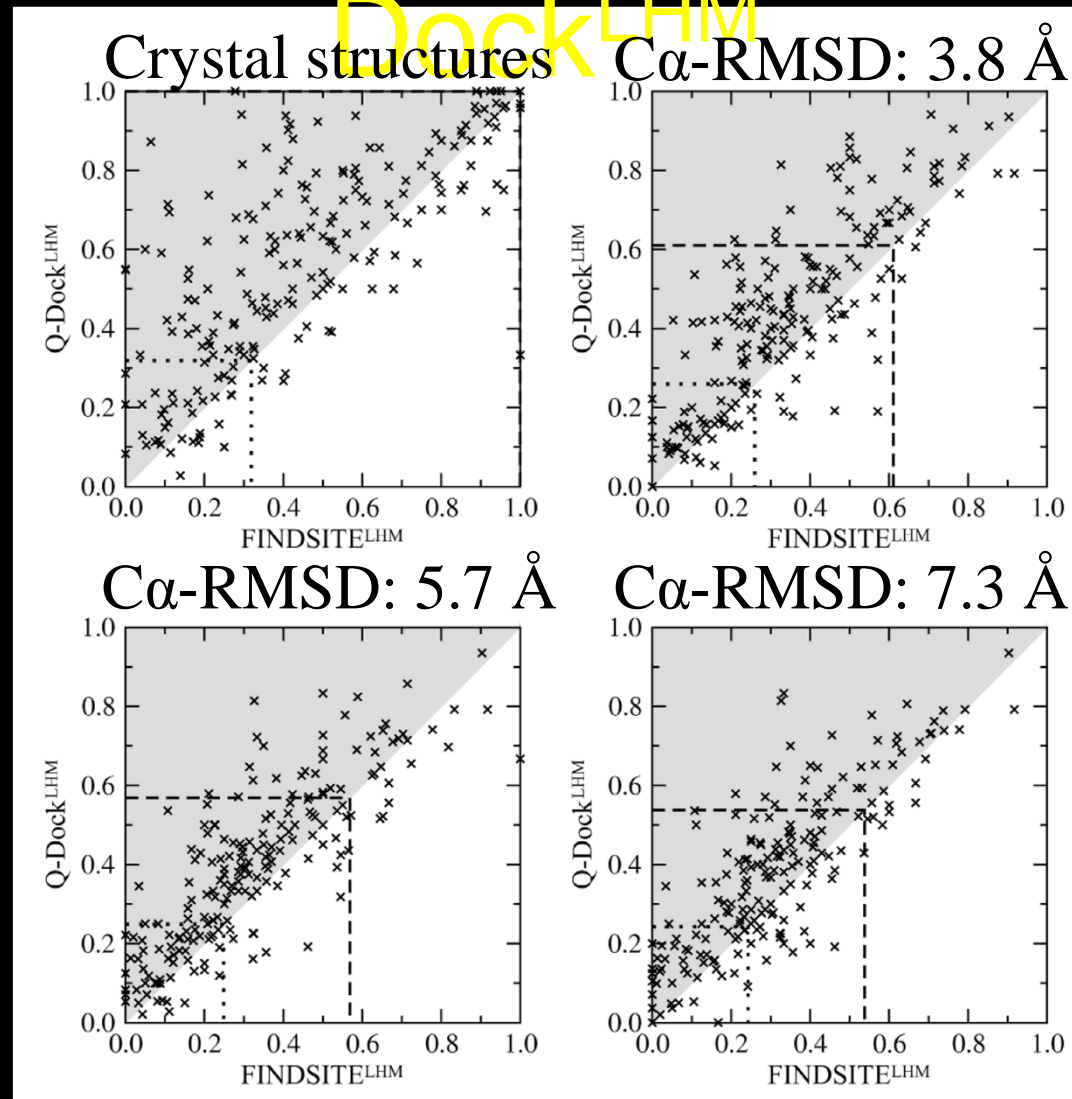
*Calculated for ~1,000  
randomized ligands (decoys)*

➤ Predicted binding affinity is highly correlated with MW

➤ Docking programs cannot distinguish native ligands from their randomized decoys

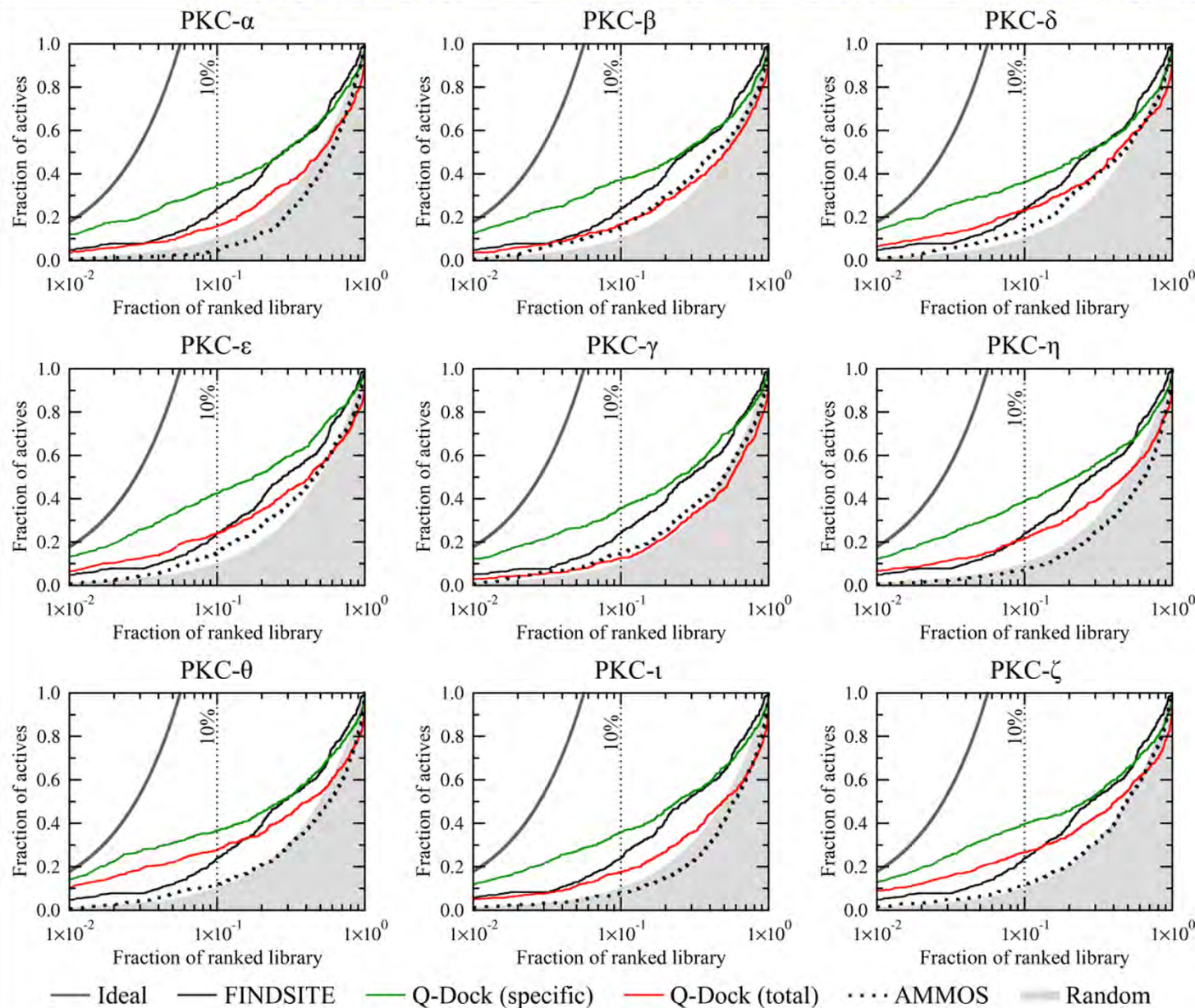
Kim & Skolnick (2008) *J Comput Chem* **29**: 1316-1331

# Ligand Homology Modeling: Q- 204 pharmacologically relevant targets from CCDC/Astex dataset



Fraction of correctly predicted specific protein-ligand contacts

# Ligand Homology Modeling:



Virtual  
screening  
against  
PKC  
isoforms

562 known  
inhibitors  
(*MDDR*)

10,000 decoy  
cmps  
(*ZINC7*)